

การพิสูจน์เอกลักษณ์และลักษณะสมบัติของยีนและโปรตีนที่เกี่ยวข้องกับการส่งสัญญาณระหว่าง
การพัฒนารังไข่ของกิ้งกูดำ *Penaeus monodon*

นางสาวสมกมล ศิริพฤกษ์

วิทยานิพนธ์นี้เป็นส่วนหนึ่งของการศึกษาตามหลักสูตรปริญญาวิทยาศาสตรมหาบัณฑิต

สาขาวิชาเทคโนโลยีชีวภาพ

คณะวิทยาศาสตร์ จุฬาลงกรณ์มหาวิทยาลัย

ปีการศึกษา 2553

ลิขสิทธิ์ของจุฬาลงกรณ์มหาวิทยาลัย

IDENTIFICATION AND CHARACTERIZATION OF GENES AND PROTEINS INVOLVED IN
SIGNAL TRANSDUCTION PATHWAY DURING OVARIAN DEVELOPMENT OF THE
GIANT TIGER SHRIMP *Penaeus monodon*

Miss Somkamon Keereepruk

A Thesis Submitted in Partial Fulfillment of the Requirements
for the Degree of Master of Science Program in Biotechnology

Faculty of Science

Chulalongkorn University

Academic Year 2010

Copyright of Chulalongkorn University

Thesis Title	Identification and characterization of genes and proteins involved in signal transduction pathway during ovarian development of the giant tiger shrimp <i>Penaeus monodon</i>
By	Miss Somkamon Keereepruk
Field of Study	Biotechnology
Thesis Advisor	Professor Piamsak Menasveta, Ph.D.
Thesis Co-advisor	Pattareeya Ponza, Ph.D.

Accepted by the Faculty of Science, Chulalongkorn University in Partial Fulfillment of the Requirements for the Master's Degree

..... Dean of the Faculty of Science
(Professor Supot Hannongbua, Dr.rer.nat.)

THESIS COMMITTEE

..... Chairman
(Assistant Professor Sanit Piyapattanakorn, Ph.D.)

..... Thesis Advisor
(Professor Piamsak Menasveta, Ph.D.)

..... Thesis Co-advisor
(Pattareeya Ponza, Ph.D.)

..... Examiner
(Sirawut Klinbunga, Ph.D.)

..... External Examiner
(Rachanimuk Hiransuchalert, Ph.D.)

สมกมล ศิริพฤกษ์: การพิสูจน์เอกลักษณ์และลักษณะสมบัติของยีนและโปรตีนที่เกี่ยวข้องกับวิถีการส่งสัญญาณระหว่างการพัฒนารังไข่ของกุ้งกุลาดำ *Penaeus monodon* (IDENTIFICATION AND CHARACTERIZATION OF GENES AND PROTEINS INVOLVED IN SIGNAL TRANSDUCTION PATHWAY DURING OVARIAN DEVELOPMENT OF THE GIANT TIGER SHRIMP *Penaeus monodon*) อ.ที่ปรึกษาวิทยานิพนธ์หลัก: ศ.ดร.เปี่ยมศักดิ์ เมนะเศวต, อ.ที่ปรึกษาวิทยานิพนธ์ร่วม: ดร.ภัทริยา พลชา, 127 หน้า.

การพิสูจน์เอกลักษณ์และลักษณะสมบัติของยีนและโปรตีนที่เกี่ยวข้องกับวิถีการส่งสัญญาณระหว่างการพัฒนารังไข่ เป็นจุดเริ่มต้นของความเข้าใจกลไกระดับโมเลกุลของการสมบูรณ์พันธุ์ของกุ้งกุลาดำ จึงนำยีนที่เกี่ยวข้องกับวิถีการส่งสัญญาณระหว่างการพัฒนารังไข่ของกุ้งกุลาดำจากห้องสมุดยีนมาคัดแยกด้วยวิธีอาร์ทีพีซีอาร์ เพื่อศึกษาแนวโน้มของรูปแบบการแสดงออกที่แตกต่างกันในรังไข่ระยะต่างๆของกุ้งกุลาดำ จากนั้นหาลำดับนิวคลีโอไทด์ที่สมบูรณ์ของยีน *PmMEK* ประกอบด้วย ORF 1227 คู่เบส พบโดเมน Serine/Threonine protein kinases (S_TKc)

เมื่อตรวจสอบการแสดงออกของยีนด้วยวิธี Quantitative real-time PCR พบว่ายีน *PmMEK* มีระดับการแสดงออกที่สูงในระยะรังไข่ที่สี่ของกุ้งแม่พันธุ์ปกติ ($P < 0.05$) แต่มีระดับการแสดงออกที่ไม่ต่างกันในกุ้งกุลาดำที่ตัดก้านตา ($P > 0.05$) และพบว่ายีน *PmLATS1* มีระดับการแสดงออกที่สูงในระยะรังไข่ที่สี่ของกุ้งแม่พันธุ์ปกติ ($P < 0.05$) และระดับการแสดงออกที่สูงขึ้นในระยะที่สามและสี่ของกุ้งกุลาดำที่ตัดก้านตา ($P < 0.05$) ส่วนระดับการแสดงออกของยีน *PmKSR* มีระดับการแสดงออกสูงในระยะที่สี่ของกุ้งแม่พันธุ์ปกติ ($P < 0.05$) แต่มีระดับการแสดงออกที่สูงในระยะที่หนึ่งของกุ้งกุลาดำที่ตัดก้านตา ($P < 0.05$) บ่งชี้ว่ายีน *PmKSR* ตอบสนองต่อการกระตุ้นการเจริญพันธุ์ระยะสุดท้ายด้วยการตัดตาหรือการกำจัด GIH แสดงให้เห็นว่าสามารถใช้ยีนดังกล่าวเป็นเครื่องหมายโมเลกุลเพื่อตรวจสอบความสมบูรณ์พันธุ์ของแม่พันธุ์กุ้งกุลาดำได้

เมื่อตรวจสอบตำแหน่งการแสดงออกของยีนที่สนใจในรังไข่ของกุ้งกุลาดำด้วยวิธี *in situ* hybridization พบว่า *PmMEK* และ *PmLATS1* มีตำแหน่งการแสดงออกของ mRNA ในส่วนของไฮโดพลาสซึมของเซลล์ไข่ระยะ previtellogenesis และพบการแสดงออกของยีน *PmLATS1* ในส่วนไฮโดพลาสซึมของเซลล์ไข่ระยะ cortical rod อีกด้วย

สร้างโปรตีนลูกผสมของ PmMEK ในแบคทีเรีย และผลิตโพลีโคลอนแอนติบอดีของโปรตีนดังกล่าวในกระต่าย เมื่อตรวจสอบระดับการแสดงออกของโปรตีนในรังไข่ของกุ้งกุลาดำ พบว่าโปรตีน PmMEK มีระดับการแสดงออกในระยะที่สองและสามสูงกว่าระยะที่หนึ่งและที่สี่ของกุ้งแม่พันธุ์ปกติ แต่ในกุ้งกุลาดำที่ตัดก้านตามีระดับการแสดงออกของโปรตีนลดลงในระยะที่สอง ผลการทดลองบ่งชี้ว่าโปรตีนดังกล่าวมีหน้าที่สำคัญเกี่ยวกับการพัฒนารังไข่ของกุ้งกุลาดำ

จากการศึกษา ยีนและ/หรือโปรตีนดังกล่าวที่เกี่ยวข้องกับวิถีการส่งสัญญาณระหว่างการพัฒนารังไข่ของกุ้งกุลาดำ บ่งชี้ว่ายีนและ/หรือโปรตีนดังกล่าวมีหน้าที่เกี่ยวข้องกับการพัฒนารังไข่ของกุ้งกุลาดำ ซึ่งสามารถนำความรู้ความเข้าใจที่ได้ไปศึกษาความสมบูรณ์พันธุ์ของกุ้งกุลาดำในอนาคตต่อไป

สาขาวิชา.....เทคโนโลยีชีวภาพ.....	ลายมือชื่อ.....
ปีการศึกษา.....2553.....	ลายมือชื่อ อ.ที่ปรึกษาวิทยานิพนธ์หลัก.....
	ลายมือชื่อ อ.ที่ปรึกษาวิทยานิพนธ์ร่วม.....

5172485023 : MAJOR BIOTECHNOLOGY

KEYWORDS : *Penaeus monodon* / GIANT TIGER SHRIMP / OVARIAN DEVELOPMENT / SIGNAL TRANSDUCTION PATHWAY/ PmMEK

SOMKAMON KEEREEPRUK : IDENTIFICATION AND CHARACTERIZATION OF GENES AND PROTEINS INVOLVED IN SIGNAL TRANSDUCTION PATHWAY DURING OVARIAN DEVELOPMENT OF THE GIANT TIGER SHRIMP *Penaeus monodon*
 ADVISOR : PROF.PIAMSAK MENASVETA, Ph.D., CO-ADVISOR : PATTAREEYA PONZA, Ph.D., 127 pp.

Identification and characterization of genes and proteins involved in signal transduction pathway during ovarian development in the giant tiger shrimp (*Penaeus monodon*) were identified and characterized. Screening of expression patterns of genes functionally related to ovarian development of *P. monodon* by RT-PCR, 4 genes including *Mitogen-activated protein (MAP) kinases (MEK)*, *Large Tumor Suppressor1 (LATS1)*, *Kinase Suppressor of RAS (KSR)* and *RAS* with differentially expresses pattern as reveal by RT-PCR were characterized.

The full length cDNAs of *PmMEK* was 1559 bp in length containing the ORFs of 1227 bp to polypeptide of 408 amino acid. Molecular mass and *pI* of the deduced *PmMEK* protein was 45.27 kDa and 6.13, respectively. *PmMEK* contained Serine/Threonine protein kinases (S_TKc).

In situ hybridization indicated that *PmMEK* was localized only in the cytoplasm of previtellogenic oocytes while *PmLATS1* was localized in ooplasm of late cortical rod oocytes as well as previtellogenic oocytes.

Quantitative real-time PCR indicated that In normal broodstock, expression levels of *PmMEK* at stages IV ovaries was greater than those other stages ($P > 0.05$) and this transcript was not significantly different during development of eyestalk-ablated brooder *P. monodon*. The expression level of *PmLATS1* was significantly increased at the final stage (IV) of ovarian development in normal broodstock. And the expression level of *PmKSR* transcript was higher in stage I, II and III ovaries of eyestalk-ablated broodstock than that of intact broodstocks *P. monodon*. Results suggested that *PmKSR* gene may be used as bioindicators for monitoring progression of oocyte maturation.

Recombinant PmMEK protein was successfully expressed *in vitro*. Polyclonal antibodies of these recombinant proteins were successfully produced. Western blot analysis indicated that PmMEK expressed at the vitellogenic ovaries and early cortical rod.

In the present study, the expression profiles of interesting genes/proteins were examined in different stages of ovarian development of normal and eyestalk-ablated *P. monodon* broodstock implied that several key genes from the signal transduction pathway may contribute ovarian development and maturation in *P. monodon*. Functionally analysis of genes/proteins involving ovarian development can be further carried out for better understanding of the reproductive maturation of female *P. monodon* in captivity.

Field of Study :.....Biotechnology..... Student's Signature

Academic Year :.....2010..... Advisor's Signature

Co-advisor's Signature

ACKNOWLEDGEMENTS

I would like to express my deepest sense of gratitude to my advisor, Professor Dr. Piamsak Menasveta, my co-advisor, Dr. Pattareeya Ponza and Dr. Sirawut Klinbunga for their guidances, encouragement, valuable suggestion and supports throughout my study.

My gratitude is also extended to Dr. Sanit Piyapattanakorn and Dr. Rachanimuk Hiransuchalert for serving as thesis committee, for their recommendations and also useful suggestion.

I wish to acknowledge to Center of Excellent in Aquatic Molecular Genetics and Biotechnology (AMGB), National Center for Genetic Engineering and Biotechnology (BIOTEC), National Science and Technology Development Agency (NSTDA), and Thailand Graduate Institute of Science and Technology (TGIST) for my financial support.

Many thanks are also excessively to everyone in the laboratory for their help, suggestion and kindness friendship that give a happy time during a study periods.

Thanks are also express to all my friends in Ratchadamri School, Biotechnology of KMITL and CU for friendships.

Finally, I would like to express my deepest gratitude to my parents and members of my family for their love, understanding and encouragement extended throughout my study.

CONTENTS

	Page
ABSTRACT (THAI)	iv
ABSTRACT (ENGLISH)	v
ACKNOWLEDGMENTS	vi
CONTENTS	vii
LIST OF TABLES	xi
LIST OF FIGURES	xiii
LIST OF ABBREVIATIONS	xvii
CHAPTER I INTRODUCTION	1
1.1 Background information	1
1.2 Objectives	4
1.3 General introduction	4
1.4 Penaeid shrimp biology.....	5
1.4.1 Taxonomy.....	5
1.4.2 Morphology.....	7
1.4.3 Distribution and life cycle.....	7
1.5 Female reproductive system.....	8
1.5.1 Morphology of female reproductive system.....	8
1.5.2 Ovarian development in Penaeid shrimps.....	10
1.6 Vitellogenesis and oocyte maturation.....	12
1.7 Hormones involving shrimp reproduction.....	12
1.8 Molecular biological approaches used in this thesis.....	15
1.8.1 PCR.....	15
1.8.2 Reverse transcription-polymerase chain reaction (RT-PCR)	15
1.8.3 Rapid amplification of cDNA ends-polymerase chain reaction RACE-PCR.....	18
1.8.4 DNA sequencing.....	20
1.8.5 Quantitative real-time PCR.....	22
1.8.6 <i>In situ</i> hybridization.....	24
1.9 Overview of oocyte meiotic resumption.....	26
1.10 Effect of MAPK signal transduction pathway and LATS1 on ovarian development in <i>P. monodon</i>	27
1.10.1 RAS.....	28
1.10.2 Kinase Suppressor of RAS (KSR).....	30

	Page
1.10.3 MEK.....	32
1.10.4 Large tumor suppressor 1 (<i>LATS1</i>).....	32
CHAPTER II MATERIALS AND METHODS.....	34
2.1 Experimental samples.....	34
2.2 Nucleic acid extraction.....	34
2.2.1 DNA extraction.....	34
2.2.2 RNA extraction.....	35
2.2.3 DNase treatment of the extracted RNA.....	36
2.3 Measuring concentrations of extracted DNA and RNA using spectro- photometry and electrophoresis.....	36
2.4 Examination of expression patterns of genes related to ovarian development by RT-PCR and tissue distribution analysis.....	37
2.4.1 Primer design.....	37
2.4.2 First strand cDNA synthesis.....	37
2.4.3 End point PCR.....	39
2.4.4 Tissue distribution analysis.....	40
2.4.5 Agarose gel electrophoresis, semiquantitative RT-PCR and data analysis	41
2.5 Isolation and characterization of the full length cDNA.....	42
2.5.1 Isolation and characterization of the full length cDNA using Rapid Amplification of cDNA Ends-Polymerase Chain Reaction (RACE – PCR).....	42
2.5.1.1 Preparation of the 5' and 3' RACE template.....	42
2.5.2.2 Primer designed for RACE-PCR and primer walking.....	43
2.5.2.3 RACE-PCR and cloning of RACE-PCR products.....	43
2.6 Examination of expression levels of interesting genes in ovaries of <i>P. monodon</i> by quantitative real-time PCR.....	47
2.6.1 Primers and construction of the standard curve.....	47
2.6.2 Quantitative real-time PCR analysis.....	47
2.7 <i>In situ</i> hybridization (ISH).....	48
2.7.1 Sample preparation.....	48
2.7.2 Preparation of cRNA probes.....	48
2.7.2.1 Addition of RNA polymerase recognition sequence (RPRS) by PCR.....	48

	Page
2.7.2.2 Synthesis of cRNA probes.....	50
2.7.2.3 Dot blot analysis.....	50
2.7.3 Hybridization and detection	51
2.8 <i>In vitro</i> expression of recombinant proteins using a bacterial expression system.....	51
2.8.1 Primers design.....	51
2.8.2 Construction of recombinant plasmid in cloning and expression vectors.....	51
2.8.3 Expression of recombinant proteins.....	52
2.8.4 Detection of recombinant proteins.....	53
2.8.5 Purification of recombinant proteins.....	54
2.8.6 Polyclonal antibody production and western blot analysis.....	54
CHAPTER III RESULTS	56
3.1 Examination of expression patterns of genes functionally related to ovarian development of <i>P. monodon</i> by RT-PCR.....	56
3.1.1 Total RNA extraction.....	56
3.1.2 RT-PCR analysis of genes functionally related to ovarian development.....	57
3.2 Tissue distribution analysis of functionally important genes.....	57
3.3 RT-PCR of functionally important genes in gonads of <i>P. monodon</i> ...	59
3.4 Isolation and characterization of the full length cDNA of genes expresses.....	60
3.4.1 Characterization of full length cDNA of <i>MEK</i>	60
3.4.2 Characterization of full length cDNA of <i>Large tumor suppressor gene 1 (LATS1)</i>	63
3.4.3 Characterization of full length cDNA of <i>Kinase suppressor of ras (KSR)</i>	67
3.5 Examination of expression levels of <i>PmMEK</i> , <i>PmLATS1</i> and <i>PmKSR</i> related with ovarian development of <i>P. monodon</i> by Quantitative real-time PCR.....	73
3.6 Localization of sex-related transcripts in ovaries of <i>P. monodon</i> broodstock.....	79
3.6.1. Quantification of the cRNA probes.....	79
3.6.2 <i>In situ</i> hybridization (ISH).....	81

	Page
3.7 In vitro expression of recombinant MEK and RAS proteins using the bacterial expression system.....	86
3.7.1 <i>In vitro</i> expression of recombinant protein.....	89
3.7.2 Purification of recombinant proteins.....	92
3.8 The production of polyclonal antibodies against recombinant PmMEK	95
3.9 Expression profiles of PmMEK protein during ovarian development of <i>P. monodon</i>	95
CHAPTER IV DISCUSSION	98
CHAPTER V CONCLUSION	106
REFERENCES	108
APPENDIX	118
BIOGRAPHY	127

LIST OF TABLES

		Page
Table 1.1	Export of the giant tiger shrimp from Thailand during 2002-2007...	6
Table 2.1	Primer sequences and the expected size of the PCR product of gene homologue of <i>P. monodon</i> initially isolated by EST analysis.	37
Table 2.2	Amplification condition for interesting gene expression level analysis in various tissues.....	40
Table 2.3	Primer sequences for the first strand cDNA synthesis for RACE-PCR.....	44
Table 2.4	Gene-specific primers (GSPs) used for characterization of the full length cDNA of functionally important gene homologues in <i>P. monodon</i> using RACE-PCR.....	44
Table 2.5	Internal primers used for primer walking of the full length cDNA fragments of functionally important gene homologues in <i>P. monodon</i> using RACE-PCR.....	45
Table 2.6	Composition of 5'- and 3'- RACE-PCR.....	45
Table 2.7	The amplification conditions for RACE-PCR of various gene homologues of <i>P. monodon</i>	45
Table 2.8	Nucleotide sequences of primers used for quantitative real-time PCR analysis of <i>MEK</i> or <i>LATS1</i> in <i>P. monodon</i>	48
Table 2.9	Primer sequences for preparation of templates for synthesis of <i>MEK</i> antisense and sense cRNA probes of <i>P. monodon</i>	49
Table 2.10	Primer sequences for preparation of <i>MEK</i> antisense and sense cRNA probes of <i>P. monodon</i>	50
Table 2.11	Nucleotide sequences of primers used for <i>in vitro</i> expression of <i>MEK</i> and <i>RAS</i> of <i>P. monodon</i>	52
Table 3.1	Relative expression levels of <i>PmMEK</i> in different ovarian stages of <i>P. monodon</i> female broodstock.....	74
Table 3.2	Relative expression levels of <i>PmLATS1</i> in different ovarian stages of <i>P. monodon</i> female broodstock.....	77
Table 3.3	Relative expression levels of <i>PmKSR</i> in different ovarian stages of <i>P. monodon</i> female broodstock.....	77

	Page
Table 3.3 Relative expression levels of <i>PmKSR</i> in different ovarian stages of <i>P. monodon</i> female broodstock.....	77
Table 3.4 Titers of polyclonal antibodies using indirect ELISA assay and read the optical density at 450 nm after rabbits was immunized with recombinant PmMEK for 5 times.....	95
Table 3.5 The intensity of MEK signals in different stages of ovaries in both normal and eyestalk-ablated of <i>P. monodon</i> broodstock.....	97

LIST OF FIGURES

		Page
Figure 1.1	Taxonomy of the giant black tiger shrimp, <i>Penaeus monodon</i> , Fabricius	5
Figure 1.2	The life history of <i>Penaeus monodon</i> shrimp.....	8
Figure 1.3	Lateral view of the external morphology of <i>P. monodon</i>	9
Figure 1.4	Lateral view of the internal anatomy of a female <i>P. monodon</i>	9
Figure 1.5	Different ovarian development stages of <i>P. monodon</i>	11
Figure 1.6	General illustration of the polymerase chain reaction (PCR) for amplification of the target DNA.....	16
Figure 1.7	Overall concepts of RT-PCR.....	17
Figure 1.8	Overview of the SMART™ RACE cDNA Amplification Kit.....	19
Figure 1.9	General illustration of the polymerase chain reaction (PCR) for amplifying DNA segments.....	20
Figure 1.10	Automated DNA sequencing.....	21
Figure 1.11	A schematic diagram illustrating principles of automated DNA sequencing.....	22
Figure 1.12	The principle of SYBR Green detection in real-time.....	23
Figure 1.13	Digoxigenin-UTP/dUTP/ddUTP, alkali-stable.....	25
Figure 1.14	Regulation of Oocyte Meiosis Resumption in LowerVertebrates...	28
Figure 1.15	Overview of Raf/MEK/ERK Pathway.....	29
Figure 1.16	The domain organization of KSR protein.....	31
Figure 3.1	A 1.0% ethidium bromide-stained agarose gel showing the quality of total RNA extracted from ovaries of <i>P. monodon</i> broodstock....	56
Figure 3.2	RT-PCR of <i>Large tumor suppressor gene 1(LATS1)</i> , <i>Rho</i> , <i>Rac1</i> , <i>Myc (cMyc)</i> , <i>interleukin (ILPK)</i> , <i>CDC like kinase2(Clk2)</i> , <i>MAP3K interacting protein (MAP3K)</i> , <i>MEK</i> , <i>Moleskin Importin-7 (MSK)</i> , <i>inositol 1,4,5-trisphosphate kinase (IP3K)</i> , <i>Phosphatidylinositol-3-kinase(PI3K)</i> , <i>Like protein kinase form (Polo)</i> , <i>Copper-specific metallothionein (CuMT)</i> , <i>Mn/Fe-dependent superoxide dismutase(SOD)</i> , <i>kinase suppressor of ras (KSR)</i> , <i>Evh1 domain</i> using the first strand cDNA template of <i>P. monodon</i> having different GSI values.....	58

Figure 3.3	Tissue distribution analysis of <i>Large tumor suppressor gene 1 (LATS1)</i> , <i>Rho</i> , <i>Rac1</i> , <i>interleukin (ILPK)</i> , <i>CDC like kinase2 (Clk)</i> , <i>MAP3K interacting protein (MAP3K)</i> , <i>MEK</i> , <i>Moleski</i> , <i>Importin-7 (MSK)</i> , <i>inositol 1,4,5-trisphosphate kinase (IP3K)</i> , <i>Phosphatidylinositol-3-kinase (PI3K)</i> , <i>Like protein kinase from (Polo)</i> , <i>kinase suppressor of ras (KSR)</i> , <i>Evh1 domain</i>	59
Figure 3.4	RT-PCR of <i>Clk2</i> (A), <i>IP3K</i> (B), <i>PI3K</i> (C), <i>ILPK</i> (D), <i>Polo</i> (E), <i>Rho</i> (F) and <i>RAC1</i> (G) using the first strand cDNA of ovaries of juveniles (lanes 1–5) and wild broodstock (lanes 11–15) and testes of juveniles (lanes 6-10) and wild broodstock (lanes 16-20) of <i>P. monodon</i> . <i>EF-1α</i> was successfully amplified from the same template (H).....	60
Figure 3.5	3' and 5'RACE-PCR products (lanes 1 and 2) of <i>MEK</i>	60
Figure 3.6	Nucleotide sequences of EST of <i>MEK</i>	61
Figure 3.7	The full length cDNA and deduced amino acid sequences of <i>MEK</i> of <i>P. monodon</i>	62
Figure 3.8	Diagram illustrating the deduced <i>MEK</i> protein sequence of <i>P. monodon</i>	63
Figure 3.9	5' and 3'RACE-PCR products of <i>LATS1</i>	63
Figure 3.10	Partial multiple alignments of the deduced amino acid sequence of <i>PmMEK</i> , <i>MEK1</i> , <i>MEK2</i> protein of various species.....	64
Figure 3.11	Nucleotide sequences of <i>PmLATS1</i>	65
Figure 3.12	Partial nucleotide and deduced amino sequences of <i>P. monodon LATS1</i> mRNA.....	66
Figure 3.13	The 3'RACE-PCR product of <i>KSR</i>	67
Figure 3.14	Nucleotide sequences of <i>PmKSR</i>	68
Figure 3.15	Partial nucleotide and deduced amino sequences of <i>KSR</i> of <i>P. monodon</i>	70
Figure 3.16	Figure 3.16 Results from BlastX indicating similarity between <i>P. monodon KSR</i> and that of <i>Harpegnathos saltator</i>	71

	Page
Figure 3.17 Partial multiple alignments of the deduced amino acid sequence of PmKSR, KSR, KSR1, KSR2 and KSR like proteins of various species.....	72
Figure 3.18 Standard curves of <i>PmMEK</i> , <i>PmLATS1</i> , <i>PmKSR</i> and <i>EF-1α</i>	73
Figure 3.19 Histograms showing the relative expression profiles of <i>PmMEK</i> during ovarian maturation of normal (A), unilateral eyestalk ablated (B) <i>P. monodon</i> broodstock.....	75
Figure 3.20 Histograms showing the relative expression profiles of <i>PmLATS1</i> during ovarian maturation of normal (A), unilateral eyestalk ablated (B) <i>P. monodon</i> broodstock.....	76
Figure 3.21 Histograms showing the relative expression profiles of <i>PmKSR</i> during ovarian maturation of normal (A), unilateral eyestalk ablated (B) <i>P. monodon</i> broodstock.....	78
Figure 3.22 The amplification product for synthesis of the cRNA probe of <i>PmMEK</i>	79
Figure 3.23 Dot blot hybridization using the antisense <i>Pm-MEK</i> probe.....	79
Figure 3.24 The amplification product for synthesis of the cRNA probe of <i>PmLATS1</i>	80
Figure 3.25 Dot blot hybridization using the antisense <i>PmLATS1</i> probe.....	80
Figure 3.26 Localization of <i>PmMEK</i> transcript during ovarian development of normal <i>P. monodon</i> broodstock.....	82
Figure 3.27 Localization of <i>PmMEK</i> transcript during ovarian development of eyestalk-ablated <i>P. monodon</i> broodstock.....	83
Figure 3.28 Localization of <i>PmLATS1</i> transcript during ovarian development of normal <i>P. monodon</i> broodstock.....	84
Figure 3.29 Localization of <i>PmLATS1</i> transcript during ovarian development of eyestalk-ablated <i>P. monodon</i> broodstock.....	85
Figure 3.30 The full length cDNA and deduced amino acid sequences of <i>RAS</i> of <i>P. monodon</i>	86
Figure 3.31 Multiple alignments of the deduced amino acid sequence of PmRAS and RAS of various species.....	87

	Page
Figure 3.32 Agarose gel electrophoresis showing RT-PCR of the mature transcript of <i>MEK</i> (A) and <i>RAS</i> (B).....	88
Figure 3.33 A 15% SDS-PAGE (A) and Western blot (B) showing <i>in vitro</i> expression of PmMEK.....	89
Figure 3.34 A 12% SDS-PAGE (A) and Western blot (B) showing <i>in vitro</i> expression of PmRAS.....	90
Figure 3.35 A 12% SDS-PAGE showing expression of recombinant PmMEK are insoluble and soluble fractions, respectively.....	91
Figure 3.36 15% SDS-PAGE showing expression of recombinant PmRAS are insoluble and soluble fractions, respectively.....	91
Figure 3.37 15% SDS-PAGE of purified recombinant PmMEK.....	93
Figure 3.38 12%SDS-PAGE of purified recombinant PmRAS.....	94
Figure 3.39 Western blotting analysis of anti-MEK PcAb.....	96

LIST OF ABBREVIATIONS

bp	base pair
°C	degree Celsius
DEPC	Diethylpyrocarbonate
dATP	deoxyadenosine triphosphate
dCTP	deoxycytosine triphosphate
dGTP	deoxyguanosine triphosphate
dTTP	deoxythymidine triphosphate
DNA	deoxyribonucleic acid
EDTA	ethylene diamine tetraacetic acid (disodium salt)
EtBr	ethidium bromide
HCl	hydrochloric acid
IPTG	isopropyl-thiogalactoside
kb	kilobase pair
M	Molar
mg	milligram
mRNA	Messenger-Ribonucleic acid
ml	millilitre
mM	millimolar
ng	nanogram
OD	optical density
PCR	polymerase chain reaction
RNA	Ribonucleic acid
rpm	revolution per minute
RNase A	Ribonuclease A

SDS	sodium dodecyl sulfate
T _m	melting temperature
Tris	Tris (hydroxy methyl) aminomethane
U	unit
UV	ultraviolet
w/v	weight/volume
μg	Microgram
μl	Microlitre
μM	Micromolar

CHAPTER I

INTRODUCTION

1.1 Background information

The giant tiger shrimp (*Penaeus monodon*) is one of the world's most economically important cultured crustaceans (Abe, 1987). Still, *P. monodon* farming relies almost entirely on ocean-caught females for farm seed supply. This open reproductive cycle and reliance on wild stocks of *P. monodon* results in heavy exploitation of female broodstock from wild populations (Klinbunga, 1996).

Reduced spawning potential and low degree of maturation of *P. monodon* in captivity crucially prohibit several possible applications including development of effective breeding programs of this species (Coman, 2006). Unilateral eyestalk ablation is used in practice to induce ovarian maturation in *P. monodon* (Benzie, 1998) It is generally believed that reproductive-inhibiting hormone (GIH) and mandibular organ inhibiting hormone (MOIH), produced and secreted from the X-organsinus gland system in the eyestalk, are eliminated upon eyestalk ablation, thus the gonadal development is no longer inhibited (Huberman, 2000; Okumura, 2004). Although this technique effectively induces maturation and spawning of female shrimp broodstock maintained in the hatcheries, the broodstock become detrimentally exhausted with deterioration in egg quality and quantity leading to the death of spawners. Therefore, predictable maturation and spawning of captive *P. monodon* without the use of eyestalk ablation is a long-term goal for a sustainable shrimp aquaculture. Study of molecular mechanisms involving ovarian/oocyte maturation in this species would suggest pathways or molecules playing a role regulating oocyte maturation. To begin with, cell cycle is the first place to be observed so that molecules would be isolated or pathways would be highlighted for this purpose.

Vertebrate oocytes, which grow within the ovarian follicles, are arrested at the first meiotic prophase. In teleosts, as in other non mammalian vertebrates, the principal events responsible for the enormous growth of oocyte are due essentially to the accumulation of yolk proteins within their cytoplasm (Devlin and Nagahama, 2002). After the oocyte completes its growth, it become ready for the next phase of

oogenesis, that is, the resumption of meiosis, which is accompanied by several maturational processes in the nucleus and cytoplasm of the oocyte. This process, called oocyte maturation, occurs prior to ovulation and is a prerequisite for successful fertilization; it consists of breakdown of the germinal vesicle (GVBD), chromosome condensation, assembly of the meiosis spindle, and formation of the first polar body.

Meiosis consists of two successive cell divisions that are under the control of the M-phase promoting factor (MPF), a heterodimer of two subunits: a catalytic subunit, cyclin-dependent kinase2 (*cdc2*) and a regulatory subunit, cyclin B (Lohka, 1988). The most important kinase is the maturation promoting factor (MPF), which performs a dominant role, in GVBD (Yano, 1988).

The signal transduction pathway crucial for the regulation of meiosis and has been identified in various species is the mitogen-activated protein kinase (MAPK) pathway (Inoue, 1991). The enzyme MAPK is a serine/threonine protein kinase that, together with its downstream substrates, is believed to stabilize MPF and facilitate the MPF-driven process of progression into meiosis (Sagata, 1996). In *Xenopus* MAPK cascade, including Mos, MEK, MAPK, as well as MEK downstream kinase p90^{Rsk}, has been shown to play an important role in establishing MPF.

Phosphorylation of MAPK mediated by MEK is a reliable index representing cytotstatic factor (CSF) activity. MAPK existed in oocytes and eggs during oocyte maturation and after egg activation; the presence of its active form was associated with MI arrest unequivocally. Similarly, the phosphorylation of MEK seen in MI-arrested eggs disappeared upon egg activation. The state of phosphorylation of MEK and MAPK apparently correlated to the progression of meiosis, as demonstrated in other animals so far examined (Tachibana *et al.*, 2000; Kishimoto, 2003; Tunquist and Maller, 2003; Kondoh *et al.*, 2006).

G-protein-coupled receptors and classical progesterone receptor were shown to activate the Src/Ras/MAPK pathway. By subunits of G proteins can recruit phosphatidylinositol 3-kinase (PI3K) γ isoform to the membrane (Stoyanov *et al.*, 1995) where they create phosphatidylinositol triphosphate docking sites for nonreceptor tyrosine kinase Src (Dikic *et al.*, 1996; Lopez-Illasaca *et al.*, 1997). Then, activated Src kinase promotes MAPK activation through the assembly of a RAS-

activating signaling complex. PI3K activity is increased in progesterone-treated oocytes and overexpression of constitutively active PI3K γ is able to induce GVBD and stimulate MAPK (Hahl *et al.*, 2001). Evidence is presented that RAS is essential component of oocyte maturation downstream of PI3K (Hahl *et al.*, 2001; Hu *et al.*, 1995)

The Ras proteins are small guanine nucleoside binding proteins that regulate multiple signal transduction pathways (Campbell *et al.*, 1998). They cycle between active (GTP-bound) and inactive (GDP-bound) forms by way of intrinsic Ras GTPase activity as well as by association with cellular regulatory proteins (guanine nucleotide exchange factors [GEFs] and GTPase-activating proteins [GAPs]). Activated RAS in turn transmits the signal to a three-tiered kinase cascade consisting RAF, MEK and ERK/MAPK. The most complex step during signal transduction pathway is the activation of RAF and this involves several events including membrane recruitment, phosphorylation, and protein oligomerization. A critical regulator of RTK and RAS dependent RAF activation is KSR (kinase suppressor of RAS).

A novel tumor suppressor protein family, lats, encodes a class of putative Ser/Thr protein kinases. LATS1 (Tao *et al.*, 1999) or Warts1 (Nishiyama *et al.*, 1999) is a mammalian homolog of *Drosophila* lats. Expression of the human LATS1 gene in *Drosophila* rescues all developmental defects in homozygous Lats mutants and suppresses tumor formation in lats mosaic flies (Tao *et al.*, 1999).

Recently evidence about other gene in signal transduction pathway, In *Xenopus*, Polo like kinase (Polo) can phosphorylate and activate Cdc25C that its ability to dephosphorylation MPF and initiate mitosis (kumagai, 1992). For *clk2* protein exhibits dual-specificity protein kinase activity and can effect changes in subnuclear compartmentalization of serine/arginine-rich protein that *clk* gene product can be involved in the control of constitutive and/or alternative splicing (Duncan, 1998) IP3K-Ca²⁺ signaling has a function in dorsoventral axis formation in *Xenopus* embryos: however, the immediate target of free Ca²⁺ is nuclear (saneyoshi, 2002) Immunoreactive interleukin1 β (ILPK-1 β) has been observed in equine follicular fluid. It has also been shown that (ILPK-1 β) increases the GVBD rate of oocytes *in vitro* in the rabbit (Takehara *et al.*, 1994) and *in vivo* in the mare (Martoriati *et al.*, 2003a) and

Martoriati *et al.*, 2003b). This demonstrates that IL-1 β plays a role in the process of oocyte nuclear) maturation. As is the case with G-Protein-coupled receptors, proteins that bind GTP play a major role in transmission of signal from the activated receptor tyrosine kinases (RTK)s into the cell. In this case, the G proteins are members of the *rho* and *rac1* referred to collectively as small G proteins.

1.2 Objectives

To determine the involvement of MAPK signal transduction pathway during ovarian development and characterize genes in MAPK pathway and other kinases that might participate in ovarian maturation in *P. monodon*.

1.3 General introduction

The giant tiger shimp, *Penaeus monodon*, is one of the most important cultured species (Asian Shrimp Culture Council, 1996; Rosenberry, 2003). Farming of *P. monodon* in Thailand relies almost entirely on wild-caught broodstock for supply of juveniles because of poor reproductive maturation of cultured *P. monodon*. As a result, breeding of pond-reared *P. monodon* is extremely difficult and rarely produced enough quality larvae desired by the industry. The high demand on wild female broodstock lead to overexploitation of the natural population of *P. monodon* in thai waters (Laubier, 1993; Klinbunga *et al.*, 1999). Total aquaculture production of the giant tiger shrimp, *P. monodon* increased gradually from 21,000 tons in 1981 to 200,000 tons in 1988; then it sharply increased to nearly 500,000 tons in 1993. Since then, the production has been quite variable, ranging from a low of 480,000 tons in 1997 to a high of 676,000 tons in 2001 (FAO Fishery Statistic, 2009). The major producers of *P. monodon* are Thailand, Viet Nam, Indonesia, India, the Philippines, Malaysia and Myanmar (Table 1.1).

Marine shrimp farms and hatcheries are located along the coastal areas of Thailand where Nakorn Sri Thammarat and Surat Thani in Peninsular Thailand are the major parts of shrimp cultivation. In addition, Chanthaburi (eastern Thailand), Samut Sakhon and Samut Songkhran (central region) also significantly contribute on the country production. The intensive farming system has resulted in consistent

production of marine shrimp of Thailand. Thailand has been regarded as the leading shrimp producer of cultivated shrimp for over a decade.

Farming of *P. monodon* has achieved a considerable economic and social importance in the region, constituting a significant source of income and employment. In Thailand, *P. monodon* had been intensively cultured for more than two decades.

1.4 Penaeid shrimp biology

1.4.1 Taxonomy

Penaeid shrimp belong to the largest phylum in the animal kingdom, the Arthropoda. This group of animals is characterized by the presence of paired appendages and a protective cuticle or exoskeleton that covers the whole animal. The subphylum Crustacea is made up of 42,000, predominantly aquatic species, that belong to 10 different classes. Within the class Malacostraca, shrimp, together with crayfish, lobsters and crabs, belong to the order Decapoda (Figure 1.1). Taxonomical recognition of *P. monodon* is illustrated below.

Phylum Arthropoda

Subphylum Crustacea

Class Malacostraca

Order Decapoda

Superfamily Penaeoidea

Family Penaeidae Rafinesque, 1815

Genus *Penaeus* Fabricius, 1798

Subgenus *Penaeus*

Species *monodon*

Figure 1.1 Taxonomy of the giant black tiger shrimp, *Penaeus monodon*, Fabricius, 1798 (Brusca and Brusca, 1990).

Table 1.1 Export of the giant tiger shrimp from Thailand during 2002-2007

Country	2002		2003		2004		2005		2006		2007	
	Quantity (MT)	Value (MB)	Quantity (MT)	Value (MB)	Quantity (MT)	Value (MB)	Quantity (MT)	Value (MB)	Quantity (MT)	Value (MB)	Quantity (MT)	Value (MB)
USA	97681.81	36,011.41	89115.28	29,032.87	58365.2	17,206.75	29116.62	17,206.75	34537.23	8,847.42	7979.91	1,909.64
Japan	16644.6	13,813.33	33235.52	11,916.87	27977.27	9,586.59	20182.85	9,586.59	15,709.39	3,832.31	3711.32	1,067.25
Canada	6455.76	3,890.48	11216.47	3,412.09	6490.03	2,072.25	3249.37	2,072.25	2798.61	744.95	1762.16	462.68
Singapore	5251.66	3,138.86	3317.14	1,258.13	3383.18	537.88	1933.5	537.88	1580.11	236.31	401.47	63.53
Taiwan	4917.65	1,276.86	3051.77	799.44	2964.62	564.58	1673.65	564.58	607.7	170.12	692.69	194.78
Australia	4481.25	1,326.06	4817.5	1,252.31	2418.19	1,042.02	2097.76	1,042.02	1418.36	445.05	658.54	225.13
Hong Kong	1365.12	533.26	1437.54	340.42	1396.98	409.93	1026.84	409.93	921.88	256.91	1569	365.91
China	1649.23	352.68	992.91	214.54	833.1	162.66	1003	162.66	710.7	85.65	1629.74	235.57
U. Kingdom	661.07	210.81	184.23	64.11	505.76	181.63	161.79	181.63	241.91	70.54	242.4	73.46
Total	180,615.81	63,822.73	160,986.48	51,524.10	118,343.12	16,629.05	69,168.96	16,629.05	64,565.41	16,178.85	23,933.1	5,922.11

Source: <http://www.fao.org/fishery/statistics/en>

1.4.2 Morphology

The external morphology of penaeid shrimp is distinguished by a cephalothorax with a characteristic hard rostrum, and by a segmented abdomen (Figure 1.2). Most organs are located in cephalothorax, while the body muscles are mainly in the abdomen. The internal morphology of penaeid shrimp is outlined by Figure 1.3. Penaeids and other arthropods have an open circulatory system and, therefore, the blood and the blood cells are called hemolymph and hemocytes, respectively.

1.4.3 Distribution and life cycle

The giant black tiger shrimp is widely distributed throughout the greater part of the Indo-Pacific region, ranging northward to Japan and Taiwan, eastward to Tahiti, southward to Australia and westward to Africa. Penaeid shrimp life cycle include several distinct stages that are found in a variety of habitats (Figure 1.2). Juveniles prefer brackish shore areas and mangrove estuaries in their natural environment. Most of the adults migrate to deeper offshore areas at higher salinities, where mating and reproduction takes place. Females produce between 50,000-1,000,000 eggs per spawning (Rosenberry, 1997). The eggs hatch into the first larval stage, which is the nauplius. The nauplii feed on their reserves for a few days and develop into the protozoeae. The protozoeae feed on algae and metamorphose into mysids. The mysids feed on algae and zooplankton and have many of the characteristics of adult shrimp and develop into megalopas, the stage commonly called postlarvae (PLs). Larval stages inhabit plankton-rich surface waters offshore, with a coastal migration as they develop.

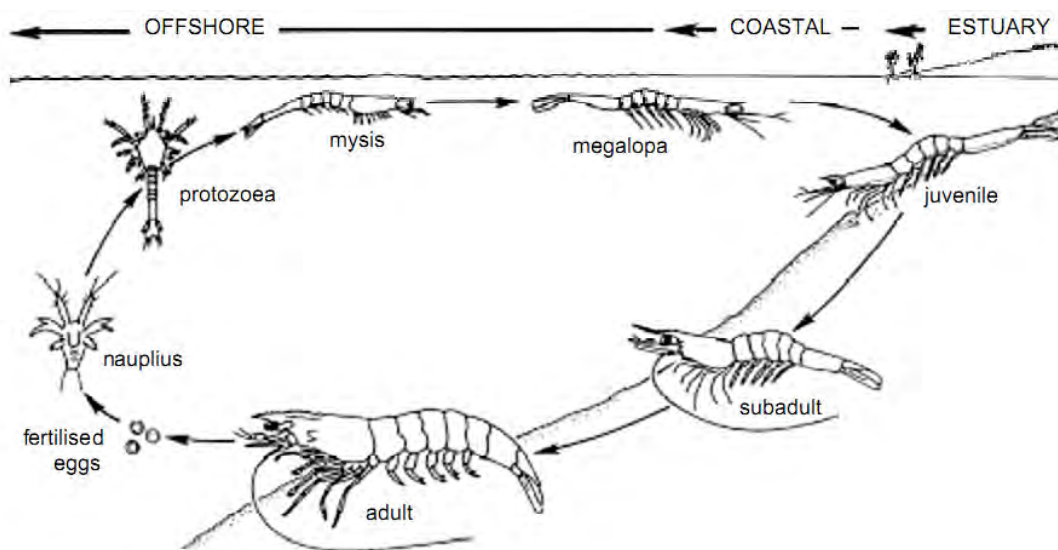


Figure 1.2 The life history of *Penaeus monodon* shrimp. Eggs hatch within 16 hours after fertilization. The larval stages comprise nauplius (6 stages in 2 days), protozoa (3 stages in 5 days), mysis (3 stages in 4-5 days) and megalopa (6-35 days). The megalopa and early juvenile are called postlarvae. Transition from juvenile to subadult takes 135-255 days and subsequently completion of sexual maturity occurs within 10 months (Motoh, 1984). The picture is not in proportion to actual size.

P. monodon is the largest, reaching 330 mm or more in body length, and exhibits the highest growth rate of all cultured penaeid shrimps (Lee and Wickins, 1992). Generally, *P. monodon* can reach a market size up to 25-30 g. within 3-4 months after PL stocking in the culture ponds and tolerates a wide range of salinities (Rosenberry, 1997). Those facts together make *P. monodon* a leading species

1.5 Female reproductive system

1.5.1 Morphology of female reproductive system

The female reproductive system consists of paired ovaries, paired oviducts and a single thelycum. The first two are internal and the last is an external organ. The ovaries are partly fused, bilaterally symmetrical bodies extending in the mature female for almost its entire length, from the cardiac region of the stomach to the anterior portion of the telson. In cepharothorax region the organ bears a slender anterior lobe and five finger-like lateral projections (King, 1948). A pair of lobes, one

from each ovary, extends over the length of the abdomen. The anterior lobes lie close to the esophagus and cardiac region of the stomach. The lateral lobes are located dorsally in the large mass of the hepatopancreas and ventrally in the pericardial chamber. The abdominal extensions lie dorsa-lateral to the intestine and ventro-lateral to the dorsal abdominal artery. The oviducts origins at the tips of the sixth lateral lobes and descend to the external genital apertures hidden in the ear-like lobes of the coxopods of the third pair of pereopods.

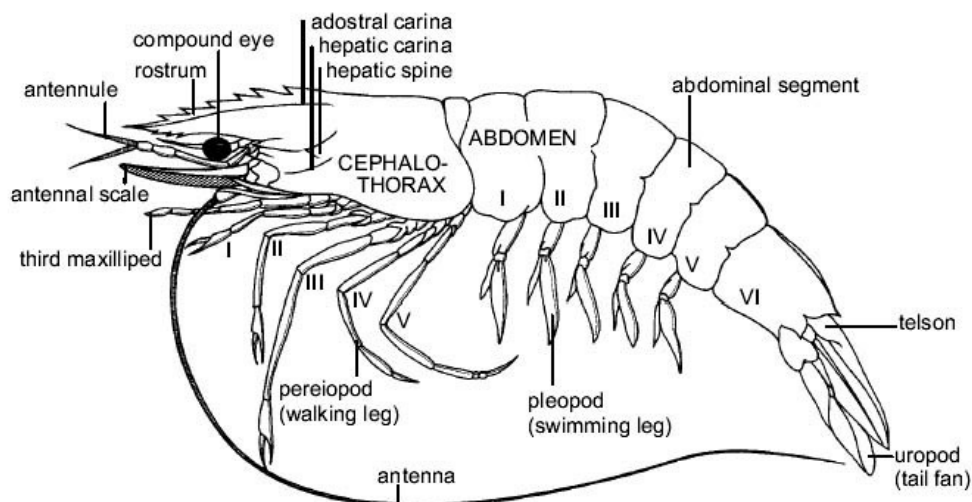


Figure 1.3 Lateral view of the external morphology of *P. monodon*. (Primavera, 1990)

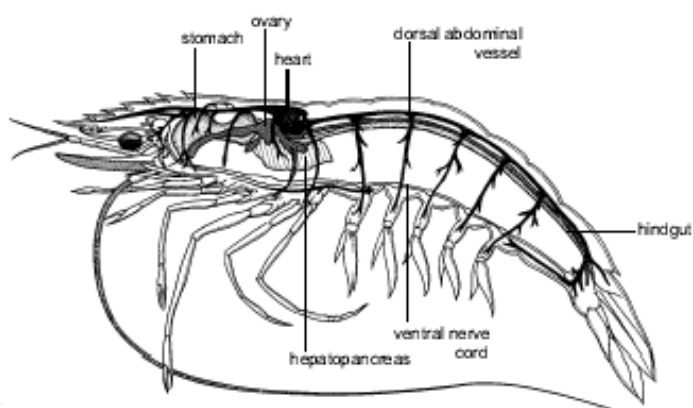


Figure 1.4 Lateral view of the internal anatomy of a female *P. monodon* (Primavera, 1990).

1.5.2 Ovarian development in Penaeid shrimps

The average *P. monodon* broodstock varies according to geographic location. Female wild broodstock are normally range from 110 g to 160 g. However, large females, those over 150 grams, which are assumed to be older females, often do not perform well in hatcheries. The ovary lies dorsal to the gut and extends from the cephalothorax (head and thorax region) along the entire length of the tail as shown in Figure 4. The ovaries are paired, but partially fused in the cephalothorax region which consists of a number of lateral lobes. The ovarian development is divided in 4 phases according to its histological features and germ cell association as shown in Figure 1.3. It consists of stages I (undeveloped phase or spent phase), II (proliferative phase), III (premature phase) and IV (mature phase) ovaries.

The stage I ovaries (Figure 1.5A) are comprised of a connective tissue capsule surrounding a soft vascular area containing future eggs, called oogonia, and accessory cells, also called follicle or nurse cells. The undifferentiated oogonia exists the germinative zone of the ovaries and became oogonia that divided mitotically and enter the meiotic prophase.

The stage II ovaries (Figure 1.5b) contain the majority of previtellogenic oocytes characterized by accumulation of ribosomes and the development of rough endoplasmic reticulums. The developing eggs are increasing in size and they are not as yet producing yolk.

In the stage III ovaries (Figure 1.5c), the majority of oocytes are vitellogenic oocytes governed by the process of vitellogenesis in which yolk proteins (vitellin) are recruited and made within the oocytes. Vitellin is the common form of yolk stored in oocytes and is a nutrient source for developing embryos. Vitellgenin is the precursor molecule of vitellin. Vitellgenin in crustacean was synthesized by fat body, hemocytes, ovaries or hepatopancreas. It is evidenced that vitellogenin fragment was cleaved into smaller size of vitellin fragment by protease function. At the end of the third phase, the oocytes become bright colored by the association of vitellin with carotenoids. By the end of vitellogenesis, the eggs develop cortical granules filled with a jelly-like substance destined to form part of egg shell membrane after ovulation.

In the stage IV ovaries (Figure 1.5d), the fully mature oocytes is composed of extracellular cortical rods. These cortical specializations are precursors of jelly layer (JL) of the egg. Spawning and direct contact of the spawned eggs with sea water leads to the release of extracellular cortical rods. Then, increasing vitellin envelope and formation of corona that is composed of a flocculent matrix around the egg consisting of jelly layer occur. The biochemical composition of the shrimp cortical rods and the nature of jelly layer still scarcely understood. Precursors isolated from mature ovaries comprised of approximately 70-75% protein and 25-30 % carbohydrate. Shrimp ovarian peritrophin (SOP) was demonstrated that it is a component of the cortical rod precursor of the jelly layer in shrimp eggs. It is glycosylated and binds chitin. The color of mature ovaries is characteristic dark green color as a result of deposition of carotenoid pigments.

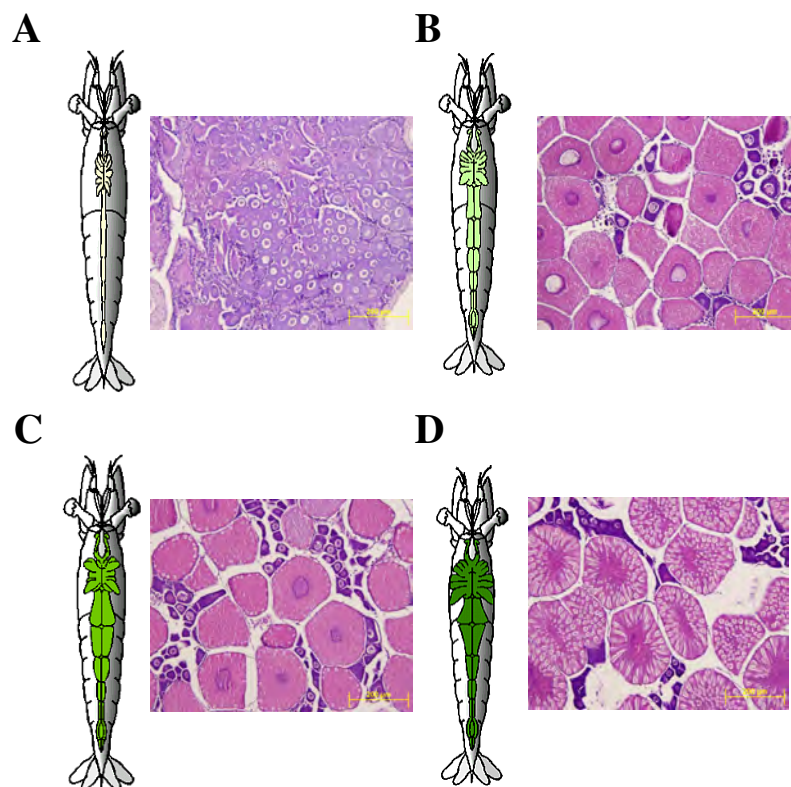


Figure 1.5 Different ovarian development stages of *P. monodon*. **Panel A.**,the underdeveloped ovaries (Stage I), **B.**, the developing stage (Stage II), **C.**, the nearly ripe stage (Stage III) and **D.**, the ripe stage (Stage IV) (www.aims.gov.au/.../mdef/images/fig01-4a.gif).

1.6 Vitellogenesis and oocyte maturation

The process of vitellogenesis involves stimulation by neurotransmitters or hormones. In this process, oocytes gain larger and accumulation of various proteins within the cytoplasm. In crustaceans, during vitellogenesis, vitellogenin, the precursor of vitellin the major yolk protein, is synthesized and is taken in by the oocytes. In the oocytes, vitellogenin is processed and accumulated. Vitellin is utilized as a nutritional source during embryogenesis. Vitellin and vitellogenin have been purified in several shrimps and determined to be large lipoprotein molecules (molecular weight, 280–700 kDa).

In *Marsupenaeus japonicus*, Yano *et al.* (1996) reported that electron dense materials showing the presence of Vg found in the irregular surface of yolk granule stage oocytes were incorporated into the micropinocytotic vesicles of the oocytes. This indicated that Vg is temporally transferred into hemolymph after its synthesis by ovarian tissue and is then incorporated into oocytes by pinocytosis.

It has long been suspected that vitellogenesis including Vg synthesis and its incorporation into oocytes in decapod crustaceans is controlled by stimulating and inhibiting antagonistic hormones. Several studies have shown that vitellogenesis is regulated by a vitellogenesis-inhibiting hormone (VIH) or gonad-inhibiting hormone (GIH) from the X organ–sinus gland complex of the eyestalk (Bomirski *et al.*, 1981; Quackenbush and Herrnkind, 1983; Meusy *et al.*, 1987; Rotllant *et al.*, 1993; De Kleijn *et al.*, 1998) (Figure 1.5). Knowledge of hormonal induction of Vg synthesis and secretion in crustaceans, however, is fragmentary. Understanding the roles of steroid hormones on vitellogenesis may lead to the development of ways to induce ovarian maturation in decapods crustaceans.

1.7 Hormones involving shrimp reproduction

Neurosecretory structures in crustacean eyestalks are known to produce the crustacean hyperglycemic hormone (CHH), molting-inhibiting hormone (MIH) and gonad-inhibiting hormone (GIH) of the CHH/MIH/GIH gene family which secreted from brain and thoracic ganglion as well as other steroids and terpenoids (Chan *et al.*,

2003). These neuropeptides are involved in blood sugar regulation, inhibition of ecdysteroid synthesis, and regulation of reproduction, respectively (Chang, 1993).

A number of physiological processes in decapod crustaceans are known to be regulated by diverse neuropeptides synthesized by a neurosecretory system called X-organ-sinus gland complex (XOSG) located in the optic ganglia of the eyestalks (De and Van, 1995). In penaeid shrimp, GIH is produced in the X-organs and stored in the sinus glands of eyestalks (Gu *et al.*, 2002).

Treerattrakool *et al.* (2007) characterized a cDNA encoding a GIH (Pem-GIH) from the eyestalk of *Penaeus monodon*. Pem-GIH cDNA is 861 bp in size with an ORF of 288 bp. The deduced Pem-GIH consists of a 17-residue signal peptide and a mature peptide region of 79 amino acids with features typical of type II peptide hormones from the CHH family. Pem-GIH transcript was detected in eyestalk, brain, thoracic and abdominal nerve cords of *P. monodon* adults. The gonad-inhibiting activity of Pem-GIH was investigated using the RNA interference technique. Double-stranded RNA, corresponding to the mature Pem-GIH sequence, triggered a decrease in Pem-GIH transcript levels both *in vitro* (eyestalk ganglia and abdominal nerve cord culture) and *in vivo* (female *P. monodon* broodstock). The conspicuous increase in *Vg* transcript level in the ovary of GIH-knockdown shrimp suggests a negative influence for Pem-GIH on *Vg* gene expression, and thus implies its role as the gonad-inhibiting hormone.

Steroid and steroid-like compounds ingested in the diet may have direct effects on reproduction and development (Benzie, 1997). While these can have unintended negative effects, it also means that inclusion of appropriate hormone in the diet may provide the means for a more controlled endocrine manipulation than eyestalk ablation. Since shrimp cannot synthesize cholesterol, an important precursor of steroid hormones (Cuzon *et al.*, 1994), diet is the only source of this substance.

An understanding the roles of steroid hormones on vitellogenesis may lead to the development of ways to induce ovarian maturation in decapod crustaceans. Progesterone has been shown to stimulate ovarian maturation of penaeid shrimp (Yano, 1985) and yolk protein synthesis in the ovary of white shrimp (Quackenbush, 2001). In addition, 17α -hydroxy-progesterone induces spawning in prawn; *P. styliifera*

(Nagabhushanam *et al.*, 1980), Vg secretion into hemolymph of kuruma prawn *M. japonicus* (Yano, 1987) and oocyte developments in white shrimp *P. vannamei* and red swamp crayfish *Procambarus clarkii* (Tsukimura and Kamemoto, 1991; Rodriguez *et al.*, 2002).

Several steroid hormones have been detected in *P. monodon* (Young *et al.*, 1992). It has been reported that 17β -oestradiol and oestrone increase in the early stages of ovary growth demonstrated that 17β -estradiol stimulated in vitro yolk protein synthesis in white shrimp which suggests that 17β -estradiol may also stimulate vitellogenesis in decapod crustaceans. Pregnenolone as well as testosterone have been document from various organs such as the mandibular organ, kidney, hepatopancreas, hemolymph, ovary and testis (Quinitio *et al.*, 1994).

Induction of ovarian maturation in *P. monodon* broodstocks by eyestalk-ablation has been practiced widely in most hatcheries. The technique may result in loss of the valuable broodstocks, as it has been known as non-reversible technique causing stress. Potential molecules that may induce maturation and spawning such as steroid, juvenoids, neurotransmitters and its antagonists have been practiced in vivo and in vitro. However, it has been reported without of success from aquaculture perspective (Alfaro *et al.*, 2004). Injection of serotonin to the female broodstocks resulted in higher hatching rate, production of nauplii that would be more or less comparable to eyestalk ablation (Wongprasert *et al.*, 2006) but the mechanisms how extogenous serotonin worked in ovaries where endogenous serotonin was available did not stated in *P. monodon*. While in marine netertean worms, the mechanisms of how serotonin causing oocyte maturation was clearly explained (Stricker and Smythe, 2001). This process of activation includes signal transduction pathway and phosphorylation of membrane proteins as initial step of oocyte maturation. Therefore, molecular mechanisms of ovarian maturation upon activation by “inducers” in this species should not be neglected to fully manipulate shrimp maturation in captivity in the future.

1.8 Molecular biological approaches used in this thesis

1.8.1 PCR

The introduction of the polymerase chain reaction (PCR) by Mullis *et al.* (1987) has opened a new approach for molecular genetic studies. This method is a technique for enzymatically replicating DNA without using a living organism, such as *E. coli* or yeast and is a method using specific DNA sequences by the two oligonucleotide primers, usually 18-25 nucleotides in length. Million copies of the target DNA sequence can be synthesized from the low amount of starting the DNA template within a few hours.

The PCR components are composed of DNA template, a pair of primers for the target sequence, dNTPs (dATP, dCTP, dGTP and dTTP), PCR buffer and heat-stable DNA polymerase (usually *Taq* polymerase). The amplification reaction typically consists of three steps; denaturation of double stranded DNA at high temperature, annealing to allow primers to form hybrid molecules at the optimal temperature, and extension of the annealed primers by heat-stable DNA polymerase. The cycles are repeated for 30-40 times (Figure 1.7). The amplification product is determined by agarose gel electrophoresis.

1.8.2 Reverse transcription-polymerase chain reaction (RT-PCR)

RT-PCR is a comparable method of conventional PCR but the first strand cDNA template rather than genomic DNA was used as the template in the amplification reaction (Figure 1.6). It is a direct method for examination of gene expression of known sequence transcripts in the target species. The template for RT-PCR can be the first stranded cDNA synthesized from total RNA or poly A⁺ RNA. Reverse transcription of total RNA can be performed with oligo(dT) or random primers using a reverse transcriptase. The product is then subjected to the second strand synthesis using gene-specific primers.

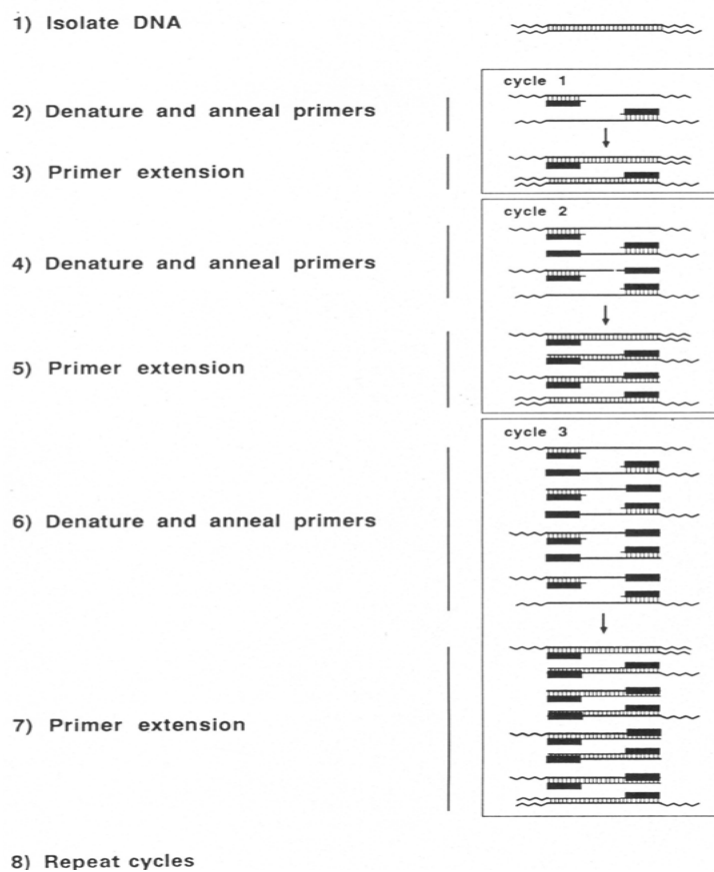


Figure 1.6 General illustration of the polymerase chain reaction (PCR) for amplification of the target DNA.

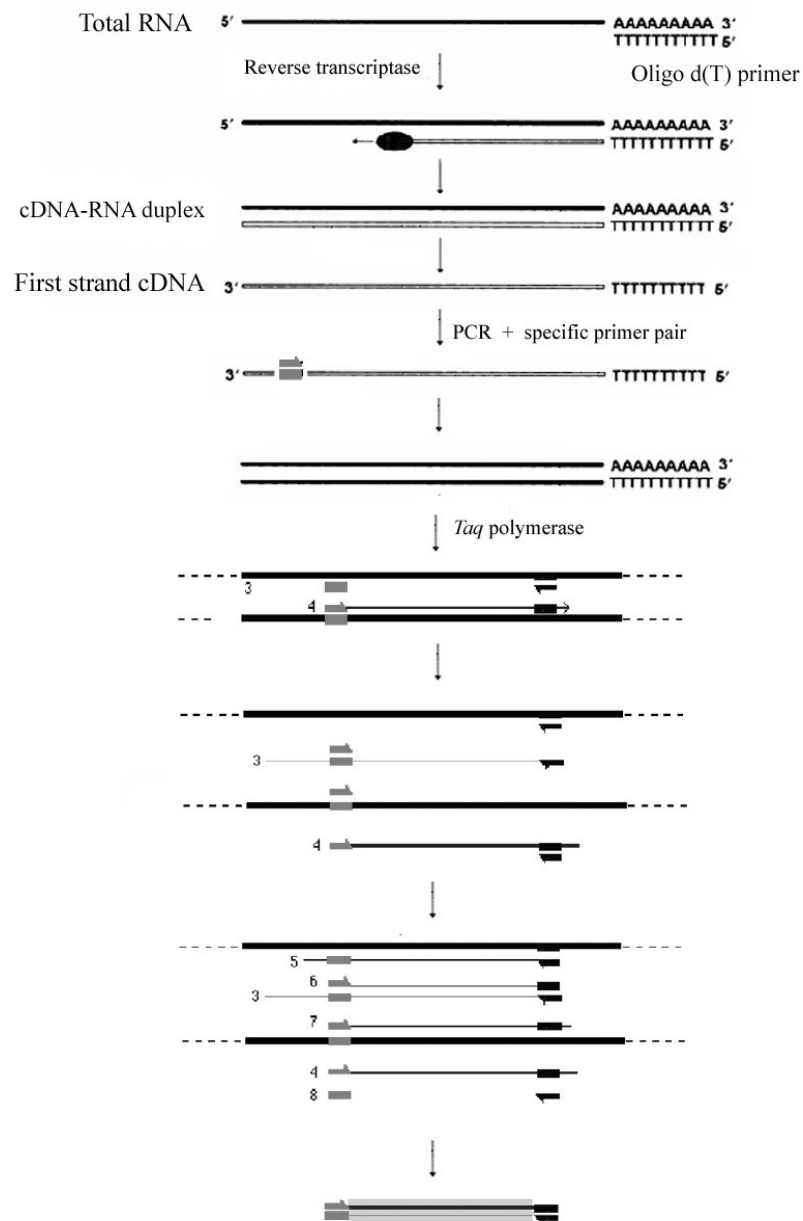


Figure 1.7 Overall concepts of RT-PCR. During the first strand cDNA synthesis, an oligo d(T) (or random primers) primer anneals and extends from sites present within mRNA. The second strand cDNA synthesis primed by the 18 – 25 base specific primer proceeds during a single round of DNA synthesis catalyzed by thermostable DNA polymerase (e.g. *Taq* polymerase).

RT-PCR can also be used to identify homologues of interesting genes by using degenerate primers and/or conserved gene-specific primers from the original species and the first strand cDNA of the interesting species is used as the template. The amplified product is further characterized by cloning and sequencing.

Semi-quantitative RT-PCR is a relatively quantitative approach where the target genes and the internal control (e.g. a housekeeping gene) were separately or simultaneously amplified using the same template. The internal control (such as *β -actin*; *elongation factor*, *EF-1 α* or *G3PDH*) is used under the assumption that those coding genes are transcribed constantly and independently from the extracellular environment stimuli and that their transcripts are reverse transcribed with the same efficiency as the product of interesting transcript.

1.8.3 Rapid amplification of cDNA ends-polymerase chain reaction RACE-PCR

RACE-PCR is the common approach used for isolation of the full length of characterized cDNA. Using SMART (Switching Mechanism At 5' end of RNA Transcript) technology, terminal transferase activity of Powerscript Reverse Transcriptase (RT) adds 3 - 5 nucleotides (predominantly dC) to the 3' end of the first-strand cDNA. This activity is harnessed by the SMART oligonucleotides whose terminal stretch of dG can anneal to the dC-rich cDNA tail and serve as an extended template for reverse transcriptase. A complete cDNA copy of original mRNA is synthesized with the additional SMART sequence at the end (Figure 1.8).

The first strand cDNA of 5' and 3' RACE is synthesized using a modified oligo (dT) primers and serve as the template for RACE PCR reactions. Gene specific primers (GSPs) are designed from interested gene for 5'- RACE PCR (antisense primer) and 3'-RACE PCR (sense primer) and used with the universal primer (UPM) that recognize the SMART sequence. RACE products are characterized. Finally, the full length cDNA is constructed.

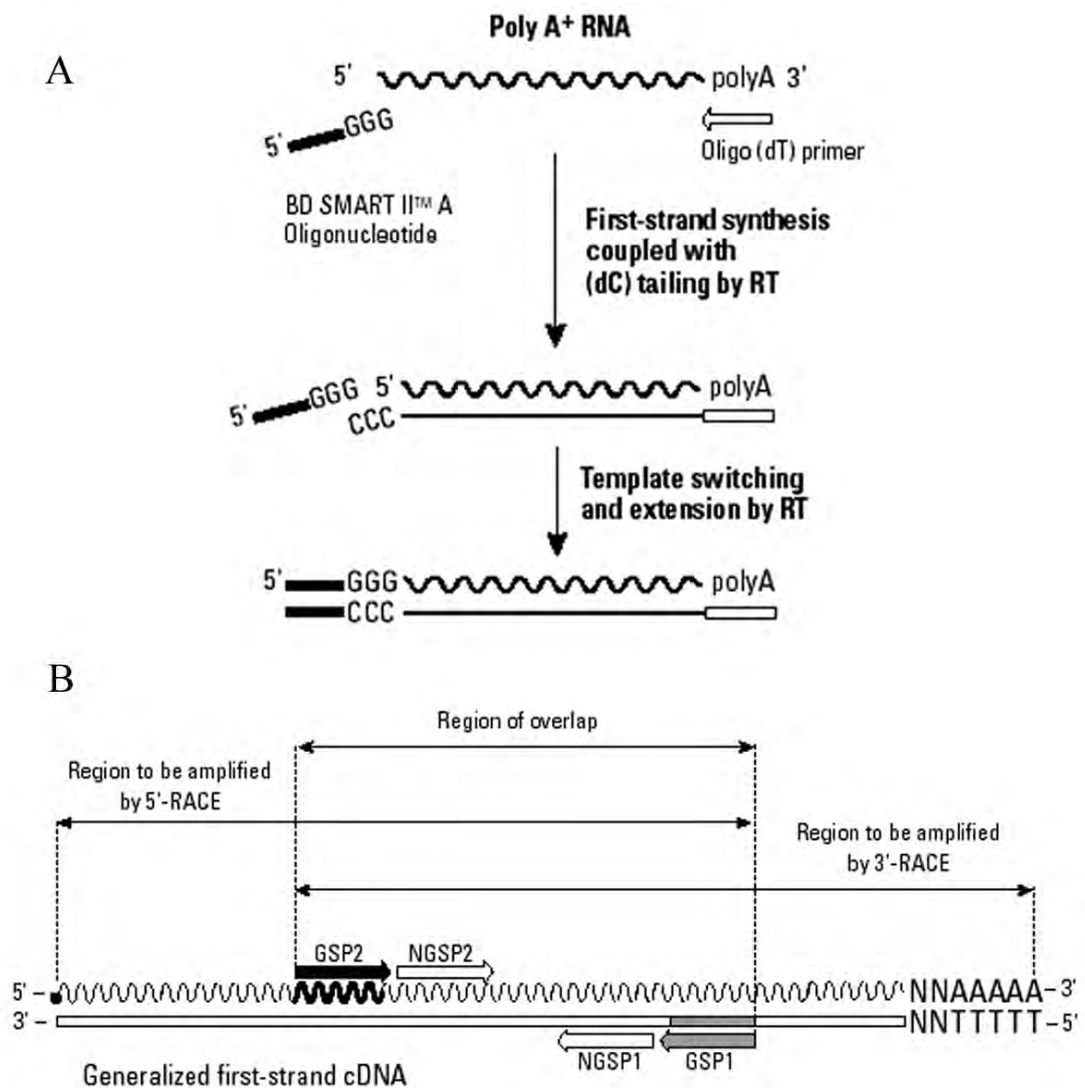


Figure 1.8 Overview of the SMART[™] RACE cDNA Amplification Kit.

A. Mechanism of SMART cDNA synthesis. First strand synthesis is primed using a modified oligo (dT) primer. After reverse transcriptase reaches the end of the mRNA template, it added several dC residues. The SMART II A Oligonucleotide anneals to the tail of the cDNA and serves as an extended template for PowerScriptRT.

B. Relationships of gene-specific primers to the cDNA template. This diagram shows a generalized first strand cDNA template.

1.8.4 DNA sequencing

Polymorphism at the DNA level can be studied by several methods but the direct strategy is determination of nucleotide sequences of a defined region. DNA sequencing is the process of determining the exact order of the bases A, T, C and G in a piece of DNA. There are two general methods for sequencing of DNA segments: the “chemical cleavage” procedure (Maxam and Gilbert, 1977) and the “chain termination” procedure (Sanger, 1977). Nevertheless, the latter method is more popular because chemical cleavage procedure requires the use of several hazardous substances.

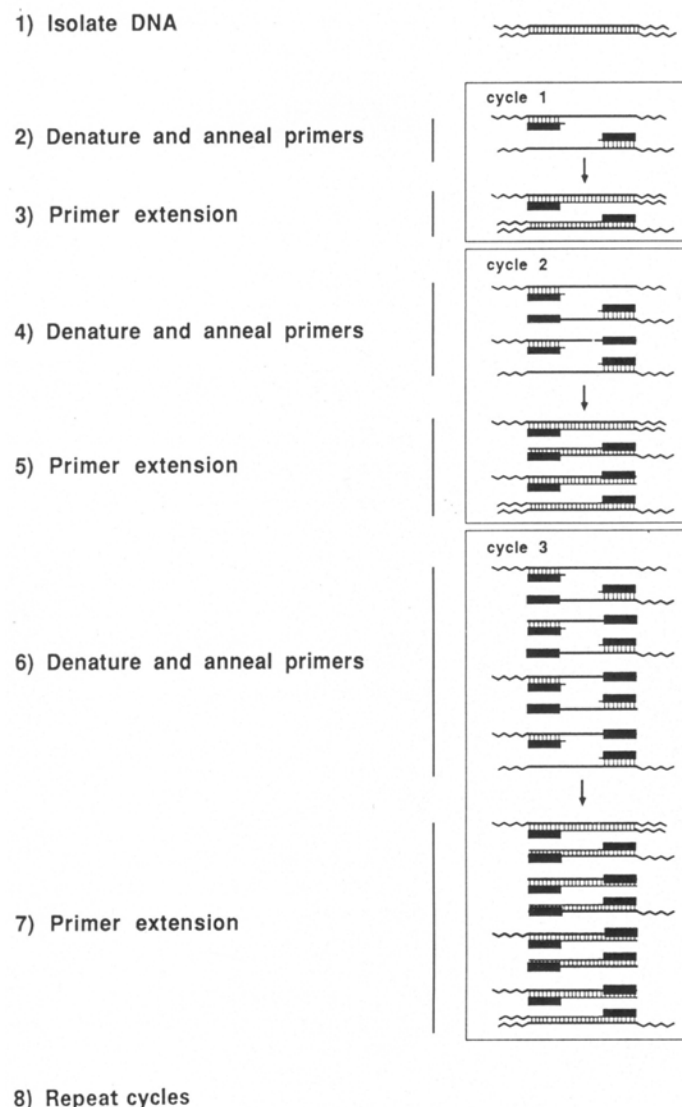


Figure 1.9 General illustration of the polymerase chain reaction (PCR) for amplifying DNA segments.

DNA sequencing provides high resolution and facilitating interpretation. DNA fragments generated from PCR can be directly sequenced or alternatively, those fragments can be cloned and sequenced. This eliminates the need to establish a genome library and searching of a particular gene in the library. However, sequencing of a large number of individuals using conventional method is extremely tedious and prohibitively possible. The enzymatic sequencing approach has presently been developed to the automated method (Figure 1.10). DNA sequences can be detected using a fluorescence-based system following labeling of a sequencing primer or incorporated nucleotides with a fluorescence dye. At present, automated DNA sequencing is commonly used. This greatly allows wider application of DNA sequencing analysis for population genetic and systematic studies.

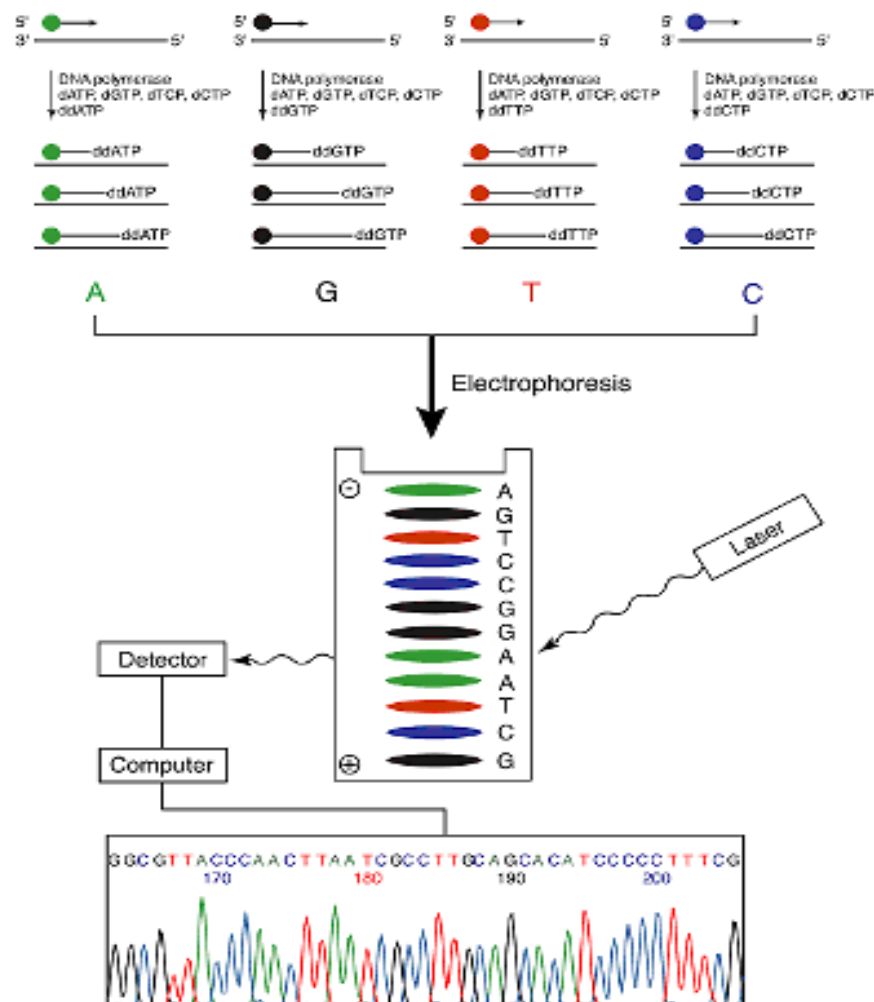


Figure 1.10 Automated DNA sequencing.

1.8.5 Quantitative real-time PCR

Real-time polymerase chain reaction, also called “quantitative real-time polymerase chain reaction” (Q-PCR/qPCR) or “kinetic polymerase chain reaction”, is a laboratory technique based on the polymerase chain reaction, which is used to amplify and simultaneously quantify a target DNA molecule. It enables both detection and quantification (as absolute number of copies or relative amount when normalized to DNA input or additional normalizing genes) of a specific sequence in a DNA sample.

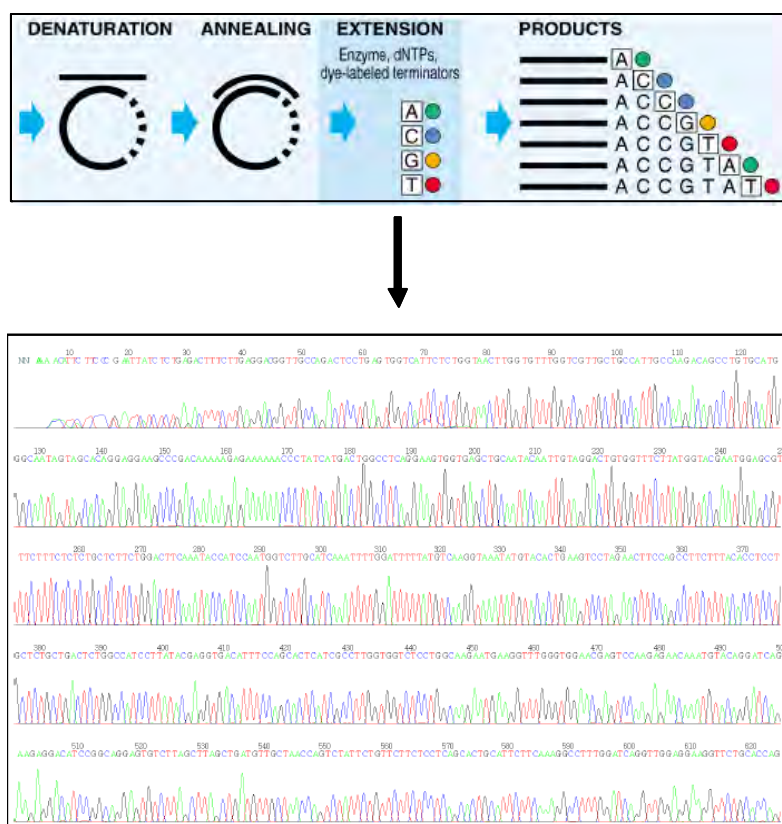


Figure 1.11 A schematic diagram illustrating principles of automated DNA sequencing.

The procedure follows the general principle of polymerase chain reaction; its key feature is that the amplified DNA is quantified as it accumulates in the reaction in real time after each amplification cycle (Figure 1.12). Two common methods of quantification are: (1) the use of fluorescent dyes that intercalate with double-stranded DNA, and (2) modified DNA oligonucleotide probes that fluoresce when hybridized with a complementary DNA (VanGuilder *et al.*, 2008)

Typically, the reaction is prepared as usual, with the addition of fluorescent dsDNA dye. The reaction is run in a thermocycler and after each cycle, the levels of fluorescence are measured with a detector; the dye only fluoresces when bound to the dsDNA

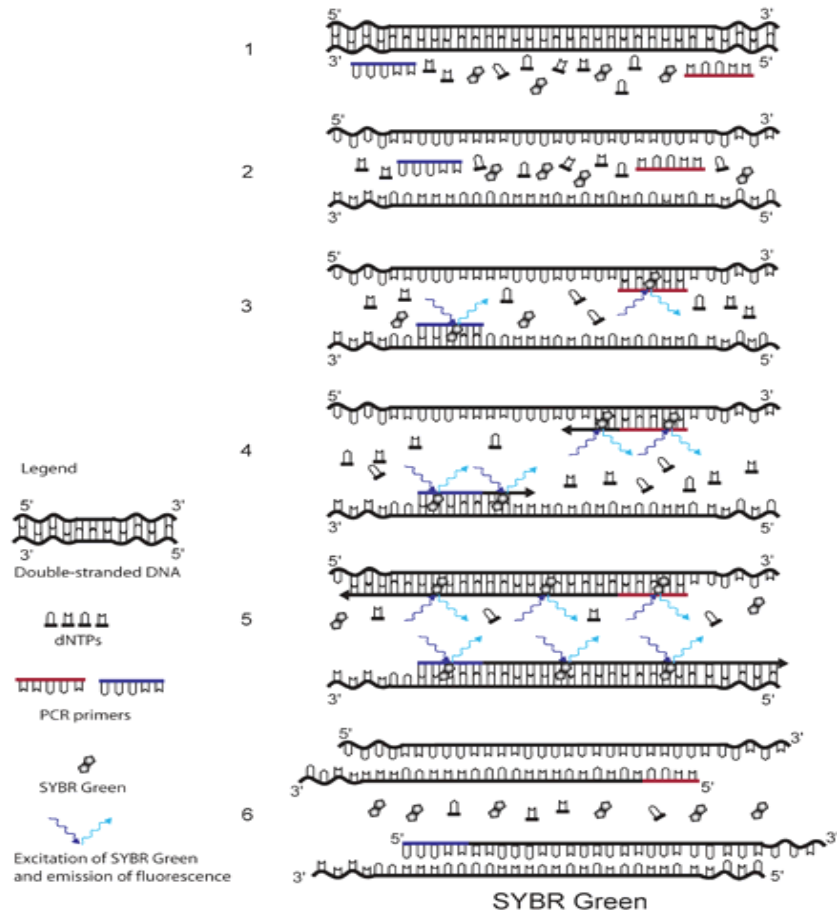


Figure 1.12 The principle of SYBR Green detection in real-time. The fluorescent dye SYBR Green is added to the PCR mixture. SYBR Green is a DNA binding dye that fluoresces strongly when bound to double-stranded DNA. At the start of the reaction, very little double stranded DNA is present, and so the fluorescent signal detected by the thermocycler is low. As the reaction proceeds and PCR product accumulates, the amount of double-stranded DNA increases and with it the fluorescence signal. The signal is only detectable during annealing and extension, since the denaturation step contains predominantly single-stranded DNA. PCR product). With reference to a standard dilution, the dsDNA concentration in the PCR can be determined.

A DNA-binding dye binds to all double-stranded (ds) DNA in PCR, causing fluorescence of the dye. An increase in DNA product during PCR therefore leads to an increase in fluorescence intensity and is measured at each cycle, thus allowing DNA concentrations to be quantified. However, SYBR Green binds to all dsDNA PCR products, including nonspecific PCR products (such as “primer dimers”). This can potentially interfere with or prevent accurate quantification of the intended target sequence.

1.8.6 *In situ* hybridization

In situ hybridization allows specific nucleic acid sequences to be detected in morphologically preserved chromosomes, cells or tissue sections. In combination with immunocytochemistry, *in situ* hybridization can relate microscopic topological information to gene localization at the DNA, mRNA, and protein level. The technique was originally developed by Pardue and Gall (1969). At that time radioisotopes were the only labels available for nucleic acids, and autoradiography was applied for detecting hybridized sequences. Furthermore, as molecular cloning was not possible in those days, *in situ* hybridization was restricted to those sequences that could be purified and isolated by conventional biochemical methods (e.g., mouse satellite DNA, viral DNA, ribosomal RNAs).

At present, non-radioactive labeling using the digoxigenin (DIG) system is commonly applied for *in situ* hybridization. Digoxigenin is linked to the C-5 position of uridine nucleotides via a spacer arm containing eleven carbon atoms (Figure 1.13).

The DIG-labeled nucleotides may be incorporated, at a defined density, into nucleic acid probes by DNA polymerases (such as *E. coli* DNA polymerase I, T4 DNA polymerase, T7 DNA polymerase, Transcriptase, and Taq DNA Polymerase) as well as RNA Polymerase (SP6, T3, or T7 RNA Polymerase), and Terminal Transferase.

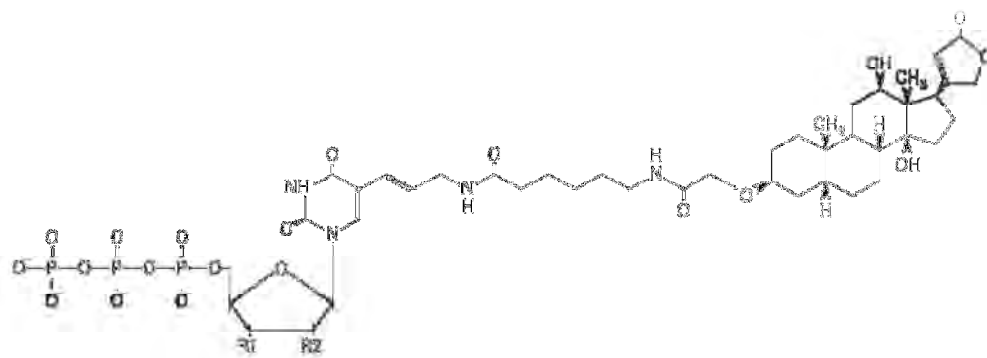


Figure 1.13 Digoxigenin-UTP/dUTP/ddUTP, alkali-stable. Digoxigenin-UTP (R1 = OH, R2 = OH) Digoxigenin-dUTP (R1 = OH, R2 = H) Digoxigenin-ddUTP (R1 = H, R2 = H)

DIG label may be carried out by random primed labeling, nick translation, PCR, 3'-end labeling/tailing, or *in vitro* transcription. Hybridized DIG-labeled probes may be detected with high affinity anti-digoxigenin (anti-DIG) antibodies that are conjugated to alkaline phosphatase, peroxidase, fluorescein, rhodamine, or colloidal gold. Alternatively, unconjugated anti-digoxigenin antibodies and conjugated secondary antibodies may be used.

Detection sensitivity depends upon the method used to visualize the anti-DIG antibody conjugate. For instance, when an anti-DIG antibody conjugated to alkaline phosphatase is visualized with colorimetric (NBT; blue tetrazolium chloride and BCIP; 5-Bromo-4chloro-3-indolyl phosphate, toluidine salt) or fluorescent (HNPP) alkaline phosphatase substrates, the sensitivity of the detection reaction is routinely 0.1 pg of the target on a Southern blot.

1.9 Overview of oocyte meiotic resumption

Oocytes in the vertebrate ovary are arrested at the prophase of first meiotic division, the principal events responsible for the enormous growth of oocytes are due essentially to the accumulation of yolk protein in cytoplasm (Devlin and Nagahama, 2002) and resumption of meiosis by several maturational processes in the nucleus and cytoplasm of the oocyte called oocyte maturation, it consists of breakdown of the germinal vesicle (GVBD).

Although oocyte maturation has been studied in a variety of vertebrates and invertebrates including mammals (Mehlmann, 2005), amphibians (Masui and Clarke, 1979; Maller and Krebs, 1980), fishes (Nagahama *et al.*, 1994) and starfishes (Kishimoto, 1999).

Oocyte maturation in fish is regulated by three mediators, gonadotropin (GTH; luteinizing hormone, LH), maturation inducing hormone (MIH) and maturation promoting factor (MPF) (Nagahama *et al.*, 1994).

MIH signal received on the surface is transduced into cytoplasm for formation and activation of MPF (consist of cdc2 and cyclinB), the final inducer of oocyte maturation. Since G protein is stimulated by MIH will decrease in intracellular levels of cAMP by down-regulation of adenylate cyclase activity (Yoshikuni and Nagahama, 1994), cAMP has a negative role in the induction of fish maturation. cAMP levels is linked to decrease in protein kinase A (PKA) activity. Consistent with this, inhibition of PKA activity is sufficient to induce oocyte in *Clarius batrachus* (Haider and Baqri, 2002). Wee1 and cdc25 are PKA substrates and that the PKA-catalyzed phosphorylation activates Wee1 and inhibits cdc25. Since Wee1 (and its relative, Myt1) has inhibits effect on MPF and cdc25 has an activating effect. MPF is maintained in an inactive form and MPF converted to active form when PKA decreases (Eyers *et al.*, 2005).

Nagahama and Yamashita (2008) investigated the components of MPF (cdc2 and cyclin B) during oocyte maturation of the goldfish. Experiments with gel filtration chromatography followed by immunoblotting analysis have shown that all cdc2 exist as monomer and cyclin B proteins are absent in mature goldfish oocytes

but a part of cdc2 forms a complex with cyclin B in mature oocyte. Phosphorylation of cdc2 T161 is phosphorylated by CAK (cdk activating kinase), which contains cdc7. CAK is active throughout the processes of oocytes maturation (Kondo *et al.*, 1997).

In contrast, immature oocytes of *Xenopus laevis* contain inactive MPF (pre-MPF), the amount of which is sufficient for inducing oocyte maturation. In this species, therefore, activation of pre-MPF consists of T161 and T14/Y15 phosphorylated cdc2 bound to cyclin B (Hochegger *et al.*, 2001)

1.10 Effect of MAPK signal transduction pathway and LATS1 on ovarian development in *P. monodon*

Activation of the MAPK (mitogen-activated protein kinase) cascade is associated about resumption of oocyte meiosis in many different species. Mos codes for a serine/threonine kinase that functions upstream of MAP kinase and MAPK normal expression is confined to germ cells. Oocytes accumulate mRNA of mos, which is translated into protein during meiotic maturation and causes activation of downstream MAPK. For a number of years, it was inferred that the signal inducing meiotic resumption is transduced through MAPK and requires mos protein accumulation, based on the ability of mos and its downstream targets to induce hormone-independent maturation (Dupre *et al.*, 2002). Furthermore, initial experiments in *Xenopus* suggested that mos synthesis is required for GVBD. However, later data obtained in various animals and with many techniques such as specific MAPK inhibitors (starfish, Sadler and Ruderman, 1998), transgenic mos RNAi (mouse, Stein *et al.*, 2003), mos gene knockouts, mos DNA antisense (mouse, O'Keefe *et al.*, 1989), and morpholino antisense treatments (*Xenopus*, Dupre *et al.*, 2002) suggest that MAPK activation is not required for the resumption of meiosis (or GVBD) in any animal. Instead, MAPK activity plays a role in acceleration of MPF activation in the oocyte at meiotic resumption show in figure 1.14 (Dupre *et al.*, 2002), and is needed for suppression of interphase (DNA replication) between two divisions of meiosis and subsequent arrest at the second metaphase of meiosis (Dupre *et al.*, 2002; O'Keefe *et al.*, 1989; Stein *et al.*, 2003).

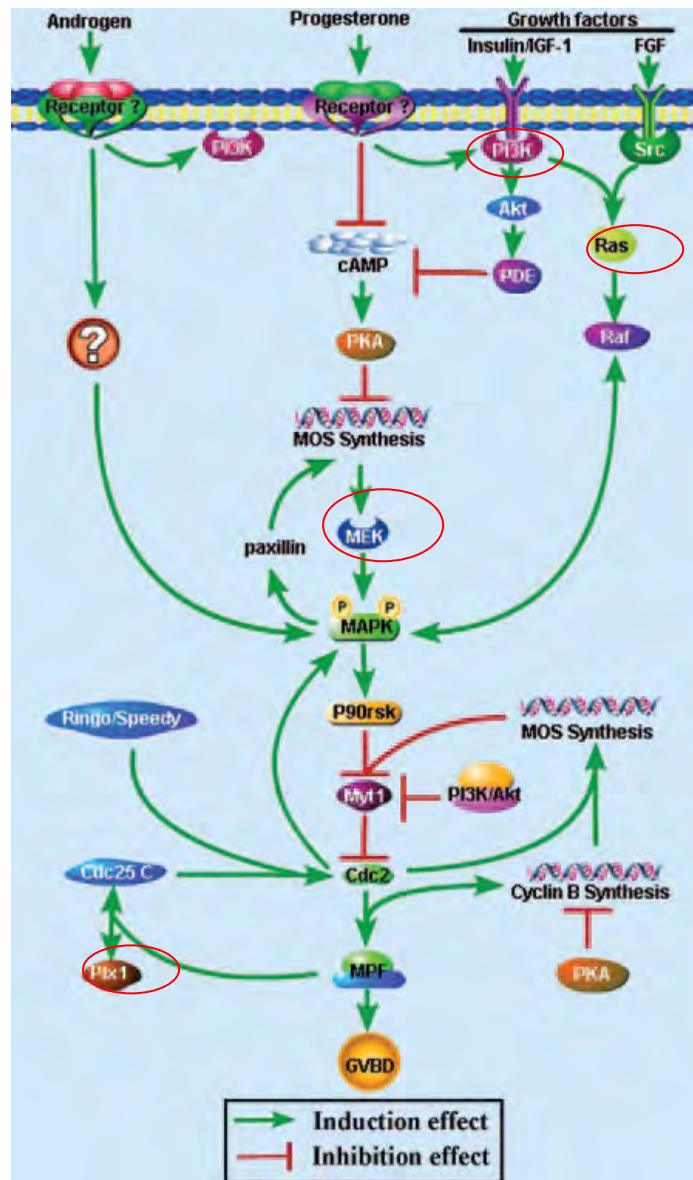


Figure 1.14 Regulation of Oocyte Meiosis Resumption in Lower Vertebrates (Dupre *et al.*, 2002).

1.10.1 RAS

The Ras/Raf/MEK/ERK cascade couples signals from cell surface receptors to transcription factors, which regulate gene expression. Furthermore, this cascade also regulates the activity of many proteins involved in apoptosis. A diagrammatic overview of the Ras/Raf/MEK/ERK pathway is presented in figure 1.15.

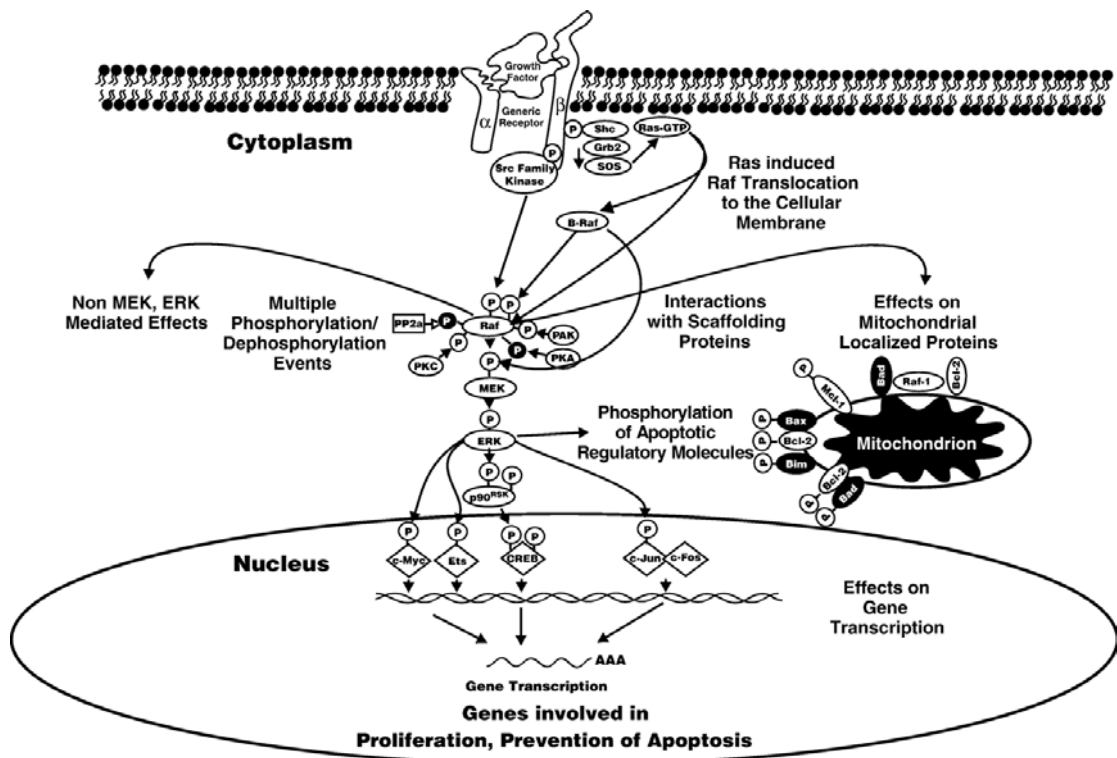


Figure 1.15 Overview of Raf/MEK/ERK Pathway. The Raf/MEK/ERK pathway is regulated by Ras as well as various kinases, which serve to phosphorylate S/T and Y residues on Raf. Some of these phosphorylation events serve to enhance Raf activity (shown by a black P in a white circle) whereas others serve to inhibit Raf activity (shown by a white P in a black circle). Moreover there are phosphatases such as PP2A, which remove phosphates on certain regulatory residues. The downstream transcription factors regulated by this pathway are indicated in diamond shaped outlines (Steelman, 2004)

Ras and other oncogenic proteins have also been shown to induce meiotic maturation when micro-injected into *Xenopus* oocytes (Birchmeier, 1985; Sagata, 1988; Daar, 1991 and Nebreda, 1991). Several lines of evidence indicate that Ras proteins are essential components in pathways of insulin-induced maturation, but not in progesterone-induced GVBD (Deshpande, 1987; Korn, 1987 and Gibbs, 1989).

Ras proteins are 21 kDa GTPases that function as molecular switches, cycling between an active GTP-bound state and an inactive GDP-bound state. This process is regulated tightly by the activities of guanine nucleotide exchange factors (GEFs) which accelerate GTP loading and GTPase-activating proteins (GAPs) which dramatically increase the rate of GTP hydrolysis. These regulatory proteins, in turn,

are controlled through the activation of cell surface receptors, a process that is conserved in eukaryote evolution. Ras proteins are essential signaling components that regulate a host of biological responses including proliferation and differentiation of mammalian cells, eye development in flies, vulva development in nematodes and mating and growth in yeast. (Bourne *et al.*, 1991).

1.10.2 Kinase Suppressor of RAS (KSR)

Kinase suppressor of Ras (KSR) has been suggested to function as scaffolds in specific MAPK pathways (Garrington and Johnson 1999); however, their precise molecular function remains ambiguous. KSR activity appears to be required in the ERK/MAPK pathway (for review, see Morrison 2001). KSR was originally identified in RAS dependent genetic screens in *Drosophila* and *C. elegans* (Kornfeld *et al.* 1995; Sundaram and Han 1995; Therrien *et al.* 1995). Interestingly, KSR proteins are mostly related to RAF serine/threonine kinase family members (Therrien *et al.* 1995).

The domain organization of the KSR proteins is shown in Figure 1.16. Vertebrate and fly KSR proteins share five conserved areas called CA1–CA5. The CA1 domain in *Drosophila* and mammals has been shown to participate in the formation of a ternary KSR–MEK–RAF complex that facilitates MEK phosphorylation (McKay *et al.*, 2009). The KSR members constitute a novel protein family that display remarkable overall structural similarity to proteins of the Raf family (Morrison, 2001). The *C. elegans* proteins lack the CA1 domain, and so it is not required for their function or they have evolved a means to compensate for its absence. The CA2 domain is a proline-rich region of unknown function. The CA3 domain is similar to the CRD domain of RAF and is required for membrane recruitment of KSR1 (Michaud *et al.*, 1997). However, it does not bind RAS and it is not able to substitute for the CRD of RAF. CA4 is a Ser/Thr-rich region similar to CR2 of RAF. CA4 contains an FXFP motif that constitutes a stimulus-dependent ERK docking site (McKay *et al.*, 2009). CA5 is highly homologous to the kinase domain (CR3) of RAF proteins. There are two forms of KSR reported in *C. elegans* and *Drosophilas*, and the similarity of these molecules was discussed. However, KSR1 and KSR2 lack the invariant lysine residue in subdomain II of the kinase domain that is necessary for catalytic activity. Interestingly, *C. elegans* KSR-1 and *Drosophila* KSR contain the invariant lysine in subdomain II, which would suggest

that they are catalytically competent. While this remains to be shown, there is compelling evidence to suggest that KSR proteins do not require catalytic activity for their function. Mutation of the invariant lysine residue in *Drosophila* KSR does not compromise its function (Roy F, 2002), and in *C. elegans*, *ksr-1* transgenes with mutations predicted to nullify catalytic activity are able to complement loss of function alleles (Stewart, 1999). The lack of demonstrable kinase activity has led some to refer to CA5 as a kinase-like or pseudo-kinase domain. The CA5 domain binds constitutively to MEK, and to RAF following stimulation.

A study of KSR1 knockout mice indicates that mammalian KSR1 plays an important role in growth factor- and RAS-dependent RAF activation (Lozano J, 2003). In addition to, apparently, regulating growth factor- and RAS-dependent RAF activation, KSR2 has several functions that are distinct from KSR1. KSR2 contains a region of 63 amino acids between CA2 and CA3 that is not present in the other KSR proteins, and this mediates KSR2- specific binding to calcineurin and AMPK. The calcineurin interaction allows KSR2 to activate ERK signaling following an increase in intracellular calcium. KSR2 regulates cellular energy metabolism in part through its interaction with AMPK, and this contributes to the obese phenotype of KSR2 knockout mice (Christian *et al.*, 2010).

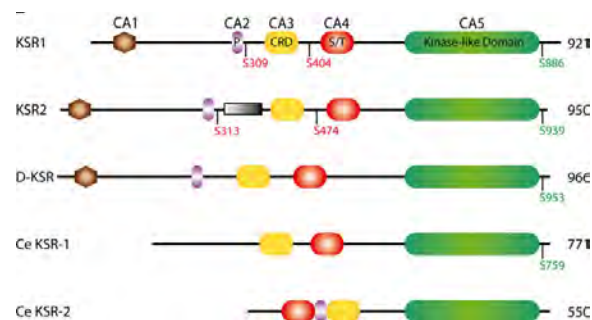


Figure 1.16 The domain organization of KSR protein. Conserved regions (CR) and conserved areas (CA) are indicated at the top of each panel. Conserved phosphorylation sites are indicated underneath each isoform. The size of each isoform is noted at the right. D-RAF and D-KSR are the *Drosophila* paralogs and Ce denotes *C. elegans* proteins. All other proteins depicted are from human. S309 and S404 in human KSR1 are the equivalent of S297 and S392 in mouse KSR1. The unique region of KSR2 is represented as a shaded box. CRD Cysteine-rich domain, P proline-rich, RBD RAS-binding domain, S/T serine/threonine-rich (Christian *et al.*, 2010).

1.10.3 MEK

Mitogen-activated protein (MAP) kinases, MEK is a dual specificity kinase that activates MAPK, also known as extracellular signal-regulated kinases (ERKs), are thought to act at an integration point for multiple biochemical signals because they are activated by a wide variety of extracellular signals, rapidly phosphorylated on threonine and tyrosine, and highly conserved. A critical protein kinase lies upstream of MAP kinase and stimulates the enzymatic activity of MAP kinase (Crews, 1992)

MEK is one of the principal cytoplasmic signal transduction systems governing the proliferation, differentiation, and survival of eukaryotic cells (Chang *et al.*, 2003 and Johnson *et al.*, 2002). In accordance with prototypical MAPK cascade architecture, the MEK-ERK cascade consists of a core unit of three serially phosphorylating protein kinases: Raf, MEK, and ERK. This basic triple kinase organization functions downstream of a diverse array of membrane receptors such as receptor tyrosine kinases and accelerated germinal vesicle breakdown (GVBD) (Bayaa *et al.*, 2000; Tian *et al.*, 2000).

1.10.4 Large tumor suppressor 1 (*LATS1*)

In cDNA library synthesized from ovaries, LATS EST was isolated. GO blast of the nucleotides suggested its duty on oogenesis. Studies on Lats1-deficient mice showed abnormal mammary gland development, infertility and growth retardation, and ovarian stromal cell tumors (Akhmedov *et al.*, 2005). This indicates that Lats1 may regulate cell proliferation and cell survival by inducing mitotic G2/M arrest and apoptotic cell death. LATS (Large Tumor Suppressor) was originally isolated from *Drosophila melanogaster* (*lats*) (Xu *et al.* 1995) and encodes a conserved Ser/Thr kinase with homologs in yeast (*dbf2*, *cbk1*, *orb6*), *C. elegans* (*cLats*), mice (*Lats1*, *Lats2*), and humans (*Ndr1*, *Ndr2*, *LATS1*, *LATS2*) (Tao *et al.* 1999; Hori *et al.* 2000; Yabuta *et al.* 2000). Since its discovery, LATS1/2 (*LATS1* and *LATS2*) have been shown to be integral to the tumorigenic process. Although loss of *LATS2* in mice is lethal, loss of *LATS1* in knockout mice leads to soft tissue sarcomas and ovarian tumors (St John *et al.*, 1999). On the other hand, overexpression of *LATS1* or *LATS2* inhibits tumor formation in mice, or reduces cell growth in human tumor cell lines (Yang *et al.*, 2001; Xia *et al.*, 2002; Li *et al.*, 2003). Hao *et al.* (2008) demonstrated

that LATS is a crucial player of tumor suppressor pathway or Hippo-LATS/Warts pathway acting by regulating cell growth, cell proliferation and cell death. Furthermore, knockout of LATS2 in mouse embryonic fibroblasts (MEFs) induces mitotic defects, genomic instability and loss of contact inhibition of growth (McPherson *et al.*, 2004; Yabuta *et al.* 2007).

Lats1 associates with Cdc2 through its N-terminal domain during early mitosis, which is a period when Lats1 is in its phosphorylated form. Lats1/Cdc2 and Cdc2/cyclinB show that in contrast to the Cdc2/cyclinB, Lats1/Cdc2 complex exhibits no detectable kinase activity for histone H1 (Turenchalk *et al.* 1999).

LATS would play a role in oogenesis by regulating cell cycle and/or cell differentiation rate in ovarian somatic cells. LATS1 is a potential kinase of Forkhead L2 protein (FOXL2) in mammalian ovary which acts as a transcriptional repressor of the steroidogenic acute regulatory (StAR) gene, a marker of granulosa cell differentiation. It was found that FOXL2 expressed abundantly in granulosa cell surrounding mouse oocyte (Uhlenhaut *et al.*, 2006). Phosphorylation of FOXL2 by LATS1 resulted in repression of StAR gene transcription and eventually controls mechanism regulating the rate of granulosa cell differentiation and maintaining follicular development in mice (Pisarska *et al.*, 2010). In zebrafish *Danio rerio*, *lats1* and *lats2* were maternally expressed and affected on gastrulation movement during embryogenesis (Chen *et al.*, 1995).

CHAPTER II

MATERIALS AND METHODS

2.1 Experimental animals

Wild female *P. monodon* broodstock purchased from Andaman Sea was construction of RT-PCR and RACE-PCR. In addition, broodstock-sized male and female *P. monodon* were purchased from Chonburi (Gulf of Thailand, east).

Ovarian developmental stages were divided to previtellogenic (stage I, GSI < 1.5%), vitellogenic (stage II, GSI >2-4%), early cortical rod (stage III, GSI >4-6%) and mature (IV, GSI >6%) ovaries, respectively. For real-time PCR analysis, female broodstock were wild-caught from the Andaman Sea and acclimated under the farm conditions for 2-3 days. Ovaries were dissected out from normal broodstock shrimps and weighed. In addition, ovaries of post-spawned normal broodstock shrimps originated from the Andaman Sea were also collected at after spawning. For the eyestalk ablation group, shrimp were acclimated for 7 days prior to unilateral eyestalk ablation. Ovaries of ablated shrimp were collected at 2-7 days after ablation. The gonadosomatic index (GSI, ovarian weight/body weight x 100) of each shrimp was calculated.

2.2 Nucleic acid extraction

2.2.1 DNA extraction

Genomic DNA was extracted from a piece of pleopod of each *P. monodon* individual using a phenol-chloroform-proteinase K method (Klinbunga *et al.*, 1999). After removing from a -80 °C freezer, a piece of pleopod tissue was briefly homogenized in 500 µl of the extraction buffer (100 mM Tris-HCl, 100 mM EDTA, 250 mM NaCl; pH 8.0), using a micropestle. SDS (10%) and RNase A (10 mg/ml) solutions were added to a final concentration of 1.0 % (w/v) and 100 µg/ml, respectively. The resulting mixture was then incubated at 37°C for 1 hour. At the end of the incubation period, a proteinase K solution (10 mg/ml) was added to the final TGconcentration of 100 µg/ml and the sample was further incubated at 55°C for 3-4

hours. An equal volume of buffer-equilibrated phenol: chloroform: isoamylalcohol (25:24:1) was added and gently mix for 15 minutes. The sample was centrifuged at 10000 rpm for 10 minutes at room temperature, and the upper aqueous phase was transferred to a newly sterile microcentrifuge tube and further extracted once with phenol and once with chloroform: isoamylalcohol (24:1). The final phase was mixed with the sample of TE buffer and subsequently with one-tenth final sample volume of 3 M sodium acetate (pH 5.2). DNA was precipitated by addition of two volume of ice-cold absolute ethanol and incubated at -80°C for 30 minutes. The precipitated DNA was recovered by centrifugation at 12000 rpm for 10 minutes at room temperature and washed twice with 1 ml of 70% ethanol (5 minutes and brief washes, respectively). The DNA pellet was then washed twice with 1 ml of -20°C-cold 70% ethanol. After air-dried, the DNA pellet was resuspended in Tricine-EDTA (TE) buffer (10 mM Tris-HCl, pH 8.0 and 0.1 mM EDTA). The DNA solution was incubated at 37 °C for 1 – 2 hours and stored at 4 °C until further needed.

2.2.2 RNA extraction

Total RNA was extracted from ovaries (or other tissues) of *P. monodon* using TRI REAGENT[®] (Molecular Research Center). A piece of tissues was immediately placed in mortar containing liquid nitrogen and ground to the fine powder. The tissue powder was transferred to a microcentrifuge tube containing 500 µl of TRI-REAGENT[®] (Molecular Research Center) (1 ml/50-100 mg tissue) and homogenized. Additional 500 µl of TRI REAGENT[®] were added. The homogenate and left for 5 minutes, before adding 0.2 ml of chloroform. The homogenate was vortexed for 15 seconds and left at room temperature for 2-15 minutes before centrifuged at 12000g for 15 minutes at 4°C. The mixture was separated into the lower phenol-chloroform phase (red), the interphase, and the colorless upper aqueous phase. The aqueous phase (inclusively containing RNA) was transferred to a new 1.5 ml microcentrifuge tube. RNA was precipitated by an addition of 0.5 ml of isopropanol and mixed thoroughly. The mixture were left at room temperature for 10-15 minutes and centrifuged at 12000g for 10 minutes at 4-25°C. The RNA pellet was washed with 1 ml of 75% ethanol prior to centrifuged at 12000g for 5 minutes at 4°C. The ethanol was removed. The RNA pellet was air-dried for 5-10 minutes. RNA was dissolved in DEPC-treated H₂O for immediately used. Alternatively, the RNA pellet was kept

under absolute ethanol in a -80 °C freezer for long storage. The quality of extracted total RNA was examined by electrophoresis on 1.0% agarose gel.

2.2.3 DNase I treatment of the extracted RNA

Ten µg of total RNA were treated with DNase I (0.5 U/1 µg of RNA, GE Healthcare) at 37°C for 30 minutes. After the incubation, the sample was gently mixed with a sample volume of phenol:chloroform:isoamylalcohol (25:24:1) for 10 minutes. The sample was centrifuged at 13,500 g for 10 minutes at 4 °C, and the upper aqueous phase was collected. The extraction process was then repeated once with chloroform:isoamylalcohol (24:1) and once with chloroform. The final aqueous phase was mixed with one-tenth final sample volume of 3 M sodium acetate (pH 5.2). After that, RNA was precipitated by adding twice the sample volume of -20 °C-cold absolute ethanol. The mixture was incubated at -80 °C for 30 minutes, and the precipitated RNA was recovered by centrifugation at 16,300 g for 10 minutes at room temperature. The RNA pellet was then washed twice with 1 ml of -20°C-cold 75% ethanol. Alternatively, the RNA pellet was kept in absolute ethanol at -80 °C until required.

2.3 Measuring concentrations of extracted DNA and RNA using spectrophotometry and electrophoresis

The concentration of extracted DNA or RNA samples is estimated by measuring the optical density at 260 nanometre (OD₂₆₀). An OD₂₆₀ of 1.0 corresponds to a concentration of 50 µg/ml of double stranded DNA, 40 µg/ml of single stranded RNA and 33 µg/ml of single stranded (ss) DNA (Sambrook and Russel, 2001). Therefore, the concentration of DNA/RNA samples were estimated in µg/ml by using the following equation.

$$[\text{DNA/RNA}] = \text{OD}_{260} \times \text{dilution factor} \times 50 \text{ (40 or 33 for RNA or ssDNA, respectively)}$$

The purity of DNA samples can be evaluated from a ratio of OD₂₆₀ / OD₂₈₀. The ratios of appropriately purified DNA and RNA were approximately 1.8 and 2.0, respectively (Sambrook and Russel, 2001).

2.4 Examination of expression patterns of genes related to ovarian development by RT-PCR and tissue distribution analysis

2.4.1 Primer design

Primers were designed, based on Expressed Sequence Tag (EST) sequences of known transcripts from ovarian cDNA libraries of *P. monodon* (Table 2.1).

2.4.2 First strand cDNA synthesis

One and a half micrograms of DNase I-treated total RNA extracted from the tissues of *P. monodon* were reverse-transcribed to the first strand cDNA using an ImProm- IITM Reverse Transcription System Kit (Promega). First, total RNA was combined with 0.5 µg of oligo dT₁₂₋₁₈ and an appropriate amount of DEPC-treated H₂O to make up the final volume of 5 µl. The mixture was incubated at 70 °C for 5 minutes and then immediately placed on ice for 5 minutes. Then, 5x reaction buffer, MgCl₂, dNTP Mix, RNasin were added to final concentrations of 1x, 2.25 mM, 0.5 mM and 20 units, respectively. Finally, 1 µl of ImProm- IITM Reverse transcriptase was added and gently mixed by pipetting. The reaction mixture was incubated at 25 °C for 5 minutes and at 42°C for 90 minutes, followed by an incubation at 70 °C for 15 minutes to terminate the reverse transcriptase activity. Concentration and quality of the synthesized first strand cDNA were examined by spectrophotometry and 1.2 %-agarose gel electrophoresis.

Table 2.1 Primer sequences and the expected size of the PCR product of gene homologue of *P. monodon* initially isolated by EST analysis

Gene/Primer	Sequence	Tm (°C)	Size (bp)
1. Large tumor suppressor gene 1(LATS1)			
F:	5'- GCGTAAAATGCT TTCTCAA -3'	51.09	201
R:	5'- ACA AACCAGTTCCCCAAT -3'	52.74	
2. Rho			
F:	5'- CTCGTCTCCCTCTTCGTGC -3'	61.88	155
R:	5'- GTCCTCCTGACCTGCTGTG -3'	61.88	
3. Rac1			
F:	5'- CCTTGTCAACCCAGCCAG-3'	59.58	157
R:	5'- CGAACCAGGGATGATACGC -3'	59.72	

Table2.1(cont.)

Gene/Primer	Sequence	Tm (°C)	Size (bp)
4 Myc (cMyc)			
F:	5'- GCAGCAGATTCGTGTCCG-3'	59.58	261
R:	5'- GAAGGCGTTGCGTAGGTC -3'	59.58	
5. Interleukin (ILPK)			
F:	5'- ACGGGCATAGGGACATTG -3'	57.30	172
R:	5'- GTCACGGCTACGAGTCTTCA -3'	59.85	
6. CDC like kinase2(Clk2)			
F:	5'- ACCAGCGGTTAGGCGACG -3'	61.5	147
R:	5'- AATGCCCAATCACCCACTCA -3'	62.2	
7. MAP3K interacting protein (MAP3K)			
F:	5'- ACCAGAATACCCCTTACACG-3'	57.80	172
R:	5'- ATGGTGACGGTGACAGTAGCA -3'	59.97	
8.MEK			
F:	5'-ATGACAACCACACGGGAA -3'	55.02	232
R:	5'-AATCTGCTGTTTCTGGACGA -3'	55.75	
9. Moleski,,Importin-7 (MSK)			
F:	5'- TGGTGGACTCAGAGGACGGA -3'	59.1	224
R:	5'- CAAAGCCATCTACCTTGAACATC -3'	55.0	
10. Inositol 1,4,5-trisphosphate kinase (IP3K)			
F:	5'-TACCCAGGGATTTAGGATAG -3'	55.75	207
R:	5'- TGGCTTTCGGTGAGTGAT-3'	55.02	
11. Phosphatidylinositol-3-kinase(PI3K)			
F:	5'- GACATTAGCCTCGCCGCA -3'	59.58	481
R:	5'- AATCCCGAAGACTTGGGTAGA -3'	56.06	
12. Like protein kinase from (Polo)			
F:	5'- AATCCACGGCACAAGTAAGC -3'	57.80	195
R:	5'- GGGGAACGAGAAAGCAGATA -3'	57.80	
13 Copper-specific metallothionein (CuMT)			
F:	5'- TAAGAATGGCGTTGGAGTGA -3'	55.0	163
R:	5'- AGAATCAGACGAGAAGATAACGA -3'	56.4	

Table2.1(cont.)

Gene/Primer	Sequence	Tm (°C)	Size (bp)
14. Mn/Fe-dependent superoxide dismutase(SOD)			
F:	5'- AAGAATGAAGATGTTGGCGATA -3'	59.3	269
R:	5'- GCCCGTGGAAGAGCAGTC -3'	60.5	
15. Kinase suppressor of ras (KSR)			
F:	5'- CCCACCACCAGTTCATCG-3'	59.58	469
R:	5'- TCTCCCAAGAGTCCCAGTA -3'	57.56	
16. Evh1 domain			
F:	5'- CATCCCCAGTCACACAGC-3'	59.58	269
R:	5'- ACACAGTCTGGTGC GTATT -3'	55.41	

2.4.3 End point PCR

One hundred nanograms of the first strand cDNA of ovaries of female broodstock *P. monodon* was used as the template in 25 µl RT-PCR reaction containing 10 mM Tris-HCl, pH 8.8 at 25°C, 50 mM KCl and 0.1% Triton X-100, 1.5-2.0 mM MgCl₂, 100 or 200 µM each of dNTPs, 0.2 µM of each primer, 1 unit of Dynazyme™ DNA Polymerase (FINNZYMES) and 2 µl of a 10 fold-diluted first strand cDNA (about 200 ng). RT-PCR was initially performed by predenaturation at 94°C for 3 minutes followed by 25 and 30 cycles of denaturation at 94°C for 30 seconds, annealing at 53 (or 55°C) for 45 seconds and extension at 72°C for 30 seconds. The final extension was carried out at 72°C for 7 minutes. Five microlitres of the amplification products were electrophoretically analyzed through 1.0-2.0% agarose gel. The electrophoresed band was visualized under a UV transilluminator after ethidium bromide staining (Sambrook and Russell, 2001). A total of 14 gene homologues were screened. Only differential expression patterns between stages of ovaries were carried out.

2.4.4 Tissue distribution analysis

Gene expression in tissues was studied in hemocytes, gills, heart, lymphoid organs, hepatopancreas, stomach, thoracic ganglion, eyestalk, pleopods, ovaries and testes of *P. monodon*.

RT-PCR was performed on 25- μ l reaction mixtures containing 150 ng of the first strand cDNA from mRNA extracted from each dissected tissue, 10 mM Tris-HCl (pH 8.8), 50 mM KCl, 0.1 % Triton X-100, 2 mM MgCl₂, 100 mM each of dATP, dCTP, dGTP and dTTP, 0.2 μ M of an appropriate primer pair and 1 unit of DynazymeTM DNA polymerase (FINNZYMES). The reaction thermal profile of each gene was shown in Table 2.2. Five μ l of the amplification products were electrophoretically analyzed on 1.5 or 1.8 % agarose gels. Tissue distribution of the target genes was studied in reference to that of a house-keeping gene, *Elongation factor-1 α* (*EF-1 α*).

Table 2.2 Amplification condition for interesting gene expression level analysis in various tissues

Gene homologue	Amplification condition
<i>Large tumor suppressor gene 1(LATS1)</i>	94°C for 3 minutes 30 cycles of 94°C for 30 seconds, 58°C for 30 seconds and 72°C for 45 seconds and the final extension at 72°C for 7 minutes
<i>interleukin (ILPK)</i>	94°C for 3 minutes 30 cycles of 94°C for 30 seconds, 56°C for 30 seconds and 72°C for 45 seconds and the final extension at 72°C for 7 minutes
<i>CDC like kinase2(Clk2)</i>	94°C for 3 minutes 30 cycles of 94°C for 30 seconds, 58°C for 30 seconds and 72°C for 45 seconds and the final extension at 72°C for 7 minutes
<i>MAP3K interacting protein (MAP3K)</i>	94°C for 3 minutes 30 cycles of 94°C for 30 seconds, 58°C for 30 seconds and 72°C for 45 seconds and the final extension at 72°C for 7 minutes
<i>MAP kinase –ERK kinase(MEK)</i>	94°C for 3 minutes 33 cycles of 94°C for 30 seconds, 55°C for 30 seconds and 72°C for 45 seconds and the final extension at 72°C for 7 minutes

Table 2.2(cont.)

Gene homologue	Amplification condition
<i>Moleski, Importin-7 (MSK)</i>	94°C for 3 minutes 30 cycles of 94°C for 30 seconds, 58°C for 30 seconds and 72°C for 45 seconds and the final extension at 72°C for 7 minutes
<i>Inositol 1,4,5-trisphosphate kinase (IP3K)</i>	94°C for 3 minutes 30 cycles of 94°C for 30 seconds, 58°C for 30 seconds and 72°C for 45 seconds and the final extension at 72°C for 7 minutes
<i>Phosphatidylinositol-3-kinase(PI3K)</i>	94°C for 3 minutes 30 cycles of 94°C for 30 seconds, 58°C for 30 seconds and 72°C for 45 seconds and the final extension at 72°C for 7 minutes
<i>Like protein kinase from (Polo)</i>	94°C for 3 minutes 30 cycles of 94°C for 30 seconds, 58°C for 30 seconds and 72°C for 45 seconds and the final extension at 72°C for 7 minutes
<i>kinase suppressor of ras (KSR)</i>	94°C for 3 minutes 33 cycles of 94°C for 30 seconds, 55°C for 30 seconds and 72°C for 45 seconds and the final extension at 72°C for 7 minutes
<i>Evh1 domain</i>	94°C for 3 minutes 30 cycles of 94°C for 30 seconds, 56°C for 30 seconds and 72°C for 45 seconds and the final extension at 72°C for 7 minutes

2.4.5 Agarose gel electrophoresis and data analysis

An appropriate amount of agarose and 1X TBE buffer (89 mM Tris-HCl, 89 mM boric acid and 2 mM EDTA, pH 8.3). The gel slurry was boiled in a microwave oven to complete solubilization, and allowed to lower than 60°C before poured into the gel mold. The gel was left to set before submerged in 1 x TBE buffer filled in an electrophoresis chamber.

Appropriate volumes of PCR products were mixed with the one-fourth volume of the 10X loading dye (0.25% bromophenol blue and 25% Ficoll in water) and loaded into the well. A 100 bp DNA ladder was used as the standard DNA marker. The electrophorised gel was stained with an ethidium bromide solution (2.5 µg/ml) for 5 min and destained in 1 x TBE buffer. Nucleic acid products were visualized under a UV transilluminator and photographed through a red filter using a Biorad gel doc machine.

The expression level of each gene was normalized by that of *EF-1α*. Significantly different expression levels between different groups of *P. monodon* were tested using one way analysis of variance (ANOVA) followed by a Duncan's new multiple range test. Significant comparisons were considered when the *P* value was < 0.05.

2.5 Isolation and characterization of the full length cDNA

2.5.1 Isolation and characterization of the full length cDNA using Rapid Amplification of cDNA Ends-Polymerase Chain Reaction (RACE – PCR)

2.5.1.1 Preparation of the 5' and 3' RACE template

Total RNA was extracted from ovaries of *P. monodon* broodstock using TRIAGENT. Messenger (m) RNA was purified using a QuickPrep *micro* mRNA Purification Kit (Amersham Pharmacia Biotech). One µg of the purified mRNA was then combined with 2 µM of 5'-CDS primer (for 5'-RACE-Ready cDNA) or 3'-CDS primer A (for 3'-RACE-Ready cDNA), 1 µl of 10 µM SMART II A oligonucleotide (only for 5'-RACE-Ready cDNA), and nuclease-free H₂O in an amount that made the final reaction volume to 5 µl. (Table 2.3) The components were mixed and spun briefly. The reaction was incubated at 70°C for 2 minutes and immediately cooled on ice for 2 minutes. The reaction tube was spun briefly. After that, 2 µl of 5X First-Strand buffer, 1 µl of 20 mM DTT, 1 µl of dNTP Mix (10 mM each) and 1 µl of PowerScript Reverse Transcriptase were added. The reactions were mixed by gently pipetting and centrifuged briefly to collect the contents at the bottom. The reactions were mixed by gently pipetting and centrifuged briefly before incubated at 42°C for 1.5 hr in a

thermocycler. The first strand reaction products were diluted with 250 µl of TE buffer and then heated at 72 °C for 7 min.

2.5.2.2 Primer designed for RACE-PCR and primer walking

Gene-specific primers (GSPs) were designed from interesting transcripts obtained from ovaries cDNA libraries and the subtraction ovaries cDNA libraries of *P. monodon*. The antisense and/or sense primers were designed for 5'- and 3'- RACE-PCR, respectively (Table 2.3). Internal forward and/or reverse primers were also designed for further sequencing of the internal regions of large RACE-PCR fragments (Table 2.4).

2.5.2.3 RACE-PCR and cloning of RACE-PCR products

Gene-specific primers (GSPs) were designed from their corresponding homologue sequences in the *P. monodon* EST libraries. GSPs used in the 5'- and 3'- RACE PCRs used to amplify fragments of each gene are summarized in Table 2.4. The master mix which is sufficient for 5'- or 3'- RACE-PCR was prepared as described in Tables 2.6. The 5'- and 3'- RACE-PCR were set up as described in Table 2.7.

After electrophoresis, The desired RACE-PCR fragments were isolated using HiYield™ Gel/PCR DNA Extraction Kit (RBC; Real Biotech Corporation). The DNA fragments were ligated to pGEM®-T Easy vector (Promega) in a 10 µl reaction volume and cloned into *Escherichia coli* JM109. Recombinant clones were selected by a lacZ' system following standard protocols (Sambrook and Russel, 2001) and randomly selected by colony PCR. Recombinant clones carrying desired DNA fragments were selected. Plasmid DNA was extracted and subjected to unidirectional sequencing.

Table 2.3 Primer sequences for the first strand cDNA synthesis for RACE-PCR

Primer	Sequence
SMART II™ A Oligonucleotide (12 μM)	5'- AAGCAGTGGTATCAACGCAGAGTACGCGGG -3'
3'-RACE CDS Primer A (3'-CDS; 12 μM)	5'- AAGCAGTGGTATCAACGCAGAGTAC(T) ₃₀ V N -3' (N = A, C, G or T; V = A, G or C)
5'-RACE CDS Primer (5'-CDS; 12 μM)	5'- (T) ₂₅ V N -3' (N = A, C, G or T; V = A, G or C)
10X Universal Primer A Mix (UPM)	Long : 5'- CTAATACGACTCACTATAGGGCAA GCAGTGGTATCAACGCAGAGT -3' Short : 5'- CTAATACGACTCACTATAGGGC -3'
Nested Universal Primer A (NUP; 12 μM)	5'- AAGCAGTGGTATCAACGCAGAGT -3'

Table 2.4 Gene-specific primers (GSPs) used for characterization of the full length cDNA of functionally important gene homologues in *P. monodon* using RACE-PCR

Primer	Sequence	Tm (°C)
<i>Large tumor suppressor gene 1(LATS1)</i>		
3'-RACE	5'- GAGGATAGACGCCCCCTTACCGCTGG -3'	76.6
<i>MAP kinase –ERK kinase(MEK)</i>		
5'-RACE	5'-TCTGAGGAGTGTCTGTTCCCGTGT-3'	63.68
3'-RACE	5'- GGATGACACACAACGCAGACGGA-3'	63.73
<i>kinase suppressor of ras (KSR)</i>		
5'-RACE	5'-CTGGTGATGGGGTTGGTTGTGGC-3'	65.52
3'-RACE	5'-CGGGTGTGCCCTTACCTCGTG-3'	65.82
<i>Evh1 domain</i>		
5'-RACE	5'-GGTGGTTGGCGTGGGAGTGGC-3'	67.78
3'-RACE	5'-CCGCAGAGGCAGAAAGTTCATCA-3'	61.95
<i>Moleski, Importin-7 (MSK)</i>		
5'-RACE	5'- TGCCTGTCGTTTCATCTTGGGCAC -3'	66.7

Table 2.5 Internal primers used for primer walking of the full length cDNA fragments of functionally important gene homologues in *P. monodon* using RACE-PCR

Primer	Sequence	T _m (°C)
<i>kinase suppressor of ras (KSR)</i>		
3KSR_GAP	5'- TAGGTCGTTCCACATCACA -3'	55.41
3KSR_GAP2	5'-TGATGTGATAGACTCCAGAC-3'	55.75
5KSR_Nested	5'-CGATGAACTGGTGGTGGGTCTC-3'	63.80
<i>Evh1 domain</i>		
3Evh1_GAP	5'- GCAGGGACAACAATGACA -3'	55.02

Table 2.6 Composition of 5'- and 3'- RACE-PCR

Component	5'-RACE Sample	3'-RACE Sample	GSP1+UPM (-Control)	GSP2+UPM (-Control)
5'-RACE-Ready cDNA	1.25 µl	-	-	-
3'-RACE-Ready cDNA	-	1.25 µl	-	-
UPM (10X)	2.5 µl	2.5 µl	2.5 µl	2.5 µl
GSP1 (10 µM)	1.0 µl	-	1.0 µl	-
GSP2 (10 µM)	-	1.0 µl	-	1.0 µl
10X BD advantage [®] 2 PCR Buffer	2.5 µl	2.5 µl	2.5 µl	2.5 µl
10 µM dNTP mix	0.5 µl	0.5 µl	0.5 µl	0.5 µl
50X BD Advantage [®] 2 polymerase mix	0.5 µl	0.5 µl	0.5 µl	0.5 µl
H ₂ O	Up to 25 µl	Up to 25 µl	Up to 25 µl	Up to 25 µl
Final volume	25µl	25µl	25µl	25µl

Table 2.7 The amplification conditions for RACE-PCR of various gene homologues of *P. monodon*

Gene homologue	Amplification condition
<i>Large tumor suppressor gene 1(LATS1) with reverse primer</i>	
3' RACE	3 cycles of 94°C for 30 seconds and 72°C for 2 minutes 5 cycles of 94°C for 30 seconds, 70°C for 30 seconds and 72°C for 3 minutes 20 cycles of 94°C for 30 seconds, 68°C for 30 seconds and 72°C for 3 minutes and the final extension at 72°C for 7 minutes

Table 2.7 (cont.)

Gene homologue	Amplification condition
<i>MAP kinase –ERK kinase(MEK)</i>	
5' RACE	3 cycles of 94°C for 30 seconds and 68°C for 2 minutes 3 cycles of 94°C for 30 seconds, 66°C for 45 seconds and 72°C for 2 minutes 3 cycles of 94°C for 30 seconds, 64°C for 45 seconds and 72°C for 2 minutes 3 cycles of 94°C for 30 seconds, 62°C for 45 seconds and 72°C for 2 minutes 20 cycles of 94°C for 30 seconds, 60°C for 45 seconds and 72°C for 2 minutes and the final extension at 72°C for 7 minutes
3' RACE	3 cycles of 94°C for 30 seconds and 68°C for 2 minutes 3 cycles of 94°C for 30 seconds, 66°C for 45 seconds and 72°C for 2 minutes 3 cycles of 94°C for 30 seconds, 64°C for 45 seconds and 72°C for 2 minutes 3 cycles of 94°C for 30 seconds, 62°C for 45 seconds and 72°C for 2 minutes 20 cycles of 94°C for 30 seconds, 60°C for 45 seconds and 72°C for 2 minutes and the final extension at 72°C for 7 minutes
<i>Kinase suppressor of ras (KSR)</i>	
3' RACE	3 cycles of 94°C for 30 seconds and 68°C for 2 minutes 3 cycles of 94°C for 30 seconds, 66°C for 45 seconds and 72°C for 2 minutes 3 cycles of 94°C for 30 seconds, 64°C for 45 seconds and 72°C for 2 minutes 3 cycles of 94°C for 30 seconds, 62°C for 45 seconds and 72°C for 2 minutes 20 cycles of 94°C for 30 seconds, 60°C for 45 seconds and 72°C for 2 minutes and the final extension at 72°C for 7 minutes
<i>Evh1 domain</i>	
3' RACE	3 cycles of 94°C for 30 seconds and 70°C for 2 minutes 3 cycles of 94°C for 30 seconds, 68°C for 45 seconds and 72°C for 2 minutes 3 cycles of 94°C for 30 seconds, 66°C for 45 seconds and 72°C for 2 minutes 3 cycles of 94°C for 30 seconds, 64°C for 45 seconds and 72°C for 2 minutes 20 cycles of 94°C for 30 seconds, 63°C for 45 seconds and 72°C for 2 minutes and the final extension at 72°C for 7 minutes
<i>Moleski, Importin-7 (MSK)</i>	
3 RACE	3 cycles of 94°C for 30 seconds and 70°C for 2 minutes 3 cycles of 94°C for 30 seconds, 68°C for 45 seconds and 72°C for 2 minutes 3 cycles of 94°C for 30 seconds, 66°C for 45 seconds and 72°C for 2 minutes 3 cycles of 94°C for 30 seconds, 64°C for 45 seconds and 72°C for 2 minutes 20 cycles of 94°C for 30 seconds, 63°C for 45 seconds and 72°C for 2 minutes and the final extension at 72°C for 7 minutes

2.6 Examination of expression levels of interesting genes in ovaries of *P. monodon* by quantitative real-time PCR

Expression levels of several transcripts related to ovarian development, such as; *MEK* or *LATS1* were examined using quantitative real-time PCR analysis. *EF1- α* was used as an internal control. The primers used for amplification *EF1- α* .

2.6.1 Primers and construction of the standard curve

Primers were applied for real-time PCR analysis. For construction of the standard curve of each gene using the according ORF-pGEMT construct prepared in section 2.5.2.3 as the templates for construction of the standard curve. Templates of each gene homologues and *EF-1 α* were tenfold diluted covering $10^3 - 10^8$ copy numbers. Real-time RT-PCR was carried out (see below) and each standard point was run in duplicate.

2.6.2 Quantitative real-time PCR analysis

The amplifications were performed in a reaction volume of 10 μ l containing 5 μ l of 2x SYBR Green Master Mix (Roach). The specific primer pairs were used at a final concentration of 0.1, 0.15, 0.2 and 0.3 μ M, respectively. The thermal profile for quantitative real-time RT-PCR was 95°C for 10 min followed by 40 cycles of denaturation at 95 °C for 15 s, annealing at 53 °C, 55 °C or 56 °C for 30 s and extension at 72 °C for 20 s. The real-time RT-PCR assay was carried out in a 96 well plate and each sample was run in duplicate using a LightCycler[®] 480 Instrument II system (Roche). The relative expression level between shrimp possessing different ovarian development were statistically tested using one way analysis of variance (ANOVA) followed by a Duncan's new multiple range test. Significant comparisons were considered when the *P* value was < 0.05.

Table 2.8 Nucleotide sequences of primers used for quantitative real-time PCR analysis of *MEK* or *LATS1* in *P. monodon*

Gene/Primer	Sequence	T _m (°C)	Size (bp)
<i>MEK</i>	F: 5'- ATGACAACCACACGGGAA -3'	60	147
	F: 5'- AATCTGCTGTTTCTGGACGA -3'	58	
<i>LATS1</i>	F: 5'-TGC GGTTGCCCTTGTCTGC -3'	60	157
	R: 5'-AGTCACCACCAGGGATGTAGTC -3'	60	
<i>KSR</i>	F: 5'- CCCACCACCAGTTCATCGC -3'	62	150
	R: 5'- GCCGCTTTGTTACCAGTTG -3'	58	

2.7 *In situ* hybridization (ISH)

2.7.1 Sample preparation

Ovaries of normal and eyestalk-ablated *P. monodon* broodstock were fixed in 4% paraformaldehyde prepared in 0.1 M sodium phosphate buffered (pH 7.2) overnight at 4°C. The fixed was washed four times with PBS at room temperature and stored in 70% ethanol at -20°C until use. Tissues were histologically prepared, embedded in paraffin and sectioned onto silane-coated slides.

2.7.2 Preparation of cRNA probes

2.7.2.1 Addition of RNA polymerase recognition sequence (RPRS) by PCR

For adding RPRS to *MEK*, gene-specific forward and reverse primers containing T7-RPRS (TAATACGACTCACTATAGGG) were designed (Table 2.10). Fifty nanograms of recombinant plasmid containing the complete ORF of target gene were used as the template in a 50 µl reaction volume containing 1X *Ex Taq*TM Buffer (2.0 mM MgCl₂), 0.2 mM of each dNTP, 0.2 µM of each primer and 1 unit of *TaKaRa Ex Taq*TM (Takara). PCR was initially performed by predenaturation at 94°C

for 2 minutes followed by 40 cycles of denaturation at 94°C for 30 seconds, annealing at 60°C and a 72°C extension for 1 minute.

For adding RPRS, a particular gene segment was amplified using gene-specific primers without the RPRS. The amplified product of each gene was diluted 100 fold. Forward and reverse gene-specific primers containing T7-RPRS; TAATACGACTCACTATAGGG and SP6-RPRS; ATTTAGGTGACACTATAGAA) was then used for the addition of it RPRS to the target genes. PCR were carried out using the same component described above except the sense and antisense probes were simultaneously synthesized. The thermal profiles were predenaturation at 94°C for 5 minutes followed by 35 cycles of denaturation at 94°C for 30 seconds, annealing at 58°C for 30 seconds and extension at 72°C for 2 minutes.

The PCR products were purified using MinElute PCR purification Kit (Qiagen). The concentrations of purified PCR product were estimated by comparing with the DNA marker after electrophoresis.

Table 2.9 Primer sequences for preparation of templates for synthesis of *MEK* antisense and sense cRNA probes of *P. monodon*

Primer combinations For synthesis of <i>MEK</i> antisense and sense cRNA probes	
ORFMEK_F	5' ATGTTGAATAAGAATAAGTTCAACC 3'
ORFMEK_R	5' TTA ACTATTGCCCTCAGCTGATGGC 3'
For synthesis of <i>LATS1</i> antisense and sense cRNA probes	
ORFLATS1_F	5' ATGTTGAATAAGAATAAGTTCAACC 3'
ORFLATS1_R	5' TTA ACTATTGCCCTCAGCTGATGGC 3'

Table 2.10 Primer sequences for preparation of *MEK* antisense and sense cRNA probes of *P. monodon*

Primer combinations	
For sense and antisense cRNA probe	
RiboMEKT7	5': TAATACGACTCACTATAGGGTTCCTCGTCCAGAAACAGCA:3'
RiboMEKSP6	5': ATTTAGGTGACACTATAGAAGCCGACCTTGGTGACCTTGA:3'
For sense and antisense cRNA probe	
RiboLATS1T7	5':TAATACGACTCACTATAGGGTTATGGACTACATCCCTGGTG:3'
RiboLAts1SP6	5':ATTTAGGTGACACTATAGAACTCTCATTGGGTTTCGCTTG:3'

2.7.2.2 Synthesis of cRNA probes

For synthesis of *MEK* antisense and sense cRNA probes, T7 or SP6 RNA polymerase (Takara, Japan) and PCR DIG labeling mix (Roche, Germany) were used for synthesis of sense and antisense cRNA probes, respectively. The mixture was incubated at 42°C (for T7) or 37°C (for SP6) for 2 hours. DNA was eliminated by treating cRNA probes with DNase I (TURBO DNA-free™ kit; Ambion) according to the manufacturer's protocols.

2.7.2.3 Dot blot analysis

The quantity of cRNA probes was determined before used for *in situ* hybridization. Plasmid DNA composing the target gene was 10 fold diluted to 10 ng/μl, 1 ng/μl, 100 pg/μl and 10 pg/μl. 1 μl of each DNA solution was spotted on the nylon membrane. Denature spotted double stranded cDNA by alkaline treatment, neutralized and fixed using UV cross linking (0.12 joules/cm²). The membranes were pre-hybridization with the DIG easyHyb solution (Roche) at 50°C for 30 minutes and hybridized with the DIG easyHyb solution containing 100 ng/ml of the denatured DIG-labeled cRNA probe at 50°C for 3 hours. The membrane was washed twice in 2X SSC (with 0.1% SDS) at room temperature for 5 minutes followed by 0.1X SSC (with 0.1% SDS) once at room temperature and twice at 68°C for 15 minutes. The membranes were washed with TBS with 0.1% tween 20. The dot blot signal was detected as described for *in situ* hybridization.

The estimation of yield can also be performed in a side by side comparison of the DIG-labeled sample nucleic acid with a DIG-label control (Roche).

2.7.3 Hybridization and detection

The sections were prehybridized in the hybridization buffer (50% Formamide, 2X SSC, 1 µg/µl tRNA, 1 µg/µl Salmon sperm DNA, 1 µg/µl BSA and 10% Dextran sulfate) (Wako) at 50°C for 30 minutes. The digoxigenin (DIG)-labeled sense or antisense cRNA probe was added to the hybridization buffer (pre-warmed at 50°C) and incubated overnight at 50°C. The sections were rinsed in 4X SSC twice at 50°C for 5 minutes, and 2X SSC containing 50% formamide at 50°C for 20 minutes. After equilibration in the RNase buffer (0.5M NaCl; 10mM Tris-HCl, pH8.0; 1mM EDTA) at 37°C for 30 minutes, single-strand RNA was digested with 10 µg/ml of RNase A at 37°C for 30 minutes. The sections were washed four times with the RNase A buffer at 37°C for 10 minutes. The sections were rinsed with 2X SSC four times at 50°C for 15 minutes and 0.2X SSC twice at 50°C for 20 minutes each. DIG was immunologically detected (anti-Digoxigenin-AP Fab fragment conjugated with alkaline phosphatase and NBT/BCIP) according to the manufacturer's instructions (Roche, Germany).

2.8 *In vitro* expression of recombinant proteins using a bacterial expression system

2.8.1 Primers design

A primer pair was designed to amplify the ORF of *MEK* and *RAS*. For *MEK* forward primer containing *Bam* HI site, and reverse primer containing *Xho*I site and six Histidine residue. For *RAS* forward primer containing *Nde* I site, and reverse primer containing *Bam* HI site and six Histidine residues encoded nucleotides were illustrated in Table 2.12.

2.8.2 Construction of recombinant plasmid in cloning and expression vectors

The full length cDNA of *MEK* amplified by PCR, ligated to pGEM[®]-T Easy vector and transformed into *E. coli* JM109. Plasmid DNA was extracted from a positive clone and used as the template for amplification using 0.5 µM of each

forward primer and reverse primer, 0.75-1.5 unit *Pfu* DNA polymerase (Promega) and 0.2 mM of each dNTPs. The thermal profiles were predenaturation at 95°C for 2 minutes followed by 25 cycles of denaturation at 95°C for 45 seconds, annealing at 60°C for 30 seconds, extension at 72°C for 4 minutes and final extension at 72°C for 7 minutes.

Table 2.11 Nucleotide sequences of primers used for *in vitro* expression of *MEK* and *RAS* of *P. monodon*

Primer	Sequence
Full length cDNA containing restriction site.	
<i>Bam</i> HI_MEK_F	F:5'- AGCGGATCCATGTTGAATAAGAATAAGT -3'
<i>Xho</i> I_MEK_R	R:5'-ATCTCGAGTCAATGATGATGATGATGATGACTA TTGCCCTCAGCTGA-3'
<i>Nde</i> I_RAS_F	F:5'- CGGCATATGCG GAATACAAGATTGTGGTG-3'
<i>Bam</i> HI_RAS_R	R:5-'CGCGGATCCTTAATGATGATGATGATGATGTAA AAG GCAACA-3'

The amplification product of *MEK* was digested with *Bam* HI and *xho*I. The digested DNA fragment was again analyzed by agarose gel electrophoresis and the gel-eluted product was ligated with pGEXaT1 vectors and transformed into *E. coli* JM109. For *RAS* was digested with *Nde* I and *Bam* HI and analyzed by agarose gel electrophoresis. The gel-elute product was ligated into pET32 and transformed into *E.coli* JM109. The corrected direction of plasmid DNA of *MEK* and *RAS* was subsequently transformed into *E. coli* BL21-CodonPlus (DE3)-RIPL

2.8.3 Expression of recombinant proteins

A single colony of recombinant *E. coli* BL21-CodonPlus (DE3)-RIPL carrying recombinant plasmid of each gene was inoculated into 3 ml of LB medium, containing 50 µg/ml ampicillin and 50 µg/ml chloramphenicol at 37°C overnight. Fifty microlitres of the cultured was transferred to 50 ml of LB medium containing 50 µg/ml ampicillin 50 µg/ml chloramphenicol and further incubated to an OD₆₀₀ of 0.4-0.6. After IPTG induction (1.0 mM final concentration), appropriate volume of the culture corresponding to the OD of 1.0 was time-interval taken (0, 1, 2, 3, 4, 6 hours

and overnight at 37°C) and centrifuged at 12000g for 1 minute. The pellet was resuspended in 1X PBS buffer and examined by 15% SDS-PAGE (Laemmli, 1970).

In addition, 20 ml of the IPTG induced-cultured cells at the most suitable time-interval were taken (6 hours or overnight at 37°C or lower), harvested by centrifugation 5000 rpm for 15 minutes and resuspended in the lysis buffer (0.05 M Tris-HCl; pH 7.5, 0.5 M Urea, 0.05 M NaCl, 0.05 M EDTA; pH 8.0 and 1 mg/ml lysozyme). The cell wall was broken by sonication using Digital Sonifier[®] sonicator Model 250 (BRANSON). The bacterial suspension was sonicated 2-3 times at 15-30% amplitude, pulsed on for 10 seconds and pulsed off for 10 seconds in a period of 2-5 minutes. Soluble and insoluble portions were separated by centrifuged at 14000 rpm for 30 minutes. The protein concentration of both portions was measured using a dye-binding assay (Bradford, 1972). Expression of the recombinant protein was electrophoretically analyzed by 15% SDS-PAGE.

2.8.4 Detection of recombinant proteins

Recombinant protein was separated with SDS-PAGE were electroblotted onto a PVDF membrane (Hybond P; GE Healthcare) (Towbin, 1979) in 25 mM Tris, 192 mM glycine (pH 8.3) buffer containing 10% methanol at a constant current of 350 mA for 1 hour. The membrane was treated in blocking solution (Roche) for 1 hour and incubated with primary antibody (Anti-His (Biorad)) 1:1000 for 1 hour at room temperature. After washing with Tris-buffered saline tween-20 (TBST; 50 mM Tris-HCl, 0.15 M NaCl, pH 7.5, 0.1% Tween-20), the membrane was incubated with a second antibody goat anti rabbit IgG (H+L) conjugated with alkaline phosphatase (Bio-Rad Laboratories) at 1:10,000 for 1 hour. The membrane was washed 3 times with 1X Tris-buffer saline tween-20 (TBST; 50 mM Tris-HCl, 0.15 M NaCl, pH 7.5, 0.1% Tween-20) and incubated with and then washed 3 times with 1X TBST. Detection was performed using NBT/BCIP (Roche) as a substrate. The color reaction was stopped by transferring the membrane into water.

2.8.5 Purification of recombinant proteins

Recombinant proteins were purified using a His GraviTrap kit (GE Healthcare). The column was pre-equilibrated with binding buffer (20 mM sodium phosphate, 500 mM NaCl, 20 mM imidazole, pH 7.4). Samples prepared from the previous step was harvested by centrifugation at 5000 rpm for 15 minutes. The pellet was resuspended in the binding buffer (20 mM sodium phosphate, 500 mM NaCl, 20 mM imidazole, pH 7.4), sonicated and centrifuged at 14000 rpm for 30 minutes. The soluble and insoluble fractions were separated. Soluble fraction composed of the recombinant protein was loaded into column. The column was washed with 10 ml of binding buffer containing 20 mM imidazole (20 mM sodium phosphate, 500 mM NaCl, 20 mM imidazole, pH 7.4), 5 ml of the binding buffer containing 50 mM imidazole (20 mM sodium phosphate, 500 mM NaCl, 50 mM imidazole, pH 7.4) and 5 ml of the binding buffer containing 80 mM imidazole (20 mM sodium phosphate, 500 mM NaCl, 80 mM imidazole, pH 7.4). The recombinant protein was eluted with 6 ml of the elution buffer (20 mM sodium phosphate, 500 mM NaCl, 500 mM imidazole, pH 7.4). Each fraction of the washing and eluting step were analyzed by SDS-PAGE and western blotting. The purified proteins were stored at 4°C or -20°C for long term storage.

2.8.6 Polyclonal antibody production and western blot analysis

Polyclonal antibody against progesterone receptor-related protein MEK and RAS was immunologically produced in a rabbit by Faculty of Associated Medical Sciences, Changmai University. Western blot analysis was carried out to examine specificity and sensitivity of the antibody.

For western blot analysis of ovaries were homogenized in the sample buffer (50 mM Tris-HCl, 0.15 M NaCl, pH 7.5) complemented with protease inhibitors cocktail EDTA free (Roche) and homogenized by centrifugation at 12,000 g for 30 min, 4°C. The supernatant was collected and determined concentrations by the dye binding method (Bradford, 1976). Twenty-five microliters of proteins were heated at 100°C for 5 min and immediately cooled on ice. Proteins were size-fractionated on a 15% SDS-PAGE (Laemmli, 1970).

Proteins separated with SDS-PAGE were transferred onto a PVDF membrane (Hybond P; GE Healthcare) (Towbin, 1979) in 25 mM Tris, 192 mM glycine (pH 8.3) buffer containing 10% methanol at a constant current of 350 mA for 1 hour. The membrane was treated in the DIG blocking solution (Roche) for 1 hour and incubated with the primary antibody (1:100 in the blocking solution) for 1 hour at room temperature. The membrane was washed 3 times with 1X Tris-buffer saline tween-20 (TBST; 50 mM Tris-HCl, 0.15 M NaCl, pH 7.5, 0.1% Tween-20) and incubated with goat anti rabbit IgG (H+L) conjugated with alkaline phosphatase (Bio-Rad Laboratories) at 1:3000 for 60 minutes and then washed 3 times with 1X TBST. Visualization of immunoreactional signals was carried out by incubating the membrane in NBT/BCIP (Roche) as a substrate. The color reaction was stopped by transferring the membrane into water.

CHAPTER III

RESULTS

3.1 Examination of expression patterns of genes functionally related to ovarian development of *P. monodon* by RT-PCR

3.1.1 Total RNA extraction

Total RNA from ovaries and ovaries, hemocytes, gills, heart, lymphoid organs, hepatopancreas, stomach, thoracic ganglion, eyestalks and pleopods and testes of a male broodstock of *P. monodon* were extracted. The quality and quantity of total RNA were determined by spectrophotometry and integrity of the total RNA was observed by agarose gel electrophoresis agarose gel electrophoresis (Figure 3.1; A). The ratio of OD260/ OD280 of the extracted RNA was 1.8 – 2.0 indicating that its quality was acceptable for further applications. Results from the agarose gel electrophoresis showed discrete ribosomal RNA bands reflecting good quality of total RNA. The first strand cDNA was successfully synthesized as illustrated on the 1.2% agarose gel (Figure 3.1; B).

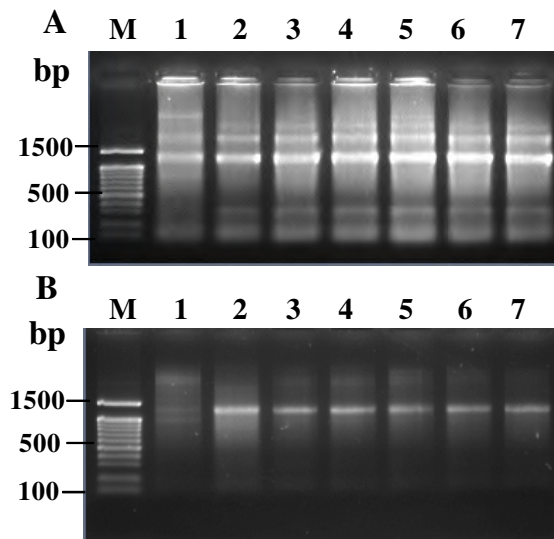


Figure 3.1 A 1.0% ethidium bromide-stained agarose gel showing the quality of total RNA extracted from ovaries of *P. monodon* broodstock (A) and the synthesized first strand cDNA (B). Lane M, 100 DNA ladder; Lanes 1 - 7, total RNA individually extracted from ovaries of *P. monodon* broodstocks.

3.1.2 RT-PCR analysis of genes functionally related to ovarian development

Expression of 17 genes from ovarian cDNA libraries of normal shrimp were examined by RT-PCR. Several genes were differentially expressed during ovarian development of wild normal broodstock of *P. monodon* including *Large tumor suppressor gene 1(LATS1)*, *interleukin (ILPK)*, *CDC like kinase2(Clk2)*, *MAP3K interacting protein (MAP3K)*, *MEK*, *Moleskin Importin-7 (MSK)*, *inositol 1,4,5-trisphosphate kinase (IP3K)*, *Like protein kinase from (Polo)*, *kinase suppressor of ras (KSR)*, *Evh1 domain* were correlated (up- or down-regulated following ovarian developmental stages) with stages of ovarian development. PCR was carried out for 25 cycles and *EF 1- α* (500 bp) was used as the positive control. Lanes M and N are a 100 bp DNA marker and the negative control (without the cDNA template), respectively (Figures 3.2).

PCR results could be categorized as 3 groups: 1) up-regulated transcripts during ovarian maturation 2) no change in gene expression level and 3) down-regulated transcripts. These genes were further analyzed in 11 tissues of a female broodstocks.

3.2 Tissue distribution analysis of functionally important genes

Tissue distribution analysis of these genes across 11 tissues including hemocytes, gills, heart, lymphoid organs, hepatopancreas, stomach, thoracic ganglion, eyestalks and pleopods, ovaries of a female and testes of a male broodstock was also carried out. These transcripts were not tissue-specific but differentially or comparably expressed in examined tissues. Results further confirmed more abundant expression of all genes in ovaries than testes of *P. monodon* broodstocks (Figure 3.3).

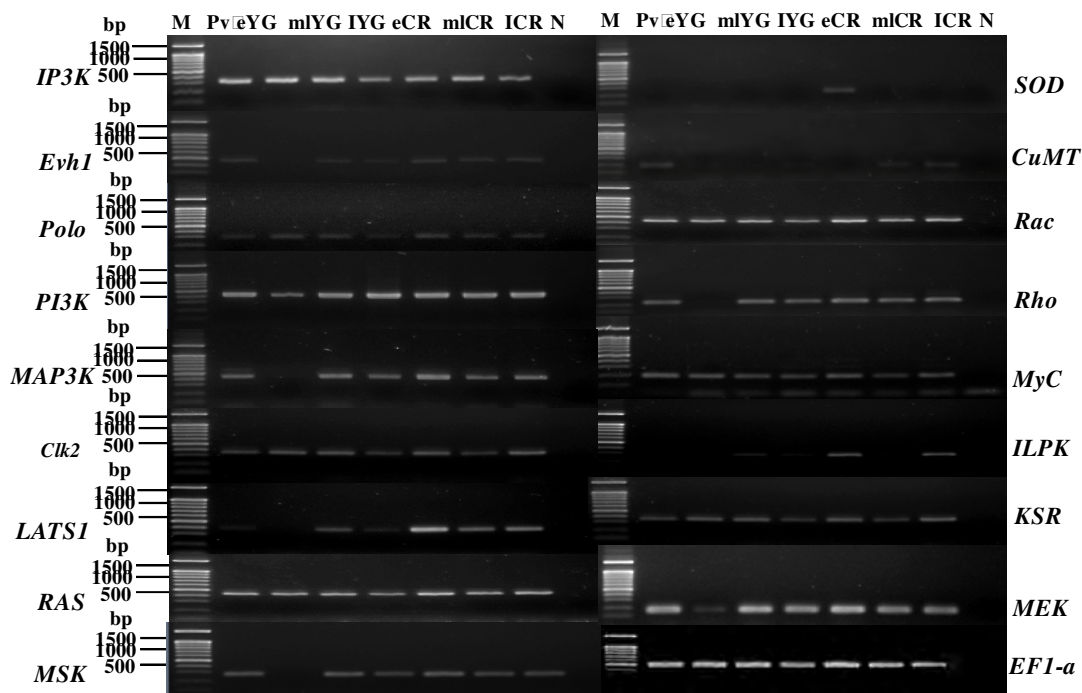


Figure 3.2 RT-PCR of *Large tumor suppressor gene 1(LATS1)*, *Rho*, *Rac1*, *Myc* (*cMyc*), *interleukin (ILPK)*, *CDC like kinase2(Clk2)*, *MAP3K interacting protein (MAP3K)*, *MEK*, *Moleskin Importin-7 (MSK)*, *inositol 1,4,5-trisphosphate kinase (IP3K)*, *Phosphatidylinositol-3-kinase(PI3K)*, *Like protein kinase form (Polo)*, *Copper-specific metallothionein (CuMT)*, *Mn/Fe-dependent superoxide dismutase(SOD)*, *kinase suppressor of ras (KSR)*, *Evh1 domain* using the first strand cDNA template of *P. monodon* having different GSI values. These transcripts were differentially expressed during ovarian development of *P. monodon*. Lanes 3 - 14 are the first strand cDNA template from pre-vitellogenic (Pv), early vitellogenic (eYG), middle vitellogenic (mLYG), late vitellogenic (IYG), early cortical rod (eCR), middle cortical rod (mlCR) and late cortical rod (ICR) ovaries. PCR was carried out for 25 cycles and *EF 1- α* (500 bp) was used as the positive control. Lanes M and N are a 100 bp DNA marker and the negative control (without the cDNA template), respectively.

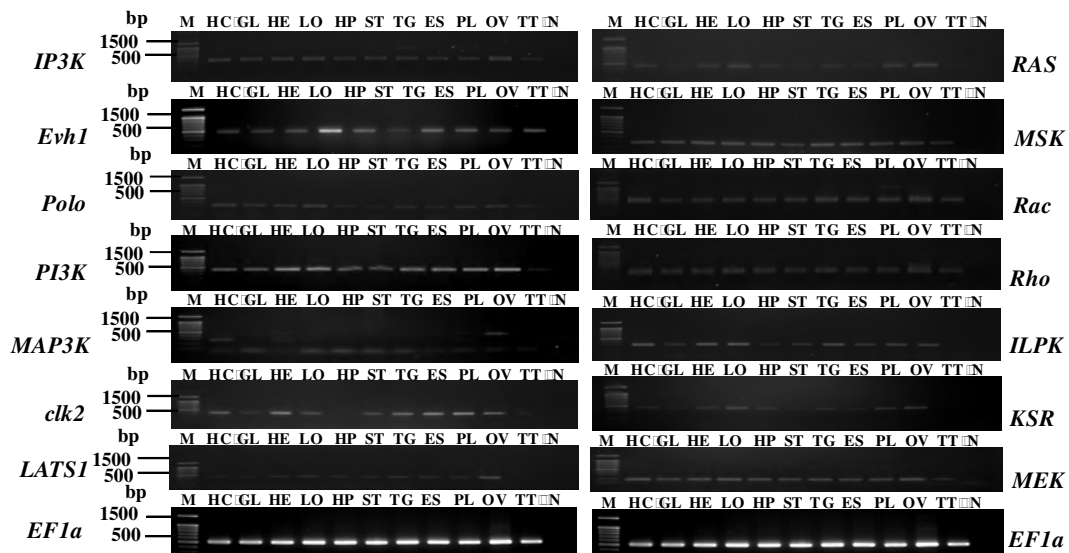


Figure 3.3 Tissue distribution analysis of *Large tumor suppressor gene 1(LATS1)*, *Rho*, *Rac1*, *interleukin (ILPK)*, *CDC like kinase2(Clk2)*, *MAP3K interacting protein (MAP3K)*, *MEK*, *Moleski,Importin-7 (MSK)*, *inositol 1,4,5-trisphosphate kinase (IP3K)*, *Phosphatidylinositol-3-kinase(PI3K)*, *Like protein kinase from (Polo)*, *kinase suppressor of ras (KSR)*, *Evh1 domain* using the cDNA template from hemocytes (HC), gills (GL), heart (HE), lymphoid organs (LO), hepatopancreas (HP), stomach (ST), thoracic ganglion (TG), eyestalks (E) and pleopods (PL), ovaries (O) of a female and testes (TT) of a male broodstock of wild *P. monodon*. *EF-1 α* was included as the positive control (H).

3.3 RT-PCR of functionally important genes in gonads of *P. monodon*

Expression of *Clk2*, *inositol IP3K*, *ILPK*, *Polo*, *PI3K*, *Rho* and *RAC1* were examined by a typical RT-PCR using the template from ovaries (female) and testes (male) of juveniles and broodstock of *P. monodon* ($N = 5$ for each group).

PI3K, *Clk2* and *IP3K* transcripts were more abundantly expressed in ovaries than testes of *P. monodon* broodstock suggesting that these genes should play the important role during oogenesis rather than the germ cell development (Figure 3.4). *ILPK* was more preferentially expressed in testes of juveniles compared to other groups of samples whereas *Rho*, *Rac1* and *Polo* were comparably expressed between ovaries and testes disregarding the developmental stages.

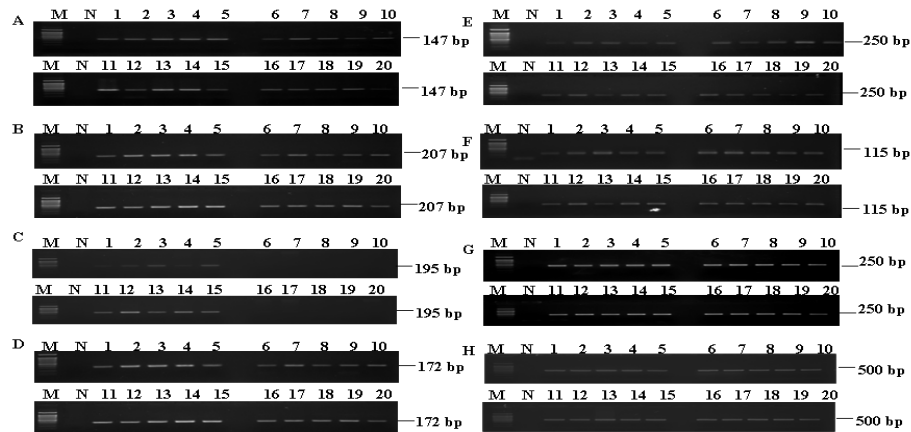


Figure 3.4 RT-PCR of *Clk2* (A), *IP3K* (B), *PI3K* (C), *ILPK* (D), *Polo* (E), *Rho* (F) and *RAC1* (G) using the first strand cDNA of ovaries of juveniles (lanes 1–5) and wild broodstock (lanes 11–15) and testes of juveniles (lanes 6–10) and wild broodstock (lanes 16–20) of *P. monodon*. *EF-1 α* was successfully amplified from the same template (H)

3.4 Isolation and characterization of the full length cDNA of genes expressed in ovaries of *P. monodon*

Several transcripts expressed in ovary of *P. monodon* were further characterized by RACE-PCR. From RT-PCR results and also literatures, four genes were screened as potential genes involving oocyte maturation. The full length cDNAs of four genes: *MEK*, *LATS1* and *KSR* were isolated and analyzed to determine the involvement during ovarian formation.

3.4.1 Characterization of full length cDNA of *MEK*

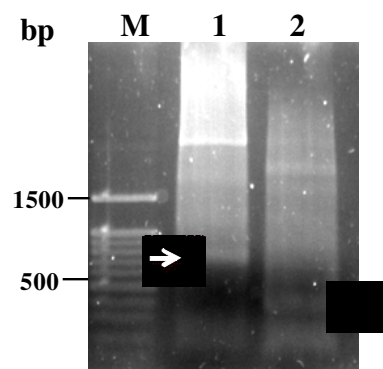


Figure 3.5 3' and 5'RACE-PCR products (lanes 1 and 2) of *MEK*. Arrowheads indicate RACE-PCR products that were cloned and sequenced. Lanes M and m are a 100 bp DNA ladder and λ -*Hind* III, respectively.

The full length cDNA of *P. monodon* MEK (*PmMEK*) was 1559 bp in length with an ORF of 1227 bp corresponding to a deduced protein of 408 amino acid and the 5' and 3' UTRs of 138 and 194 bp, respectively (Figure 3.7 and 3.8). It exhibited a high homology to *MAP kinase-ERK kinase* of *Bombyx mori* (E-value = 3×10^{-159}).

The predicted molecular mass and *pI* of the deduced *PmMEK* protein was 45.27 kDa and 6.13, respectively. *PmMEK* contained Serine/Threonine protein kinases (S_TKc) located at figure 3.6 and 3.7. For MAPK1 docking motif and Glycosylation sites were shadow (figure 3.8). The docking interaction in the MAP kinase cascades is achieved through specific conserved regions on docking motif is usually

A.

```
AGAACGCGGCTCCTTGCGTCAATCTAGATAAAAGTGTATCCCCTTCGAGTTCGCCGAAATCGCCGGAATCG
GAGCGAGCAGGAGCTGTTAGTCTGTTGATCATAATCAATATCTGACGTCTACCCCTCTCACAGCTGAAC
ATGTTGAATAAGAATAAGTTCAACCTGAAGCTGCCGCCGGCTCCATCGAACAGAACAATGACAATGAC
AACACACGGGAACAGACACTCCTCAGAGGAAAGCCAGCACTGGGGCTACAGGTAGCTTTGGGAACATG
TCCTTAGAATCTCTTCTAAAGTGCATACAAGAGCTGGACATGGATGACACACAACGCAGACGGATGGAA
ATATTCCTCGTCCAGAAACAGCAGATTGGTGAAGTGAATGCAGATGACTTTGAGAAACTC
```

B.

```
GGGGAGCTTGGAGCCGGAAATGGAGGCGTAGTCAACAAAGAAAAGCACAAACCCACAGGACTGTCAATG
GCTCGTAAGCTTATACATTTAGAAGTGAAGCCAGCAGTTAGAAACCAGATAATTCGTGAATTGAAAGTA
CTTCATGAGTGTAACCTCTCCATTTATTGTTGGATTCTATGAAGCTTTTACAGTGAAGGTGAAATTTCA
ATTTGTATGGAGTATATGGATGGTGGGTCACTTGATCTTTGCTTGAAGAAAGCTATACGCATCCCAGAG
CCAATCTTAGGGAAAATATGTTCAACAGTCCCTTAAGGGTTTAGCATATCTTCGAGAAAAACACCAGATA
ATCCATAGAGACGTAAGCCTTCCAATATTTTG
```

C.

```
GTCAATTCTCGTGGGGAGATTAAGATTTGTGACTCCGGTGTGTCAGGACAACCTTATTGATAGTATGGCC
AACACCTTTGTGGAACTAGAAGCTATATGTCGCCAGAACGATTAACCGGTGACCACTACTCTGTTGCC
AGCGATATATGGAGTTTAGGGTTGTCTCTTGTAGAAATGGCTATTGGAATGTATCCCATCCACCACCA
GACCCTGCCACTCTACAGAAAATCTTTGGACAGAAAGGTCGAGGGAGTGAGTCCGTCGCCAACGTCAAGG
TCACCAAGGTCGGCTGGACTACCAGGAGAACCACGACCAATGGCAATATTTGAGCTGCTGGACTACATT
GTGAACGAACCGCTCCGCGCCTGCCACCTGGGGTATTTTTTCCAGAATTCGTAGACTTGGTTGATCGA
TGCCTTAAAAAGAGCCCCAATGAGAGAGCAGATCTAACCCTTTGCAGAATCATGAATGGATAAAAACGT
GCAGAAAGAGAAAATGTTGATATAGCTGGTTGGGTGTGCAAGACAATGGACATCACACCTTTTACTCCG
ACTAAGCCATCAGCTGAGGGCAATAGTTAAAAAAGTTATGAAGAGTGCTACACATATTTTGTGGCTGGA
GGAGCACCAGAACGACCTTAAACCCCTTTTACTCTATGTGATGTATAAATCATAATTTAATCGTTCCAAA
TGGATAATAGTGTGTTTATTGTATGTCCAGATTAATGTGCAACTAGTCCCGGTGATTAATAAAAAAAAAA
AAAAAAAAAAAAAAAAAAAA
```

Figure 3.6 Nucleotide sequences of EST (A), 5' RACE-PCR and 3' RACE-PCR (B) of *MEK* of *P. monodon*. A primer for 5' RACE-PCR and 3' RACE-PCR (underlined) was used as the forward primer for RT-PCR analysis of this gene.

```

AGAACGCGGCTCCTTGGCTCAATCTAGATAAAAGTGTATCCCCTTCGAGTTCCCGAAATCG 60
CCGGAATCGGAGCGAGCAGGAGCTGTTAGTCTGTTGATCATAATCAATATCTGACGTCTA 120
CCCCTCTCACAGCTGAACATGTTGAATAAGAATAAGTTCAACCTGAAGCTGCCGCCCGGC 180
      M L N K N K F N L K L P P G 14
TCCATCGAACAGAACAAATGACAATGACAACCACACGGGAACAGACACTCCTCAGAGGAAA 240
S I E Q N N D N D N H T G T D T P Q R K 34
GCCAGCACTGGGGCTACAGGTAGCTTTGGGAACATGTCCTTAGAATCTCTTCTAAAGTGC 300
A S T G A T G S F G N M S L E S L L K C 54
ATACAAGAGCTGGACATGGATGACACACAACGCAGACGGATGGAAAATATTCCTCGTCCAG 360
I Q E L D M D D T Q R R R M E I F L V Q 74
AAACAGCAGATTTGGTGAAGTGAATGCAGATGACTTTGAGAACTCGGGGAGCTTGGAGGC 420
K Q Q I G E L N A D D F E K L G E L G A 94
GGAAATGGAGGCGTAGTCAACAAAAGAAAAGCACAAACCCACAGGACTGTCAATGGCTCGT 480
G N G G V V N K E K H K P T G L S M A R 114
AAGCTTATACATTTAGAAAGTGAAGCCAGCAGTTAGAAAACCAGATAATTCGTGAATTGAAA 540
K L I H L E V K P A V R N Q I I R E L K 134
GTACTTCATGAGTGTAACCTCCATTTATTGTTGGATTCTATGAAGCTTTTTACAGTGAA 600
V L H E C N S P F I V G F Y E A F Y S E 154
GGTGAATTTCAATTTGTATGGAGTATATGGATGGTGGGTCACTTGATCTTTGCTTGAAG 660
G E I S I C M E Y M D G G S L D L C L K 174
AAAGCTATACGCATCCCAGAGCCAATCTTAGGGAAAATATGTTCAACAGTCCTTAAGGGT 720
K A I R I P E P I L G K I C S T V L K G 194
TTAGCATATCTTCGAGAAAAACACCAGATAATCCATAGAGACGTAAAGCCTTCCAATATT 780
L A Y L R E K H Q I I H R D V K P S N I 214
TTGGTCAATTCTCGTGGGGAGATTAAGATTTGTGACTCCGGTGTGTCAGGACAACCTTATT 840
L V N S R G E I K I C D S G V S G Q L I 234
GATAGTTGGCCAACACCTTTGTGGGAAGTAAAGCTATATGTCGCCAGAACGATTAAC 900
D S M A N T F V G T A R S Y M S P E R L N 254
GGTGACCACTACTCTGTTGCCAGCGATATATGGAGTTTAGGGTTGTCTCTTGTAGAAATG 960
G D H Y S V A S D I W S L G L S L V E M 274
GCTATTGGAATGTATCCCATCCCACCACCAGACCCTGCCACTCTACAGAAAATCTTTGGA 1020
A I G M Y P I P P P D P A T L Q K I F G 294
CAGAAGGTCGAGGGAGTGAGTCCGTCGCCAACGTCAAGGTCACCAAGGTCGGCTGGACTA 1080
Q K V E G V S P S P T S R S P R S A G L 314
CCAGGAGAACCACGACCAATGGCAATATTTGAGCTGCTGGACTACATTGTGAACGAACCG 1140
P G E P R P M A I F E L L D Y I V N E P 334
CCTCCGCGCCTGCCACCTGGGGTATTTTTCCAGAATTCGTAGACTTGGTTGATCGATGC 1200
P P R L P P G V F F P E F V D L V D R C 354
CTTAAAAAGAGCCCCAATGAGAGAGCAGATCTAACCACTTTGCAGAATCATGAATGGATA 1260
L K K S P N E R A D L T T L Q N H E W I 374
AAACGTGCAGAAAGAGAAAATGTTGATATAGCTGGTTGGGTGTGCAAGACAATGGACATC 1320
K R A E R E N V D I A G W V C K T M D I 394
ACACCTTTTACTCCGACTAAGCCATCAGCTGAGGGCAATAGTTAAAAAAGTTATGAAGAGT 1380
T P F T P T K P S A E G N S * 414
GCTACACATATTTTGTGGCTGGAGGAGCACCAAGACCTTAAACCCTTTTACTCTAT 1440
GTGATGTATAAATCATAATTTAATCGTTCCAAATGGATAATAGTGTGTTTATTGTATGT 1500
CCAGATTAATGTGCAACTAGTCCCAGGTGATTAAAAAAAAAAAAAAAAAAAAAAAAAAAA 1559

```

Figure 3.7 The full length cDNA and deduced amino acid sequences of *MEK* of *P. monodon* (1559 bp in length with an ORF of 1227 bp corresponding to a deduced polypeptide of 408 aa). The putative start (ATG) and stop (TGA) codons are underlined. The poly A tail is illustrated in boldface. The predicted Serine/Threonine protein kinases (S_TKc; 2.53e-75, positions 86th-374th) domains are highlighted.

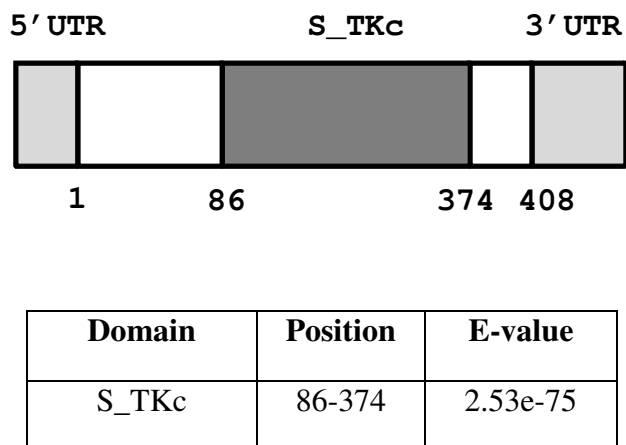


Figure 3.8 Diagram illustrating the deduced *MEK* protein sequence of *P. monodon*. The predicted S_TKc domains were found in this deduced protein.

3.4.2 Characterization of full length cDNA of *Large tumor suppressor gene 1 (LATS1)*.

The partial cDNA sequences of *P. monodon LATS1 (PmLATS1)* was 2508 bp in length which was deduced to 472 amino acids. This sequence significantly similar to *serine/threonine-protein kinase (LATS1)* of *Pediculus humanus corporis*, putative (E -value =0.00) analyzed by BLAST. The putative stop (TGA) codons were included underlined and the 3' UTRs of 194 b (Figure 3.12).

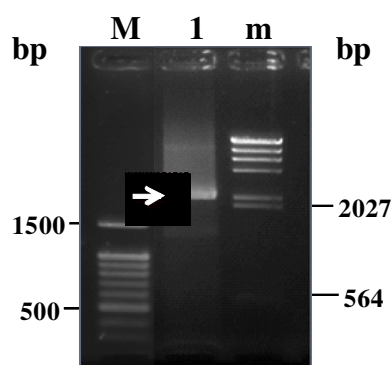


Figure 3.9 5' and 3'RACE-PCR products (lanes 1) of *LATS1*. The arrow indicates the specific RACE-PCR product that were cloned and sequenced. Lanes M and m are a 100 bp DNA ladder and λ -*Hind* III, respectively.

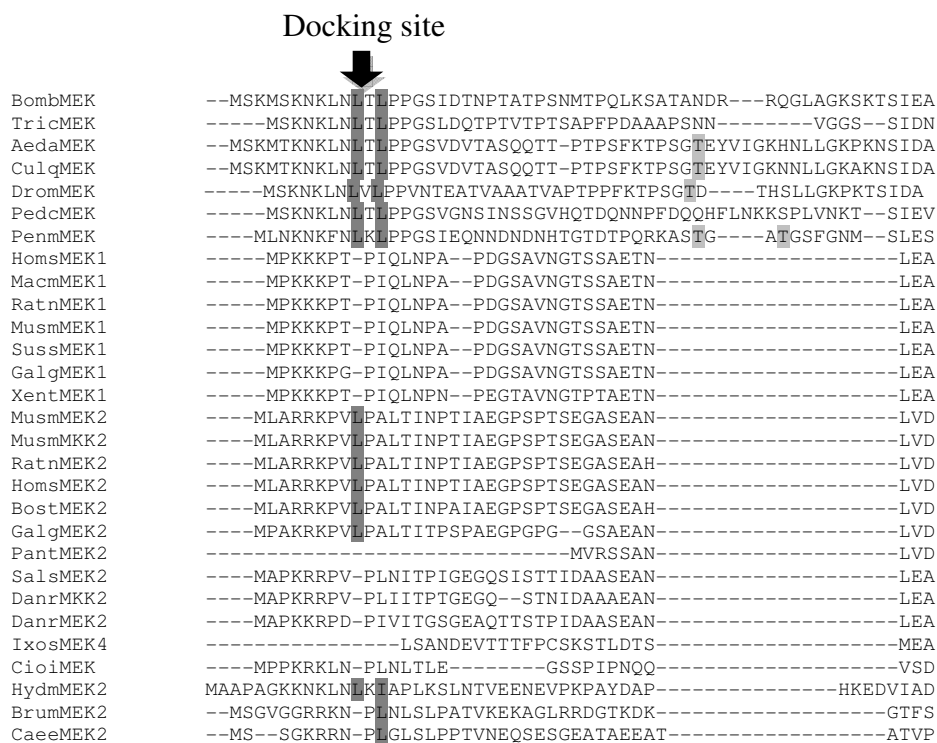


Figure 3.10 Partial multiple alignments of the deduced amino acid sequence of PmMEK, MEK1, MEK2 protein of various species. The analysis included PmMEK sequence of *Bombyx mori* (NP_001036922), *Tribolium castaneum* (XP_001966804), *Aedes aegypti* (XP_001662837), *Culex quinquefasciatus* (XP_001866069), *Drosophila melanogaster* (AAN17594.1), *Pediculus humanus corporis* (XP_002428982), *Homo sapiens* (NP_002746.2), *Macaca mulatta* (XP_001110225.1), *Sus scrofa* (NP_001137188.1), *Gallus gailus* (NP_001005830.1), *Gallus gailus* (NP_001005830.1), *Xenopus (Silurana) tropicalis* (NP_0010080581), Asterisks, colons, and dots indicate residues identical in all sequence, conserved substitutions, and semiconserved substitutions, respectively i.e KN for some of Arthropods, KK in MEK1 chordates, RR in MEK2 Chordates, KR in lower Chordates (frog and fish) where the position of these residues were not similar in BrumMEK2 and *C. elegans* MEK2. Arrows indicated CD domain or docking site for interacting with its substrates (MAPK) at carboxyl terminal of amino acid sequences. Consensus sequence of MAPK docking site (R/K)xxxx#x#, where # is a hydrophobic residue. R/K residues were marked with a frame and hydrophobic residues were indicated in bold.

A.

CGCGGGTCAAAAAGTTCGAAATTTATCTCCTCAGGCCCTTTAAACTTTACATGGAACAGCACATTGAAAAT
 GTGATAAAATCTTGTGAAGAAAAGAGAAAACAGAAAGATGCAGCTTGAGCAAAGAAATGAAAAAATTTGG
 ACTGTCAGACAAGGATCAATCCCAAATGCGTAAAATGCTTTTCTCAAAGGAATCAAACCTCATAAGCXG
 TTAAAGAGAGCAAAAATGGACAAAACAACCTTTCCGCAAAAATAAAAACCATAGGTGTTGGTGCATTTGGT
 GAGGTTGCCCTTGTCTGCAAGCTTGATACACACCGGCTGTATGCAATGAAGACCTTGCGCAAAGCTGAT
 GTCTTGAAGAGGAATCAAGTGGCTCATGTGAAAGCAGAGAGAGACATTTTAGCAGAAGCTGACAACGAG
 TGGGTTGTCAAACCTCTATTATTCATTTCAAGATAAAGACAACCTTTACTTTGTTATGGACTACATCCCT
 GGTGGTGAATTAATGTCTCTGCTCATCAAATTTGGAATATTTAAAGAGCAGTTGGCAAGATTCTACATT
 GGGGAACCTGGTTTGT

3' RACE-PCR**B.**

GCAATTGAGAGCGTGCACAAGATGGGTTTTATTACCGTGATATCAAGCCAGATAACATTCTTATTGAT
 CGCGATGGCCACATTAACCTCACTGATCTTGGTCTGTGCACTGGCTTTAGGTGGACACACAATTCCAAA
 TATTATCAGCGAGTTGGTGACCACAACAGACAAGATTCATAGACCCGCTGTGGTGACAACGATATTGTG
 TGCCGATGCAATGACCTGAAGCCCTTGGAGAGAAGACGCAGAAAGACAGCACCTTCGCTGTCTAGCCCAT
 TCACTCGTAGGAACCCCAAATTACATAGCTCCAGAGGTGCTATCCCGTACAGGTTACACACAGCTCTGC
 GATTGGTGGAGTGTGCGGAGTAATTCGTACGAGATGTTAGTAGGGCAGCCACCATTCTTGCCAGTACC
 CCGCCAGAAAACACAGTATAAGGTCATAAACTGGGAGGCAACCCTGAGAATCCCCAAACAAGCCAAATTG
 TCACCAGAAGCCAAGGACTTGATCCTGAGCCTGTGCACCCACCCTGAACAAAGACTAGGACGCAATGGT
 GCTCAGGAGGTAAAGGCGCATCCCTTCTTCAAGGAGCTGGACTTCGAAGGCGGCCCTGAGAAAAGCAGCAA
 GCACTCTACACTCCCACTATAAAAACACCCACAGACACCTCGAATTTTCGATCCCATCGATCCAGACAAG
 CTCCGACCAAGCGAAACCCCAATGAGAGTGACCTGGAGTGGGTCAACAATAGCAATCAACCACTACATGCA
 TTCTTCGAGTTTACCTTCAGAAGATTTTTTTGACAGTACTCCCGGAGGATCTGGTAACGATGAGAAGGAC
 AGTCAACATCCAGTCTATGTATGAATTGGGTCCAATGTGGCAGCTCTAGATGTGATGAAATCAGGAAATA
 TGATATATTTTTAGATATCTACTTTTATAAATTGAGAAAAAATATTTTAAACATGTCAGGGATCTAAATT
 ACTGATCACATGAATAATATGGTAGTGGCAGACTGTGGTAGCAGCCACTGTCACATTAGGTTGAGTTGC
 CCTATGAAGGGAATTCTTGCTAGACAGAAGTGAACAGTGACTTACCTCAGCCTACCACCAAATTGAAC
 ATATTTAGGTACAGGTGGCAGAAAAGGAGTAGCAATCTCGTGTGTTAAGCCCAGTGATGGGAAAGGCAA
 GCTGTGATTTTGTATATTTTTGAGTGTAGATATGGTGATATAGTTGAAAAGCAGGGTATGTATGATAT
 GGGACTCCATGAACCAAAGAGACACAAATAACAGATTGAATTTTCAGCTAATAGGGACACATTCCCAATA
 TCTTCCAGAAATGCTTTTAATTAATAGTGAGTAATTTGGTGCCTTCTGTAGTGTTTTATTGCTTAATAT
 ATTGGTAAATCATATGATGCTTATATCAGGGTGGAAAGTCACCCATTCTTCTTCTTATTGTGAACAA
 TATGAAGCAAAGAGTTTGGATGTGCCTATTGTTTCTTTGTCAAGGTATTGCTCTCACTTGTCTTGATTA
 CTACAAGACCAAAGTCAAAAAGTCCCAATTAGCAAAATGTTAATTTGTTTTATAATGTAATACACTTTT
 ACAGTGAAATGTGAAATACTCGTATGTTTGTGCATAGACAACCTGTAAATATATTTTTTTATTGTATGATA
 AGGTCTTGAGTGGATGAACTTTGTTTTTCATCTAAACAGAATGAGCGTGAGGGCCCTTGGAATATGTGCG
 AATTAAGGAATCCCTTTTCTCCCTATAGCAACCTTGTGTCTTCCCATCTGGGATAGGGTCTTTCCTCAA
 GTGTCTTCGAGTATCTAATGGTAGTTCTTCTACCAGTATATTTGTAAATTGTGTATAGCCTGATCTTAT
 ATGCTGTAAATGGCTGTATTGTTTTATGTAATAATTGCAGAGAAAACGAAAAAAAAAAAAAAAAAAAAA
 AAAAAAAAAA

Figure 3.11 Nucleotide sequences of EST (A) and 3' RACE-PCR (B) of *LATS1* of *P. monodon*. A primer for 3'RACE-PCR (underlined) was used as the forward primer for RT-PCR analysis of this gene.the poly adenylation site was italic.

```

CGCGGGTCAAAGTTCGAAATTTATCTCCTCAGGCCTTTAAACTTTACATGGAAACAGCAC 60
R G S K V R N L S P Q A F K L Y M E Q H 20
ATTGAAAATGTGATAAAATCTTGTGAAGAAAGAGAAAACAGAAAGATGCAGCTTGAGCAA 120
I E N V I K S C E E R E N R R M Q L E Q 40
AGAAATGAAAAAATGGACTGTCAGACAAGGATCAATCCCAAATGCGTAAAATGCTTTC 180
R N E K N W T V R Q G S I P N A * N A F 60
TCAAAAGGAATCAAATTCATAAGCXGTTAAAGAGAGCAAAAATGGACAAACAACCTTTC 240
S K G I K L H K X L K R A K M D K Q L F 80
CGCAAAAATAAAACCATAGGTGTTGGTGCATTTGGTGGAGTTGCCCTTGTCTGCAAGCTT 300
R K I K T I G V G A F G E V A L V C K L 100
GATACACACCGGCTGTATGCAATGAAGACCTTGCACAAAGCTGATGTCTTGAAGAGGAAT 360
D T H R L Y A M K T L R K A D V L K R N 120
CAAGTGGCTCATGTGAAGCAGAGAGAGACATTTTAGCAGAAGCTGACAACGAGTGGGTT 420
Q V A H V K A E R D I L A E A D N E W V 140
GTCAAACCTTATTTTCAATTTCAAGATAAAGACAACCTTTACTTTGTTATGGACTACATC 480
V K L Y Y S F Q D K D N L Y F V M D Y I 160
CCTGGTGGTACTTAATGTCTCTGCTCATCAAATTTGGAATATTTAAGGAGCAGTTGGCA 540
P G G D L M S L L I K F G I F K E Q L A 180
AGATTCTACATTTGGGAACCTGTTTGTGCAATTGAGAGCGTGCACAAGATGGGTTTTATT 600
R F Y I G E L V C A I E S V H K M G F I 200
CACCGTGATATCAAGCCAGATAACATTTCTTATTGATCGCGATGGCCACATTAACACTACT 660
H R D I K P D N I L I D R D G H I K L T 220
GATCTTGGTCTGTGCACTGGCTTTAGGTGGACACACAATCCAAAATATTATCAGCGGTT 720
D L G L C T G F R W T H N S K Y Y Q R V 240
GGTGACCACAACAGACAGATTCCATAGACCCGTGGTGGTACCAACGATATTTGTGTGCCGA 780
G D H N R Q D S I D P C G D N D I V C R 260
TGCAATGACCTGAAGCCCTTGGAGAGAAGACGCAGAAGACAGCACCTTCGCTGTCTAGCC 840
C N D L K P L E R R R R R R Q H L R C L A 280
CATTCACTCGTAGAACCCCAAATTACATAGCTCCAGAGGTGCTATCCCGTACAGGTTAC 900
H S L V G T P N Y I A P E V L S R T G Y 300
ACACAGCTCTCGGATTTGGTGGAGTGTGGAGTAATTCGTACGAGATGTTAGTAGGGCAG 960
T Q L C D W W S V G V I L Y E M L V G Q 320
CCACCATTCCCTTGCAGTACCCCGCCAGAAACACAGTATAAAGTCATAAACTGGGAGGCA 1020
P P F L A S T P P E T Q Y K V I N W E A 340
ACCCTGAGAAATCCCAAACAGCCAAATTTGTCACCAGAAGCCAAAGGACTTGATCCTGAGC 1080
T L R I P L K Q A K L S P E A K D L I L S 360
CTGTGACCCACCCTGAACAAAGACTAGGACGCAATGGTGTCTCAGGAGTAAAGCGCAT 1140
L C T H P E Q R L G R N G A Q E V K A H 380
CCCTTCTCAAGGAGCTGGACTTCGAAGGCGCCTGAGAAGCAGCAAGCACTCTACACT 1200
P F F K E L D F E G G L R K Q Q A L Y T 400
CCCCTATAAAACACCCACAGACACCTCGAATTCGATCCCATCGATCCAGACAAGCTC 1260
P T I K H P T D T S N F D P I D P D K L 420
CGACCAAGCGAACCCAATGAGAGTGACCTGGAGTGGTCAACAATAGCAATCAACACTA 1320
R P S E P N E S D L E W V N N S N Q P L 440
CATGCAATTCAGGTTTACCTTCAGAAGATTTTTGACAGTACTCCCGGAGGATCTGGT 1380
H A F F E F T F R R F F D S T P G G S G 460
AACGATGAGAAGGACGTCAACATCCAGTCTATGTATCAATTGGGTCCAATGTGGCAGCTC 1440
N D E K D S Q H P V Y V * 472
TAGATGTGATGAAATCAGGAAATATGATATATTTTTAGATATCTACTTTTATAATTGAGA 1500
AAAAAATATTTAACAATGTCAGGGATCTAAATTTACTGATCACATGAATAATATGGTAGTG 1560
GCAGACTGTGGTAGCAGCCACTGTCACATTAGGTTGAGTTGCCCTATGAAGGGAATTCCT 1620
GCTAGACAGAAGTGAACAGTGAATCCTCAGCCTACCACAAATTTGAACATATTTAGG 1680
TACAGGTGGCAGAAAGGAGTAGCAATTCGTGTTGTTAAGCCAGTGATGGGAAGGC 1740
GCTGTGATTTTGTATATTTTGTAGTGTAGATATGGTATATAGTTGAAAAGCAGGGTAT 1800
GTATGATATGGGACTCCATGAACCAAGAGACACAATAAACAGATTGAATTTACGCTAAT 1860
AGGGACACATCCCAATATCTCCAGAAATGCTTTTAAATTAATAGTGAGTAATTTGGTGC 1920
CTTCTGTAGTGTTTTATTGCTTAATATATTTGGTAAATCATATGATGCTTATATCAGGGTG 1980
GAAAGTCACCCCTTATTCTTCTTATTGTGAACAATATGAAGCAAGAGTTTGGATGTG 2040
CCTATTGTTTCTTTGTCAAGGTATTGCTCTCACTTGTCTTATTACTACAAGACCAAAAGT 2100
CACAAAGTCCCAATTAGCAAATGTTAATTTGTTTTATAATGTAATACACTTTTACAGTG 2160
AAATGTGAAATACCTGATGTTTGTGATAGACAACCTGAAATATATTTTTTATTGTATG 2220
ATAAGGTCTTGAGTGGATGAACTTGTTTTTTCATCTAAACAGAAATGAGCGTGAGGGCCCT 2280
TGGAATATGTGCAATTAAGGAATCCCTTTTCCCTATAGCAACCTTGTGTCTTCCCATC 2340
TGGGATAGGGTCTTCTCAAGTGTCTTCGAGTATCTAATGGTAGTTCTTCTACCGATAT 2400
ATTTGTAATTTGTGATAGCCTGATCTTATATGCTGTAATGGCTGTATTGTTTTATGTA 2460
AATAATTGCAGAGAAAACGAAAAAAAAAAAAAAAAAAAAAAAAAAAAAAAAA 2510

```

Figure 3.12 Partial nucleotide and deduced amino sequences of *P. monodon* *LATS1* mRNA. The stop codon (TGA) is illustrated in boldfaced and underlined. The poly A tail is boldfaced. The predicted Serine/Threonine protein kinases (S_TKc; 1.08e-78, positions 89th-402th) and Extension to Ser/Thr type protein kinase (S_TK_X; 3.98e-02, positions 403th-469th) domains are highlighted.

3.4.3 Characterization of full length cDNA of *Kinase suppressor of ras (KSR)*

The partial cDNA sequence of *P. monodon KSR (PmKSR)* was 3309 bp in length deduced to 969 amino acids. This sequence significantly matched Kinase suppressor of Ras 2 of *Harpegnathos saltator*, putative (E -value =0.00). The putative stop (TGA) codons are underlined and the 3' UTRs of 194 bp (Figure 3.15). The putative *PmKSR* contained a Protein kinase C conserved region 1 and Serine/Threonine protein kinases (figure 3.15). The protein kinase C conserved region 1 (C1) in each protein sequence are shaded (Figure 3.16)

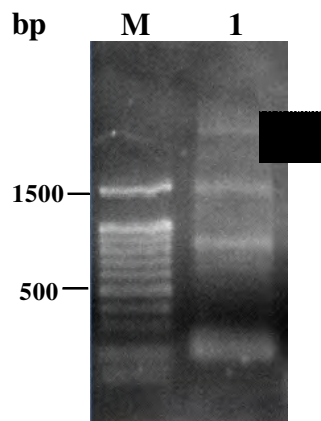


Figure 3.13 The 3'RACE-PCR product (lanes 1) of *KSR*. Arrowheads indicate RACE-PCR products that were cloned and sequenced. Lanes M ;100 bp DNA ladder.

A.

TATGATGGCGGCCAGTGC GCGGCGCTCCGCTCGGCGTTCTGTGTAAGGCAACGGCTCAGCGCGGAGAGGGCGGCGAC
 CAAGCATGAAGGGAACGCGCGGGTACGGCGCCTCGTCTTGTGTGCAGTGTCTATAGACAGATAGTAAGGGAGACC
ATGTCTGGGGCGGCGGAGGGAGGCTGGCGGCGGGAGGGCTCCACGGGGATGGCCACAACCAACCCCATCACC
 AGCAGCAGCAGGTGGGCGTGGGCGTGGACGTGGGCGTGCAGGAGGTGATAGCGGGGCGTGGAGACGTGTGAGAC
 CCACCACCAGTTTCATCGCTCGCAGGCAGAGCACCTGGAACGCTGAGGTGCAGTGTGCCACCAGCGCCAGCTC
 ACGCAGCAGGAGATCCGACGCTCGAGGGCAAGTTAGTGAAGCTGTTTACGCTACAACCTGTTAACAAGCGGCACT
 TACCCTCGGGTGTGCCCTTACCTCGTGTAGCTGCAGCTTTACCCTCGCTCAAGCAATGGTGTCAAGTGGTTGGACT

3' RACE-PCR

CTGCAAAGATTCTGTTATTGGTATGTGCCAGAGAGTCTCCACACTAGAAAGGATTACTTGAAAAA

B.

CTGCAAAGTGGTTGGACTCTGCAAAGATTCTGTTATTGGTATGTGCCAGAGAGTCTCCACACTAGAAAGGATTACTTG
 AAAAAAGAGAAAATGAATTACGCAACATCCTCAATGATTATGGAGCCGACAAAAGTGAAGCCATAAACTGGCAAG
 GGCCATGCACAATCTCAAACGATACACAGAGATACAAATGCAAGGTCAGGCAGGAGACCCAAACAACCTCAGACCTG
 CCTCTATACTGGGACTCTTGGGAGAAGTGCCTCCTTCTCCTCGAGCCTTACTCGAGCACAGAGATCCTCCACTC
 TTAACCTTCTGGGAGTATCACGGTCTTCTGTGAGAAGCGATATACTCTCCCAACTCTAGTATTATCCAAA
 GGGCAAGAGTTTCAAGTGACAAGAAATCCCAACAACACCTCCTCCTGGCAAGAAATACCAAACTGGCCTCTTAAAT
 CCCCTGCAGCCATCTTTAGGTCGTTCCACATCACATGAGTGCAGCTTGCGCCAAGGGCTGAGGGTCATGAACAGC
 AGTCTTCAGCGCTTCTCAGCTTGGAGCAACTTGTGACTCGAAGGACACGCCTTCACTCAGAGTCTGAGGCTCAGC
 AGACAACCTTGGCAAGAGGGTGGATGGGAGCCGGACCAGAACGGAGGTGCAGACCTAAAGACGCCTCAGAACTCT
 CCAGCACCTTCGACTCTTGGCAGCCCCATCAAGTCACCTCACTACCCAGATCCTGCCAAAGATGACAGTCAATAA
 TGAATCTACTCTTTCAGTACCAAAGTCTCCACGCACCCCTACTCTAGCTGGTTCAATGGGTCAATGTGCAGCA
 TCGCTTCATAAAGACGATCAAGTCTGCCACTTGTGGTTACTGTGCATCACAAAGTTTCTATTTAGGTGGTCTGAAG
 TGCAAGGAGTGCAGCTACAAATGTCATCGTGAATGTGAGCCAAAAGTGCACCTTCTGTGGATTGCCACAAGAGT
 TGCTCATATATTTGCTGATACTTGGAAAGGTTGGTATGGATGGAAGTGGTGGGCTGCACAGAGGAGGCACTCC
 TGGGGTCTCTCCTTCTCACCATCATCAAATGATGTCTTCTCCTCTACGGGTGGCCAGATGTCCAACCTCTCAG
 CCGTCCATTAGCATACCATCCTTCCAGGACCCCAATTCAGTTCGAACACATCCAGCTGCAACTCCTCAACCTCT
 CCAGCCCAGCCCTCATCATTTCTGCCTCCTCGAAGGCATGATGCATTCCATTTTCCAACCACTCGAGGATTCCA
 TTTCCAGAGGTTGAATGAGGACTGTGGGATATGCGGCTTATTTCCGCCGACCCCTACCAAGGCCCTATATCA
 GCTTCCCTCCCAAGTGAATGATGTGATAGACTCCAGACAGTCTCATGATTCTGACCGCACTGTGTACAAAACCTCAG
 GTGGCAGTACTGGCACTGATGATTCTGAGCGCACAAATAGCGGGTCTGTGATGATTGCAAGATTCCACAGTATCTGA
 TGGAGAAAATGCAGATCCGCGATGTACTCGTCAGAACAGTGTGAGTAGTGTGCCAGTCTCTCCGAGAATGGGAT
 ATTCCCTATGATGAACCTGATAGAGGAGAAGTCATTGGACGAGGAAGATTGGCATTGTATATTAGGAAATGGC
 ATGGACAAGTGGCTATAAAAAGAGTTGCGAATGGACTATGTTAATGATGAGAAAACCTCTTGAAGCATTAAAGCAGA
 GGTGAGCACTTTCCGCAAGACCCGACATGAGAATTTGGTCTGTTTTCATGGGTGCATGTATGAAGCCCCAAGACTA
 GCCATAGTGACAAGCCATGCAAGGGCATGACACTCTACAACACATTTCATGTACTGAAAGACAAATTCATATGT
 CACGCACCATCTTGATTGCTCAGCAAATTTACAGGGTATGGGCTACCTCCATGCAAGGGGCATCGTTACAAGGA
 CCTTAAGACCAAGAATATATTTCTGGAGAGTGGCAAGGTTGTGCATCACAGACTTTGGTCTCTCAATGTTACGAGA
 CTCTGTGCATGATAGCAGACGAGGCAACTGGTTAAGTATTCCTCCTGGTTGGTTGTGTTATCTCTCCCTGAGGTC
 TGAGGAACTTGCCTGTGATACAGAAACAGACGATGGCTTCCCTTCCACACGATTCAGATGTTTATTGTTTCGG
 TACTGTGTTGATGAATTATATGTGGTGAATGGCCCCATAAAGGCCTTCTCCAGAGGCCATAATATGGCAGGTT
 GGACGTGGAATGAAGCCTTCCCTAGCACATCTACAGGCTTACCGGATGTTAAGGACATACTCATGGCTGCTGGA
 GTTACCAGCCGGATGAAAGGCCAGAGTTCTCCACCATGTGAACAGCTCGACAAGGCTTCTTAAGAAGCGGCTCCA
 CCGCTCCCTTCCCATCTATCCACCTCTCACGTTTGGCAGAGAGCGTCTTGTAGACTTCGGTTTTCAAGTCGCAA
 GGACATGATGCAACTGTGGTTGAATTTGGAGAGTAAGTCCCTTGCCTCCAATATTCAGACTTTTTATTTTTCGGA
 GGGTTTTCTTATTTTCTTGTGTCTTACTTTGTTCCAATGAATTTTAAAGCAGCCAAAAGTGAATGCAGCAAGTG
 TGCCCAACACTGATTTGGGATGGATGGTGTAGGATAACCATTTTTCCAAATATGTTTGTCTTAGAGAACATGC
 AGATAGGAGGTAGAAGCACAACCTTTTGCAGTTTTTTTTACTAGTGGTGGGTGACAAAGTGTCACTTTTTGTTTT
 TGTTAGGAAATTAGATTTTGTGCTCAATTTGCTCTGCAATTTGCTGCTTACTACTTTGTTGTAAAATCTGTAT
 AATGAATCTTGAAGTAAGCCCCAAAAA

Figure 3.14. Nucleotide sequences from shrimp'sEST library (A) and 3' RACE-PCR (B) of *KSR* of *P. monodon*. A primer for 3'RACE-PCR (underlined) was used as the forward primer for RT-PCR analysis of this gene during ovarian development.

ATGTCCTGGGCGGCGGCGGAGGGAGGCTGGCGGCGGAGGGCTCCACGGGGATGGCCAC 60
 M S W G G G G G R L A A G G L H G D G H 20
 AACCAACCCATCACCAGCAGCAGCAGGTGGGCGTGGGCGTGGACGTGGGCGTGCAGGAG 120
 N Q P H H Q Q Q V G V G V D V G V Q E 40
 GTGATAGCGGCGGCTGGAGACGTGTGAGACCCACCACAGTTCATCGCCTCGCAGGCA 180
 V I A R A L E T C E T H H Q F I A S Q A 60
 GAGCACTGGAAAGCCTGAGGTGCGAGTGTGCCACCAGCGCCAGCTCACGCAGCAGGAG 240
 E H L E R L R S Q C A T S A Q L T Q Q E 80
 ATCCGCACGCTCGAGGGCAAGTTAGTGAAGCTGTTACGCCTACAACCTGGTAAACAAAGCGG 300
 I R T L E G K L V K L F S L Q L V T K R 100
 CACTTACCCTCGGGTGTGCCCTTACCTCGTGAGTGCAGCTTTACCCCTCGCTCAAGCAA 360
 H L P S G V P L P R E L Q L Y P S L K Q 120
 TGGCTGCAAGTGGTGGACTCTGCAAGATTCTGTTATTGGTATGTGCCAGAGAGTCTCC 420
 W L Q V V G L C K D S V I G M C Q R V S 140
 AACTAGAAAGATTACTTGAAGAAAGAGAAATGAATTACGCAACATCCTCAATGATTAT 480
 T L E G L L E K R E N E L R N I L N D Y 160
 GGAGCCGACAAAAGTGAAGCCATAAACTGGCAAGGGCCATGCACAACTCAAACGATAC 540
 G A D K S E A H K L A R A M H N L K R Y 180
 ACAGAGATACAAATGCAAGGTGACGAGGAGACCCAAACAACCTCAGACCTGCCTCTATAC 600
 T E I Q M Q G Q A G D P N N S D L P L Y 200
 TGGACTCTGGGAGAAGTCCCTCTCTCTCGAGCCTTACTCGAGCACAGAGATCC 660
 W D S W E N C P P S P R A S T R A Q R S 220
 TCCACTCTTAACCTTCCTGGGAGTATCACGGTCTTCTCTGAGAAGCGATATACTCCTCCC 720
 S T L N L P G S I T V F S E K R Y T P P 240
 CCAACTCTAGTATTATCCCAAAGGGCAAGAGTTGAGGTGACAAGAAATCCCAACAACA 780
 P T P S I I P K G K S S G D K K F P T T 260
 CCTCCTCGGCAAGAAATACCAAAGTGGCTCTTAAATCCCTCGAGCCATCTTTAGGT 840
 P P P G K K Y Q T G L L N P L Q P S L G 280
 CGTTCCACATCACATGAGTACAGCTTGCGCCAAGGGCTGAGGTCATGAACAGCAGTCT 890
 R S T S H E S Q L A P R A E G H E Q Q S 300
 TCAGCGCTTCTCAGCTTGGAGCAACTTGTGACTCGAAGGACACGCCTTCACTCAGAGTCT 960
 S A L S L S L E Q L V T R R R T R L H S E S 320
 GAGGCTCAGCAGCAACTTGGCAAGAGGTGGATGGAGCCGACCAAGAGGAGGTG 1020
 E A S A D N S G K R V D G S R T R T E V 340
 CGAGACCTAAAGACGATCAGAACTTCCAGCACCTTCACTCTTGGCCAGCCCATCAAG 1080
 R D L K T P Q N S P A P S T L A S P I K 360
 TCACCTCACTACCCAGATCTGCAAGATGACAGTCATATAATGAAATCTACTCTTTCA 1140
 S P H Y P D P A K D D S H I M K S T L S 380
 GTACCAAAGTCTCCAGCAGCCCTACTCTAGCTGGTTCATGGGTCAAAATGTGACGAT 1200
 V P K S P R T P T L A G S M G H N V Q H 400
 CGTCTCAAAAGACGATCAAGTCTGCCACTTGTGGTACTGTATCACAAGTTTCTATT 1260
 R F I K T I K S A T C G Y C H H K F S I 420
 TTAGTGGTCTGAAGTGAAGTGCAGCTACAATGTATCGTGAATGTGAGCCAAA 1320
 L G G L K K C K E C S Y K C H R E C E P K 440
 GTGCCACTTCCGTGGATTGCCACAAGAGTGTCTCATATTATTGCTGATCTGGAAAG 1380
 V P P S C G L P Q E L L I L F A D T W K 480
 AAGGTTGGTATGGATGGAAGTGGTGGGCTGCACAGAGGAGGCACTCCTGGGGTCTCTCCT 1440
 K V G M D G S G G L H R G G T P G V S P 500
 TCTCACCATCAAAATGATGCTTCTCTCTACGGGTGCGCCAGATGTCCAACCTCT 1500
 S H H H P N D V F S P L R V G Q M S N S 520
 CAGCCGTCCATTAGCATAACCTCTCCAGGACCCCAATCCAGTTCGAACACATCCAGC 1560
 Q P S I S I S F Q D P N S S S N T S S 540
 TGCAACTCCTCAACCTCTCCAGCCAGCCCTCATATTCTGCCTCTCCTGCAAGGCAT 1620
 C N S S T L S S P A L I I S A S P A R H 560
 GATGCATTCCATTTCACCAACTCGAGGATTCCATTCCAGAGGTGAATGAGGACTGT 1680
 D A F H F P T T R G F H F P E V N E D C 580
 GGGGATATCGGGTATTTCGCCCGACCCCTACCAAGGCCCTATATCAGCTTCTCC 1740
 G D M R L I S P R P P T K A P I S A S S 600
 ACCCAAAGTGTATGATAGACTCCAGACAGTCTCATGATTCTGACCGACTGTGTCACAA 1800
 T Q S D V I D S R Q S H D S D R T V S Q 620
 ACCTCAGGTGGCAGTACTGGCACTGATGATTCTGAGCGCACAAATAGCGGGTCTGTAGAT 1860
 T S G G S T G T D D S E R T I A G R V D 640
 TCCAAGATTCCACAGTATCTGATGGAGAAAATGCAGATCCCGGATGACTCGTCAGAAC 1920
 S Q D S T V S D G E N A D P R C T R Q N 660
 AGTGTAGTGTGTCCAGTCTCTCCGAGAATGGGATATCCCTATGATGAACCTGAT 1980
 S V S S V S Q S L R E W D I P Y D E L D 680
 AGAGGAGAAGTCATGGACGAGGAAGATTGGCATTGTATATTGAGAAAATGGCATGGA 2040
 R G E V I G R G R F G I V Y S G N W H G 700
 CAAGTGGCTATAAAGAGTGGCAATGGACTATGTTAATGATGAGAAAACCTTGAAGCA 2100
 Q V A I K E L R M D Y V N D E K T L E A 720
 TTTAAGCAGAGGTGAGCACTTCCGCAAGCCGACATGAGAATTTGGTCTGTTTCATG 2160
 F K A E V S T F R K T R H E N L V L F M 740
 GGTGCATGATGAAGCCCCAAGACTAGCCATAGTGACAAGCCTATGCAAGGGCATGACA 2220
 G A C M K P P R L A I V T S L C K G M T 760
 CTCTACAAACACATTGATGACTGAAAGACAAAATCAATATGTCACGCACCACTTGTATT 2280
 L Y K H I H V L K D K F N M S R T I L I 780
 GCTCAGCAAATTCACAGGTATGGGCTACCTCCATGCAAGGGCATCGTTCACAAGGAC 2340
 A Q Q I S Q G M G Y L H A R G I V H K D 800
 CTTAAGACCAAGAAATATTTCTGGAGAGTGGCAAGGTTGTATCAGAGACTTGGTCTC 2400
 L K T K N I F L E S G K V V I T D F G L 820
 TTCAATGTTACGAGACTCTGTCATGATAGCAGACGAGGCAACTGGTAAAGTATTCCTCCT 2460
 F N V T R L C H D S R R G N W L S I P P 840
 GGTGGTGTGTTATCTCTCCCTGAGGTGATGAGGAACTTGGTGTGATACAGAAACAA 2520
 G W L C Y L S P E V M R N L R V I Q K Q 860
 GACGATGGCTTCCCTTACCACGATTCAGATGTTATTGTTTCGGTACTGTGGTAT 2580
 D D G L P F T T Y S D V Y C F G T V W Y 880
 GAATTATTATGTTGATGGCCCAATAAGGCCCTCCTCCAGAGGCCATAATATGGCAG 2640
 E L L C G E W P H K G L P P E A I I W Q 900

```

GTGGACGTGGAATGAAGCCTTCCCTAGCACATCTACAGGCTTACGGGATGTTAAGGAC 2700
V G R G M K P S L A H L Q A S R D V K D 920
ATACTCATGGCTGCTGGAGTTACCGCCGGATGAAAGGCCAGAGTTCTCCACCATGTTG 2760
I L M A C W S Y R P D E R P E E F S T M L 940
AACAGCTCGACAAGCCTTAAAGAAGCGGCTCCACCGCTCCCCTTCCCATCCTATCCAC 2820
N S S T R L L K K R L H R S P S H P I H 960
CTCTCACGTTTGGCAGAGCGTCTTAGACTTCGGTTTTCAAGTCGCAAGGACATGAT 2880
L S R L A E S V L * 980
GCAACTGTGGTTGAATTTGGAGAGTAAGTCCCCTTGGCGCTCCAATATTCAGACTTTTATT 2940
TTTCGGAGGGTTTCTTATTTCTTTGTGTCTTACTTTGTCCAATGAATTTTAAAGCA 3000
GCCAAAAGTGAATGCAGCAAGTGTGCCCAACTGATTTGGGATTGGATGGTGTAGGAT 3060
AACCATTTTTCCAAATATGTTTGTCTTAGAGAACATGCAGATAGGAGGTAGAAGCACAA 3120
CCCTTTGCAGTTTTTTTACTAGTGGTGGGTGACAAAGTGTCACTTTTGTTTTTTGTTA 3180
GGAAATGAGATTTTGTGCTCAATTTTGTCTGCAATTTTGTCTGCTTACTACTTTGTTGT 3230
AAAATCTGTATAATGAATCTTGAAGTAAGCCCAAAAAAAAAAAAAAAAAAAAAAAAAAAA 3300
AAAAAAAA 3320

```

Figure 3.15 Partial nucleotide and deduced amino sequences of *KSR* of *P. monodon*.

The stop codon (TGA) is illustrated in boldfaced and underlined. The poly A tail is boldfaced. The predicted Protein kinase C conserved region 1 (C1; 1.08e-78, positions 89th-402th) and Serine/Threonine protein kinases (S_TKc; 1.08e-78, positions 89th-402th) domains are highlighted.

Kinase suppressor of Ras 2 [Harpegnathos saltator]
Length=899

Score = 752 bits (1941), Expect = 0.0
Identities = 489/942 (51%), Positives = 612/942 (64%), Gaps = 90/942 (9%)
Frame = +1

```

Query 124 IARALETCEHHQFIASQAEHLERLRSQCATSQQLTQQEIRTLEGKLVKLFSLQLVTKRH 303
I RAL+ ++ I A+ LE LR+QC+TSA+LTQQEIRTLEGKLVKLFSLQLVTK
Sbjct 12 IRRALDVVQS---MIDLSADRLEGLRQCSTSAELTQQEIRTLEGKLVKLVK 68

Query 304 LPSGVPLPRELQLYPSLKQWLQVVGKLDKDSVIGMCQRVSTLEGLLEKRENELRNILNDYG 483
L + LP +++ YPSL+QWLQVVG +S+ +C + ++LE L EK E+EL +IL +
Sbjct 69 LAAD-SLPAKMRQYPSLQWLQVVGKLPESIQIVCSKANSLEALKEKSEHELSSILGENN 127

Query 484 AD-KSEAHKLARAMHNLKRYTEIQMQGQAGDPNNSDLPLYWDSWENCPPSPRASTRAQRS 660
+ E +L RA+HNL+RY ++ ++G D N+D+ LYWDSW+ AS R RS
Sbjct 128 ERYEELRRLRYRALHNLRRYIDVLRG---DMENNDMNLWDSWDRHQLRTGASPRPIRS 184

Query 661 STL-----NLPGSI-----TVFSEKRYTPPPTPSIIPKKGSSGdkkfpt 777
T NL I +V S +PP TP + +G + K PT
Sbjct 185 RTTRCSVPLEDSIPYHNNNLSNDILAQASSVSSLMSTSPCTPLLSRQGC---EIKCPT 241

Query 778 tpppgkkyQTGLLNPL-QPS---LGRSTSHESQLAPRAE-GHeqqssallsleqlVTRRT 942
TPPP KK+Q G+ N + QP L +S SHESQLA R E G + S + RR
Sbjct 242 TPPPYYKHQIGVKNMSPQPEMFPLTKSKSHESQLAERLENGDAASNCGNNSHVGAIRRRN 301

Query 943 RLHSESEASADNSGKRVDGSRTRTEVRDLKTPQNSPAPSTLASPIKSPHYDPKDDSHI 1122
RL +E + + T V + P ++ SPIKSP Y DD+
Sbjct 302 RLPTEPGSCYN-----TPDFVGESLLPNSN-----SPIKSPYSSAESDDNSF 344

Query 1123 MKS--TLSVPKSPRTP-TLAGSMGHNVQHRFIKTIK-SATCGYCHHKFSILGGLKCKECS 1290
+ +L VPKSPRTP T+ MGH + HRF KT K TC YC + I GLKCKEC
Sbjct 345 KGTVTSLQVPKSPRTPVTVTRGMGHVIAHRFTKFKIKTTCDYCEKQMF IGSGLKCKECK 404

Query 1291 YKCHRECEPKVPPSCGLPQELLILFADTWKKVGMDSGGLHRGGTPGVSPSHHPNDVFS 1470
YKCHR+CE KPPPSCGLPQEL F T + GM + + PG++ +HH +++ +
Sbjct 405 YKCHRDCESKVPSCGLPQELFDEFKRTVQADGMINASPIL--SKPGITSPNHNSNLLA 462

Query 1471 PLRVGQMSNSQP--SISIPSFQDPnssntsscsnstlsspaliiaspARHDAFHFPPT 1644
L S P S++IP FQ +SSNTSSCNSST SSPAL+ + + A P
Sbjct 463 SLNRRDRKRSHPHSSMNIP-FQADSSNTSSCNSSTPSPALLPANTTQTPQA---PVK 518

Query 1645 RGFHFPEVNEDCGDMRLISPRPPTKAPISASSTQSDVIDSRQSHSDRIVSQtsggstgt 1824
+ FHFP+V +++ R T + + I S DS++T++ SG +
Sbjct 519 QGFHFDPV-----VLNERGVT---LETHKLEGTISS---DSEKTIN-VSGSGNV 562

```


Query	1825	ddsERTIAGRVDSDSTVSDGENADPRCTRQNSVSSVSQSLREWDIPYDELDRGEVIGRG	2004
Sbjct	563	DSERT RVDSQDS VSDGE D R RQNS+S +REWDIP+DEL GE IG+G	616
Query	2005	RFGIVYSGNWHGQVAIKELRMDY-VNDEKTLLEAFKAEVSTFRKTRHENLVLFMGACMKPP	2181
Sbjct	617	RFGIVY GNWHG VAIK L MDY ++D+KTLLEAFK EV+TFRKTRHENLVLFMGACMKPP	676
Query	2182	RLAIVTSLCKGMTLYKHIHVLKDKFNMSRTILIAQQISQGMGYLHARGIVHKDLKTKNIF	2361
Sbjct	677	RLAIVTS+ KGMTLY HIH+LKDKFNM++T IAQQISQGMGYLHARGIVHKDLK+KNIF	736
Query	2362	LESGKVITDFGLFNVTRLCHDSRRGNWLSIPPGWLCYLSPEVMRNLRVIQKQD-DGLPFF	2538
Sbjct	737	LE+GKVITDF LF+VT+LC+ +R+ + LSIP GWLCYL+PE++R LR Q +D + LPF	796
Query	2539	TTYSDVYCFGTVWYELLCGEWPHKGLPPEAIIWQVGRGMKPSLAHLQASRDVKDILMACW	2718
Sbjct	797	T SDVY FGTVWYELLCGEW KG PPEAIIWQVG+GMK +LA+LQASR+VKDILM CW	856
Query	2719	SYRPDERPEFSTMLNSSTRLLKRLHRSPSHPIHLSRLAESV	2844
Sbjct	857	SY + RP+F+ +L + +L +KRL RSPSHPIHLSR AESV	898
		SYHAENRPDFAKLLTTFEKLPRKRLARSPSHPIHLSRSAESV	

Figure 3.16 Results from BlastX indicating similarity between *P. monodon* KSR and that of *Harpegnathos saltator*.

	← C1 domain
HarsaKSR2	NSFKGTVTSLQVPKSPRTPVTVTRGMGHVIAHRETKTFKIKTT-CDYCEKQMF-IGSGLK
ApimeKSR1	NSFKGTVTSLQVPKSPRTP-TVTRGMGHVIAHRETKTFKMMT-CDYCDKQMF-IGTGLK
CamflKSR2	NCFKGTVTSLQVPKSPRTP-TMTRTMGHVIAHRETKTFNMATRCDYCEKPMWGWGTILK
TricaKSR	NSYK-SAPSLQVPKSPRTPPVGRSMHQINHRETKTFKMIAT-CGYCQKPIY-FGAGLK
PenmoKSR	HIMK---STLSVPKSPRTP-TLAGSMGHNVQHREIKTIK-SAT-CGYCHHKFS-ILGGLK
DromeKSR	TNASSGGSSSNVLMVPCSPGVGHVGMGHAIKHRFTKALG-FMATCTLCQKQVF--HRWMK
DrosiKSR	TNASSGGSSSNVLMVPCSPGVGHVGMGHAIKHRFTKALG-FMATCTLCQKQVF--HRWMK
AedaeKSR	HSVSIPPKS-----PCTPIITRV-MGHMIQHRETKKFVTKSTCDLONKQMF--FG-FK
IxoscKSR	PGVGQLPTSLPEPFAALQPDRLLEILSCHPVCRFTSSVK--VTTCCQCDKAMF---FGYK
MondoKSR1	-----HGSPQMVRRDIGLSVTHRES-TKSWLSQICHVCQKSM---FGVK
HomsaKSR1	-----HGSPQMVRRDIGLSVTHRES-TKSWLSQVCHVCQKSMI---FGVK
GalgaKSR	-----QGSPQMVRDFGLAVTHRES-TKSWLSQICQVCQKSM---FGVK
Xent rKSR1	-----QGSPQMVRRDIGLSVTHRES-TKSWLSQMVCHVCQKSM---FGVK
DanreKSRlike	LQEEHSGLRNNVTVHRSSPQALRRDIGLAVTHRES-TKSWLSQTCCVCQKNMI---FGVK
OrycuKSR2	VHTEASFSANTLSVPRWSPQIPRRDLGNSIKHRES-TKYWMSQTCVCGKGM---FGLK
	C1 domain * :. ** * * : *
HarsaKSR2	CKECKYKCHRDCESKVPPSCG--LPQELFDEFKRTVQADGMINASPI--LSKPGITSPNH
ApimeKSR1	CKECKYKCHRDCESKVPPSCG--LPQELFDEFKRTVQGDGMVNVSP I--LSKPGITSPNH
CamflKSR2	CKECKYKCHRECESKVPPSCG--LPQELFNEFKRTLQGDG-INASPI--LSKPGITSPNH
TricaKSR	CKECKYTCHRECDRVTPSCG--LPPELLDEFKKLSCEVQVFPSPN--PSR-ASNTKNI
PenmoKSR	CKECSYKCHRECEPKVPPSCG--LPQELLILFADTWKVGMDGSGGLHRGGTPGVSPSHH
DromeKSR	CTDCKYICHKSCAPHVPPSCG--LPREYVDEFRIKEQGGYASLPHV----HGAAKGSPL
DrosiKSR	CTDCKYICHKSCAPHVPPSCG--LPREYVDEFRIKEQGGYASLPHV----HGATKGSPL
AedaeKSR	CTECKYRCHDKCKSNVPPSCG--LPQEFVDEFKKSLSQSD--TLIPNV----SPNLCNRLM
IxoscKSR	CKECKFRCHRDCKDKVPPSCG--LPNELVDVFAEHIQKGVQQTSLRTTWTARCAGIQSPN
MondoKSR1	CKHCKRLKCHNKCTKEAPVCRISFLP---LSKLRRTESVPSDINNVPVDR-STEPHFH---T
HomsaKSR1	CKHCKRLKCHNKCTKEAPACRISFLP---LTRLRRTESVPSDINNVPVDR-AAEPHFH---T
GalgaKSR	CKYCKRLKCHNKCTKEAPACRISFLP---ITKIRRRTESVPSDINNVPVDR-PTEPQFH---T
Xent rKSR1	CKHCKRLKCHNKCTKDAPACRISFLP---IAKIRRRTESVPSDINNVPVDR-PAEPHFH---T
DanreKSRlike	CKHCKRLKCHNKCTKEAPPACRISFLP---ITKIRRRTESVPSDINNVPVDRPPEAPQFH---T
OrycuKSR2	CKNCKRLKCHNKCTKEAPPCHLLIHRGDPARLVRTESVPCDINNPLRKPPIRYDLHISQT
	* . * * . . * . . . : :

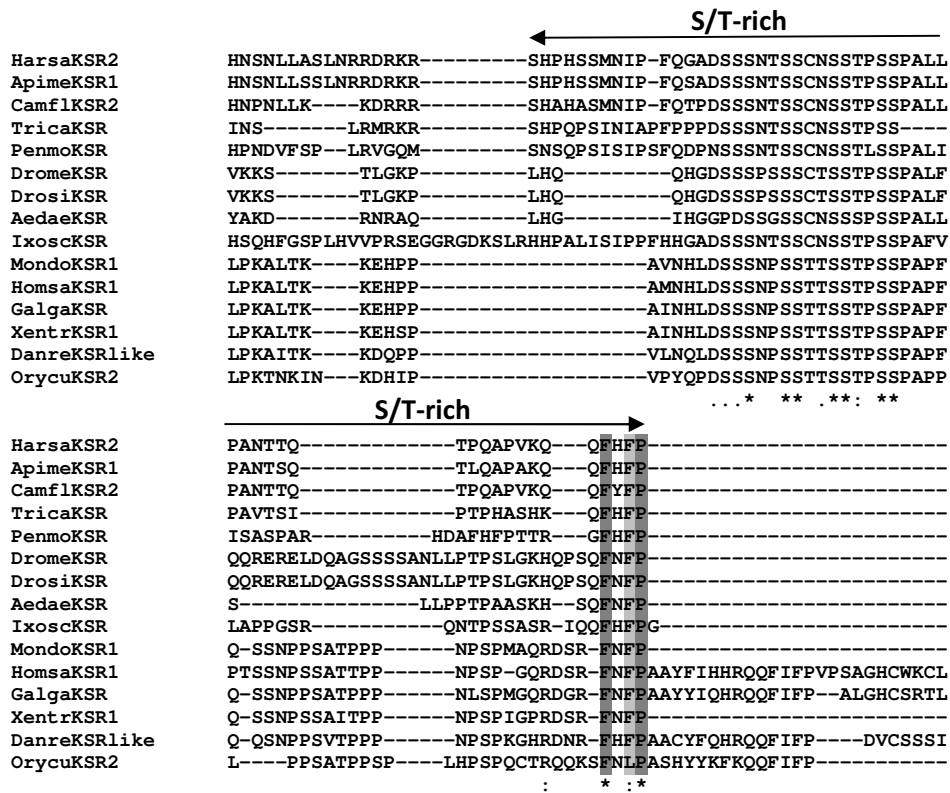


Figure 3.17 Partial multiple alignments of the deduced amino acid sequence of PmKSR, KSR, KSR1, KSR2 and KSR like proteins of various species. The analysis include PmKSR; KSR sequence of *Tribolium castaneum* (XP_001812757.1), *Drosophila melanogaster* (AAN17651.1), *Aedes aegypti* (XP_001653307.1), *Ixodes scapularis* (XP_002404769.1) and *Gallus gallus* (XP_425413.2); KSR1 sequence of *Apis mellifera* (XP_393005.2), *Monodelphis domestica* (XP_001375506.1) and *Xenopus (Silurana) tropicalis* (NP_001186688.1); KSR2 sequence of *Harpegnathos saltator* (EFN87977.1) and *Camponotus floridanus* (EFN61908.1); KSR like sequence of *Danio rerio* (XP_002660744.1). Asterisks, colons, and dots indicate residues indentical in all sequence, conserved substitutions, and semiconserved substitutions, respectively. Aminoacid sequence analysis of PmKSR on its C1 domain and S/T-rich (FXFP) at amino terminal and hyphen indicated gap.

3.5 Examination of expression levels of *PmMEK*, *PmLATS1* and *PmKSR* during ovarian development of *P. monodon* by Quantitative real-time PCR

The expression levels of *PmMEK*, *PmLATS1* and *PmKSR* in different ovarian stages of intact and unilateral eyestalk-ablated *P. monodon* broodstock were quantitatively estimated by real-time PCR (Figure 3.19, Figure 3.20 and 3.21).

The standard curves of each target gene and the control (*EF-1 α*) were constructed from a 10-fold dilution covering 10^3 - 10^8 copy numbers of each gene. High R^2 values and efficiency of amplification of examined transcripts were found (Figure 3.18). Therefore, these standard curves were acceptable to be used for quantitative estimation of all genes.

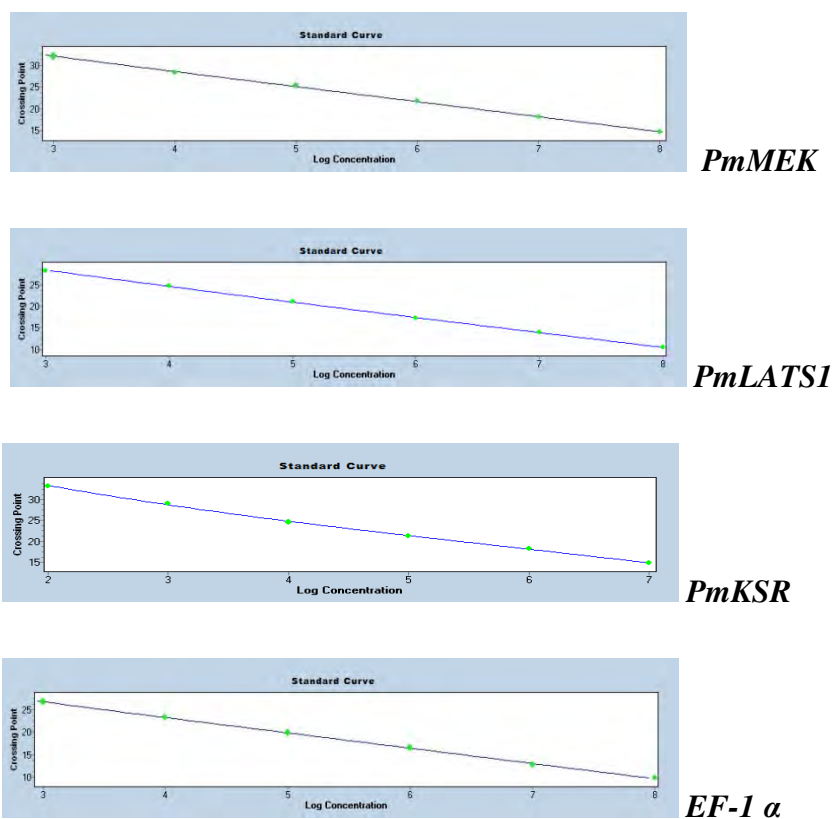


Figure 3.18 Standard curves of *PmMEK* (A; $R^2 = 0.975$, efficiency = 1.949 and equation; $Y = -3.451 * \log(X) + 42.72$), *PmLATS1* (A; $R^2 = 0.976$, efficiency = 1.953 and equation; $Y = -3.441 * \log(X) + 39.10$), *PmKSR* (A; $R^2 = 1.02$, efficiency = 2.049 and equation; $Y = -3.441 * \log(X) + 39.10$) and *EF-1 α* (B; $R^2 = 0.992$, efficiency = 1.984 and equation; $Y = -3.362 * \log(X) + 36.74$).

PmMEK in ovaries of intact and eyestalk-ablated broodstock were greater than that of juveniles (4 month olds shrimp) ($P > 0.05$). In intact broodstock, the expression level of *PmMEK* at stages IV ovaries was greater than that of other stages ($P > 0.05$) (Figure 3.19a). This transcript was not significantly different during development of eyestalk-ablated *P. monodon* (Figure 3.19b). Eyestalk ablation did not significantly promote the transcription of *PmMEK* in ovaries of wild *P. monodon* (Figure 3.19C).

Table 3.1 Relative expression levels of *PmMEK* in different ovarian stages of *P. monodon* female broodstock.

Ovarian stage	Relative expression level	N	Relative expression level	N
	Intact broodstock		Eyestalk-ablated broodstock	
Juveniles	0.0772±0.239 ^a	5	-	-
Stage I (GSI < 1.5)	0.1603±0.255 ^{ab}	8	0.3099±0.106 ^{bc}	4
Stage II (GSI 2.0 – 4.0)	0.2839±0.540 ^{bc}	7	0.1794±0.048 ^{ab}	5
Stage III (GSI 4.0 - 6.0)	0.1904±0.212 ^{ab}	5	0.3141±0.139 ^{bc}	12
Stage IV (GSI > 6.0)	0.4238±0.496 ^c	9	0.3219±0.114 ^{bc}	8
post-spawning (GSI 1.86 – 3.49)	0.2340±0.571 ^{ab}	3	-	-

The *PmLATS1* mRNA in ovaries of 4-month-old juveniles was comparable with that in stages I, II and III ovaries of intact broodstock. *PmLATS1* was significantly up-regulated in stage IV (mature) ovaries ($P < 0.05$) and returned to the basal level after spawning (Figure 3.20a).

In eyestalk-ablated broodstock, its expression level in stages III (early cortical rod) and IV (mature) ovaries was significantly greater than that in stages I (previtellogenic) and II (vitellogenic) ovaries ($P < 0.05$) (Figure 3.20b).

Eyestalk ablation resulted in a lower expression of *PmLATS1* in vitellogenic and mature ovaries of *P. monodon* broodstock (Figure 3.19C).

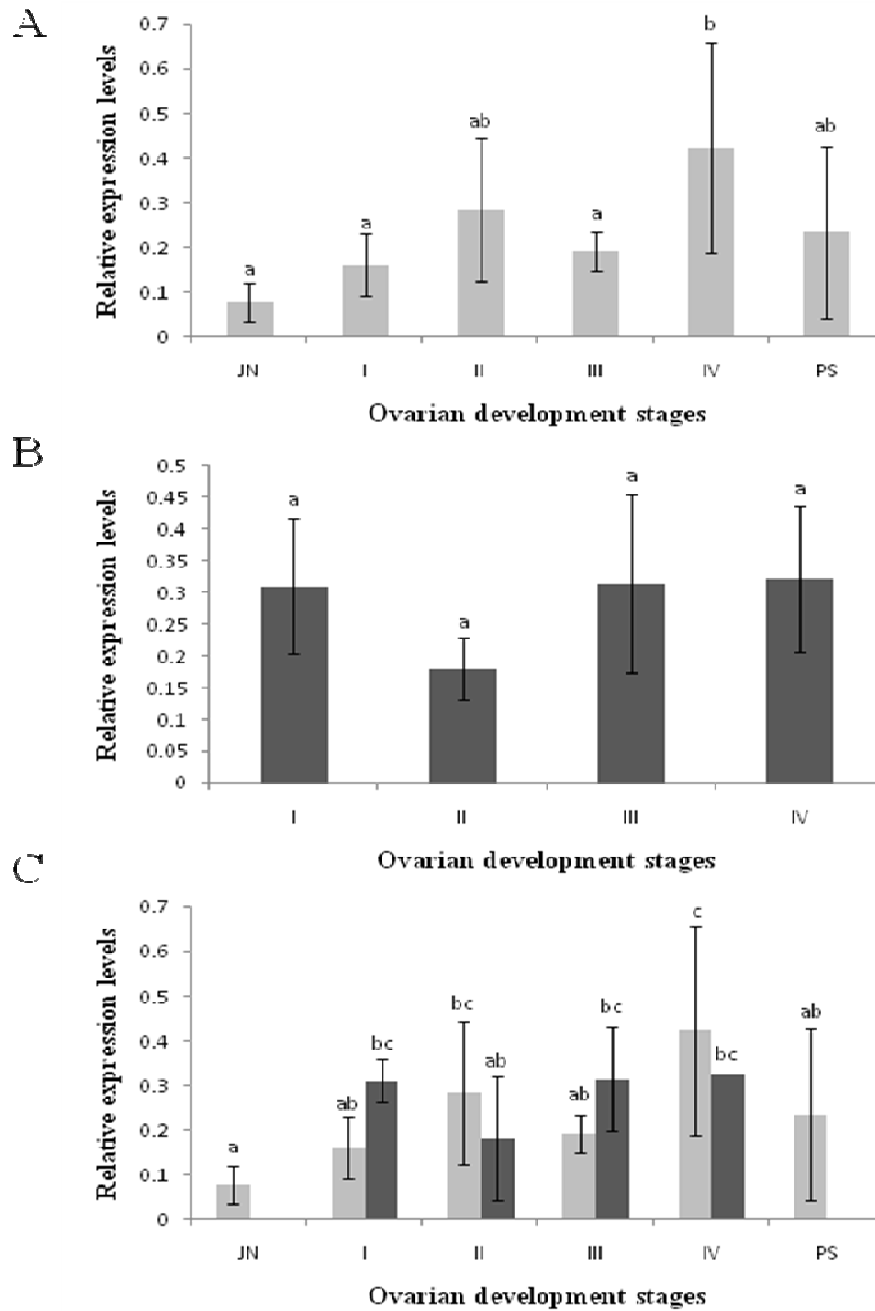


Figure 3.19 Histograms showing the relative expression profiles of *PmMEK* during ovarian maturation of intact (A), unilateral eyestalk ablated (B) *P. monodon* broodstock. Data of intact and eyestalk-ablated broodstock were also analyzed together (C). Expression levels were measured as the absolute copy number of *PmMEK* mRNA (50 ng template) and normalized by that of *EF-1 α* mRNA (5 ng template). Each bar corresponds to a particular ovarian stage. The same letters indicate that the expression levels were not significantly different ($P > 0.05$). Relative expression levels and standard deviation were also shown.

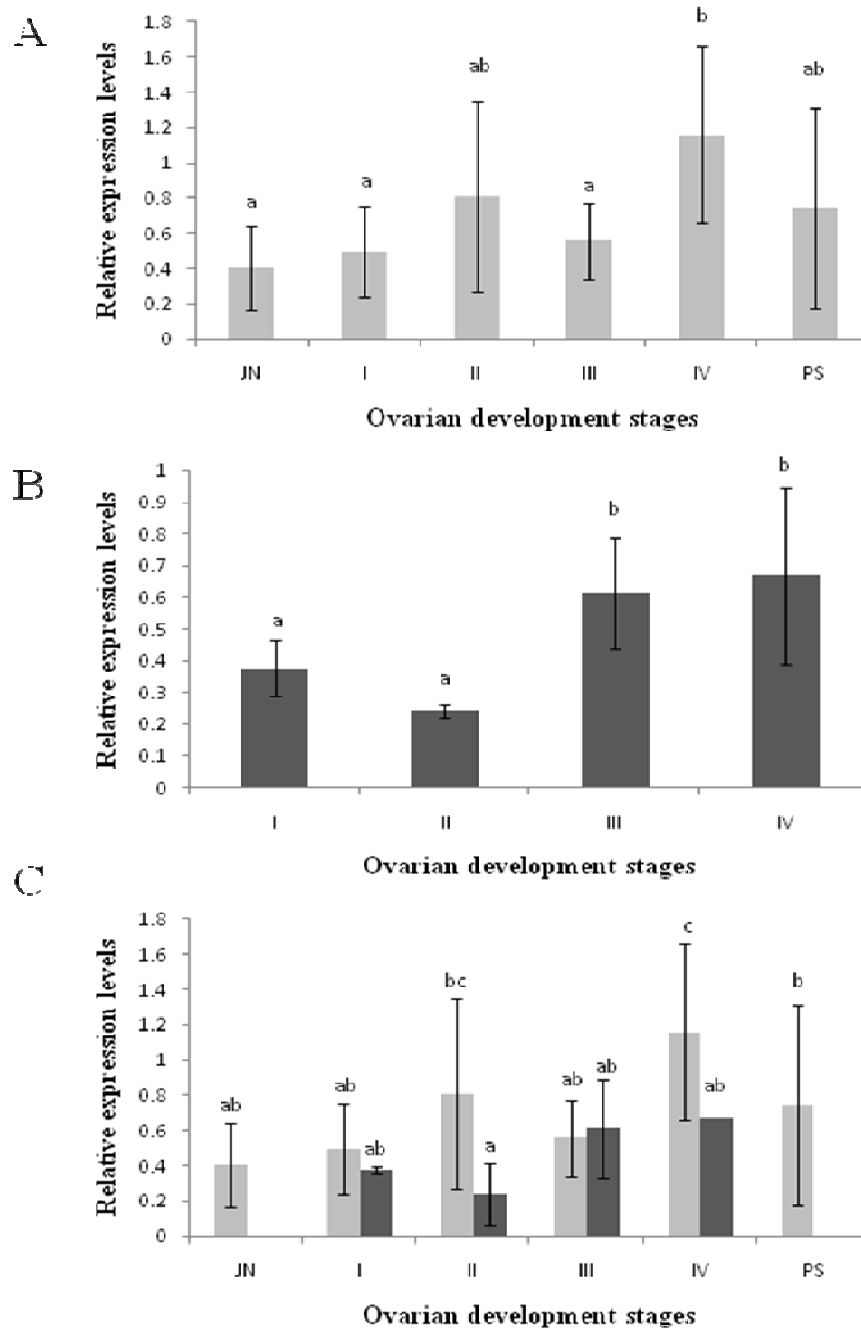


Figure 3.20 Histograms showing the relative expression profiles of *PmLATS1* during ovarian maturation of intact (A), unilateral eyestalk ablated (B) *P. monodon* broodstock. Data of intact and eyestalk-ablated broodstock were also analyzed together (C). Expression levels were measured as the absolute copy number of *PmLATS1* mRNA (50 ng template) and normalized by that of *EF-1 α* mRNA (5 ng template). Each bar corresponds to a particular ovarian stage. The same letters indicate that the expression levels were not significantly different ($P > 0.05$). Relative expression levels and standard deviation were also shown.

Table 3.2 Relative expression levels of *PmLATS1* in different ovarian stages of *P. monodon* female broodstock.

Ovarian stage	Relative expression level	N	Relative expression level	N
	Intact broodstock		Eyestalk-ablated broodstock	
Juveniles	0.4047±0.239 ^{ab}	5	-	-
Stage I (GSI < 1.5)	0.4971±0.255 ^{ab}	8	0.3763±0.088 ^{ab}	4
Stage II (GSI 2.0 – 4.0)	0.8048±0.540 ^{bc}	7	0.2429±0.019 ^a	5
Stage III (GSI 4.0 - 6.0)	0.5569±0.212 ^{ab}	5	0.6130±0.174 ^{ab}	12
Stage IV (GSI > 6.0)	1.1607±0.496 ^c	9	0.6697±0.277 ^{ab}	8
post-spawning (GSI 1.86 – 3.49)	0.7421±0.571 ^b	3	-	-

Variations in expression of *PmKSR* during ovarian development of *P. monodon* were found (Figure 3.21A). *PmKSR* showed fluctuations of expression in intact female broodstock. The transcript was significantly up-regulated at the stage IV (mature) ($P < 0.05$) before returned to the basal level at the post-spawning stage ($P > 0.05$) (Figure 3.21A).

Interestingly, its expression level peaked in stage I ovaries and comparably expressed during stages II - IV in eyestalk-ablated broodstock (Figure 3.21B).

As can be seen in Figure 3.21C, the expression level of *PmKSR* in stages I and III ovaries of eyestalk ablated females was significantly greater than that in the same stages of intact females.

Table 3.3 Relative expression levels of *PmKSR* in different ovarian stages of *P. monodon* female broodstock.

Ovarian stage	Relative expression level	N	Relative expression level	N
	Intact broodstock		Eyestalk-ablated broodstock	
Juveniles	0.3263±0.307 ^{ab}	5	-	-
Stage I (GSI < 1.5)	0.1204±0.064 ^a	8	0.6416±0.343 ^c	4
Stage II (GSI 2.0 – 4.0)	0.1934±0.132 ^{ab}	7	0.3896±0.145 ^b	5
Stage III (GSI 4.0 - 6.0)	0.1348±0.056 ^a	5	0.4185±0.163 ^b	12
Stage IV (GSI > 6.0)	0.3837±0.179 ^b	8	0.2915±0.122 ^{ab}	8
post-spawning (GSI 1.86 – 3.49)	0.2347±0.138 ^{ab}	3	-	-

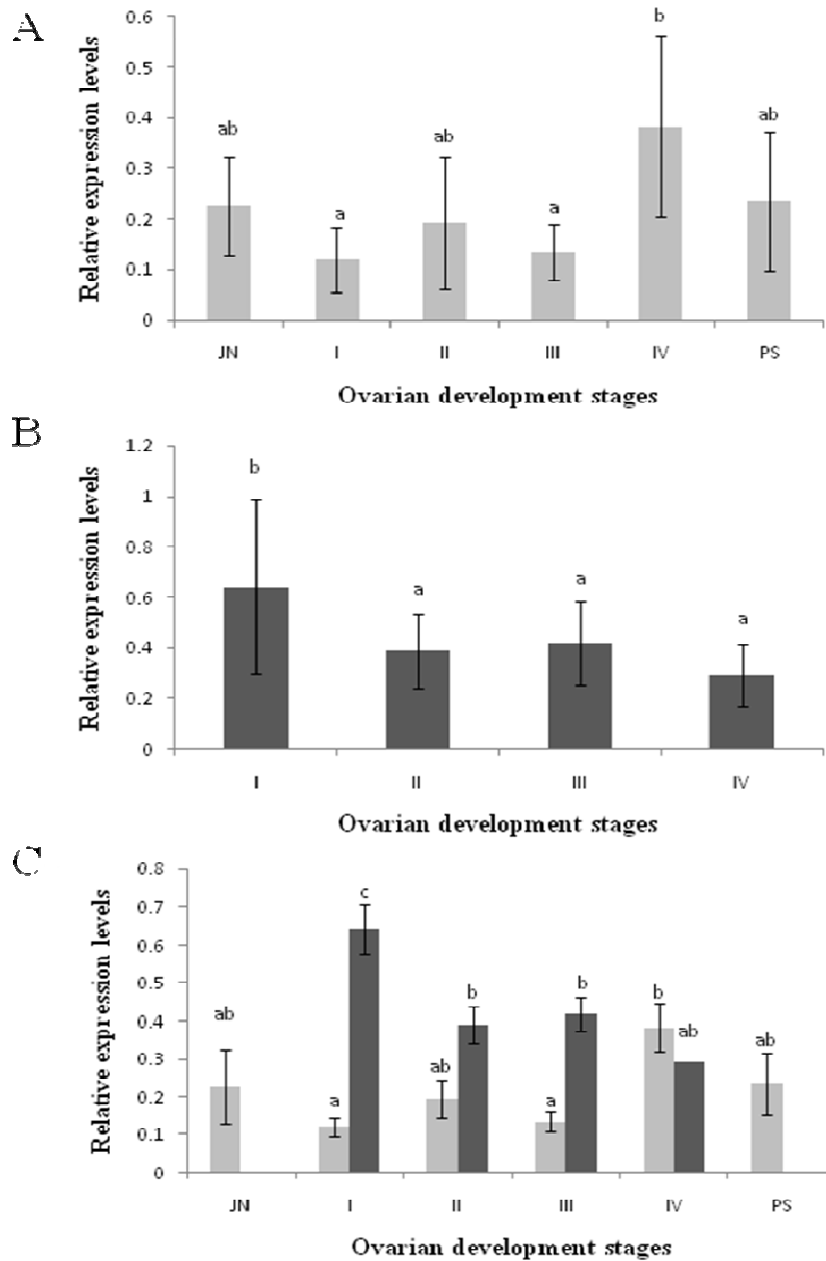


Figure 3.21 Histograms showing the relative expression profiles of *PmKSR* during ovarian maturation of intact (A), unilateral eyestalk ablated (B) *P. monodon* broodstock. Data of intact and eyestalk-ablated broodstock were also analyzed together (C). Expression levels were measured as the absolute copy number of *PmKSR* mRNA (50 ng template) and normalized by that of *EF-1 α* mRNA (5 ng template). Each bar corresponded to a particular ovarian stage. The same letters indicated that the expression levels were not significantly different ($P > 0.05$). Relative expression levels and standard deviation were also shown.

3.6 Localization of sex-related transcripts in ovaries of *P. monodon* broodstock

3.6.1. Quantification of the cRNA probes

The amount of cRNA probes was estimated by dot blot analysis. The sense and antisense cRNA probes were synthesized from PCR product (Figure 3.22 and 3.24). The sensitivity of each probes was tested by dot blot analysis compared to control RNA. The control RNA was used as the positive control demonstrating the positive signal between 10 pg - 10 ng. The antisense and sense probes of *PmMEK* and *PmLATS1* exhibited the signal from 100 pg - 10 ng (Figure 3.23 and 3.25). An appropriate amount of the cRNA probe of each transcript was applied for examination of transcriptional localization using *in situ* hybridization.

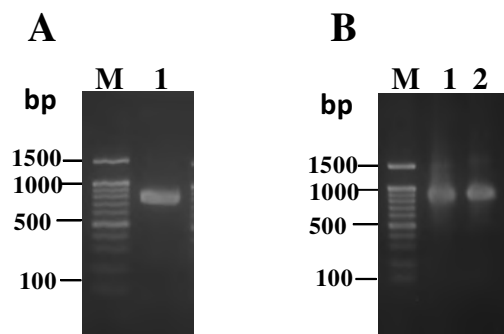


Figure 3.22 (A) The amplification product for synthesis of the cRNA probe of *PmMEK* (lane 1, A). (B) The antisense (lane 1, B) and sense (lane 2, B) were synthesized from elute PCR template. A 100 bp ladder (M) was used as the DNA maker.

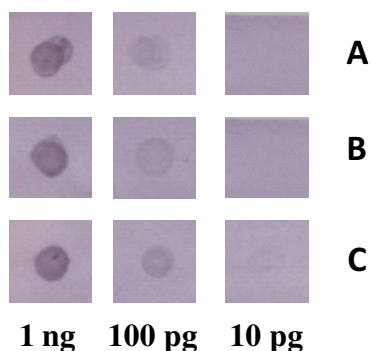


Figure 3.23 Dot blot hybridization for estimation of the concentration of the antisense (A), and sense *PmMEK* (B) and the control RNA probes(C).

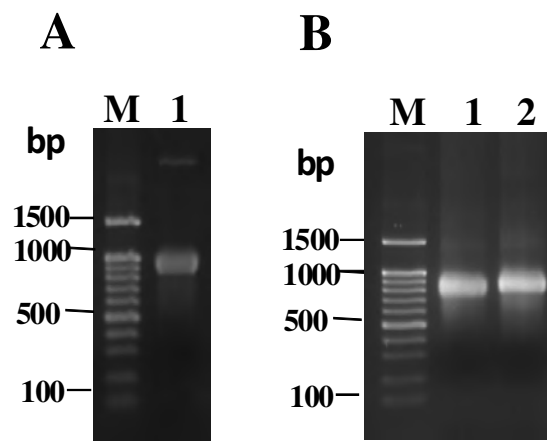


Figure 3.24 (A) The amplification product for synthesis of the cRNA probe of *PmLATSI* (lane 1, A). (B) The antisense (lane 1, B) and sense (lane 2, B) were synthesized from elute PCR template. A 100 bp ladder (M) was used as the DNA maker.

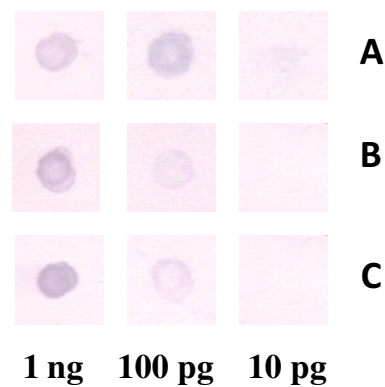


Figure 3.25 Dot blot hybridization for estimation of the concentration of the antisense (A), and sense *PmLATSI* (B) and the control RNA probes(C).

3.6.2 *In situ* hybridization (ISH)

The subcellular localization of *PmMEK* and *PmLATS1* transcripts in ovaries of *P. monodon* broodstock was determined by *in situ* hybridization. The positive signal (blue precipitate) was observed when the tissue sections were hybridized with the antisense probe of *PmMEK* and *PmLATS1* and no signal was observed with sense probe for all transcripts (Figure 3.26 a,b; Figure 3.28 a,b; Figure 3.30 a,b and 3.29 a,b).

The antisense *PmMEK* and *PmLATS1* probes gave an intense signal in ooplasm of previtellogenic oocytes during development in both normal and eyestalk-ablated broodstocks (Figure 3.26- Figure 3.29).

As described previously, localization of *PmMEK* was not observed in more mature (vitellogenic oocytes and late cortical rod oocytes) but *PmLATS1* was localized in ooplasm of late cortical rod oocytes as well as previtellogenic oocytes (Figure 3.28d and 3.29d).

HE staining (Figure 3.26 e,f; Figure 3.27 e,f; Figure 3.28 e,f and 3.29 e,f) showed the oocytes in developing ovaries of *P. monodon* broodstocks. The ovarian stages were categorized by judging from majority of the oocytes appeared from HE staining. Previtellogenic oocytes could be observed in all stages but the quantity was not increased.

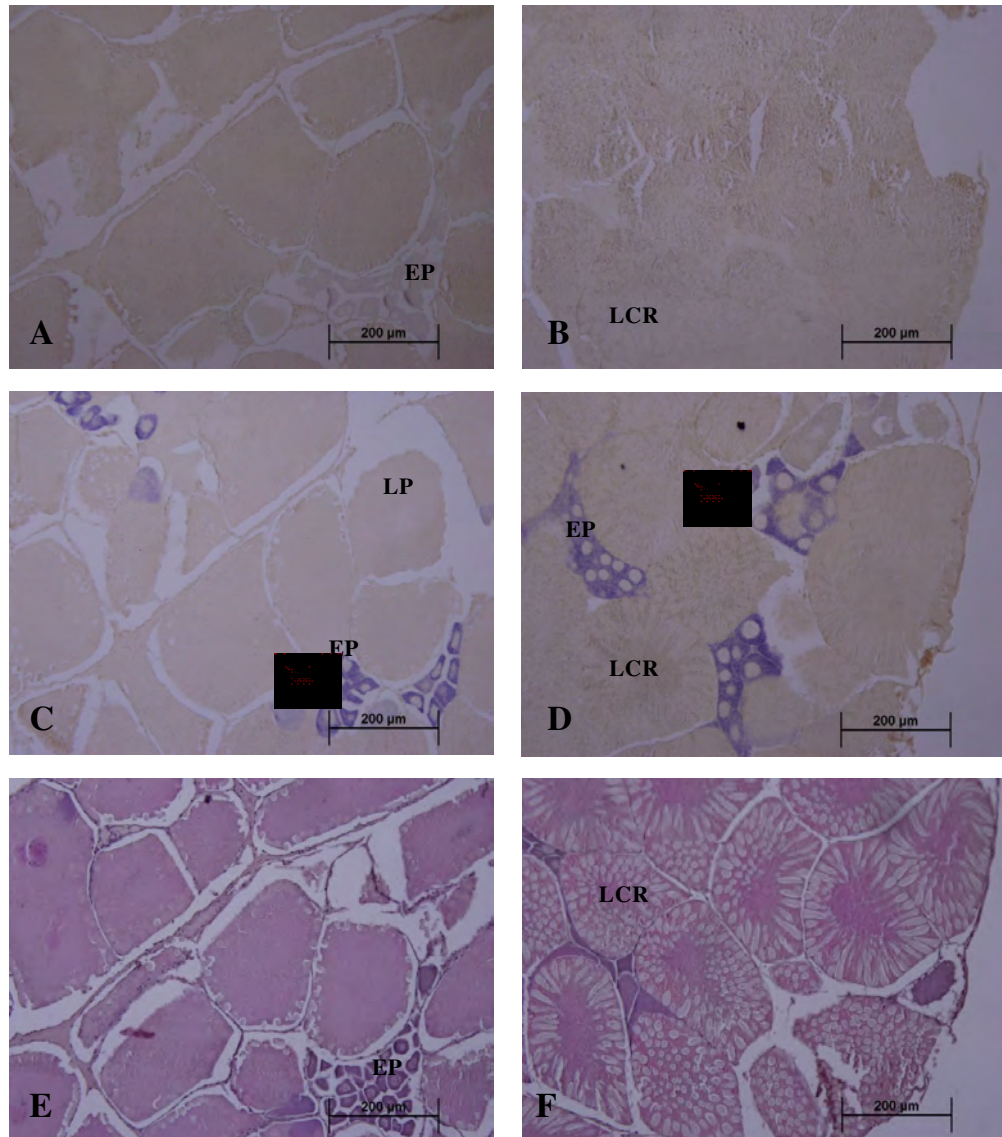


Figure 3.26 Localization of *PmMEK* transcript during ovarian development of normal *P. monodon* broodstock visualized by *in situ* hybridization using the sense *PmMEK* probe (A and B), antisense *PmMEK* probe (C and D). Conventional HE staining was carried out for identification of oocyte stages (E and F). EP = early previtellogenic oocytes; LP = late previtellogenic oocytes and LCR = late cortical rod oocytes.

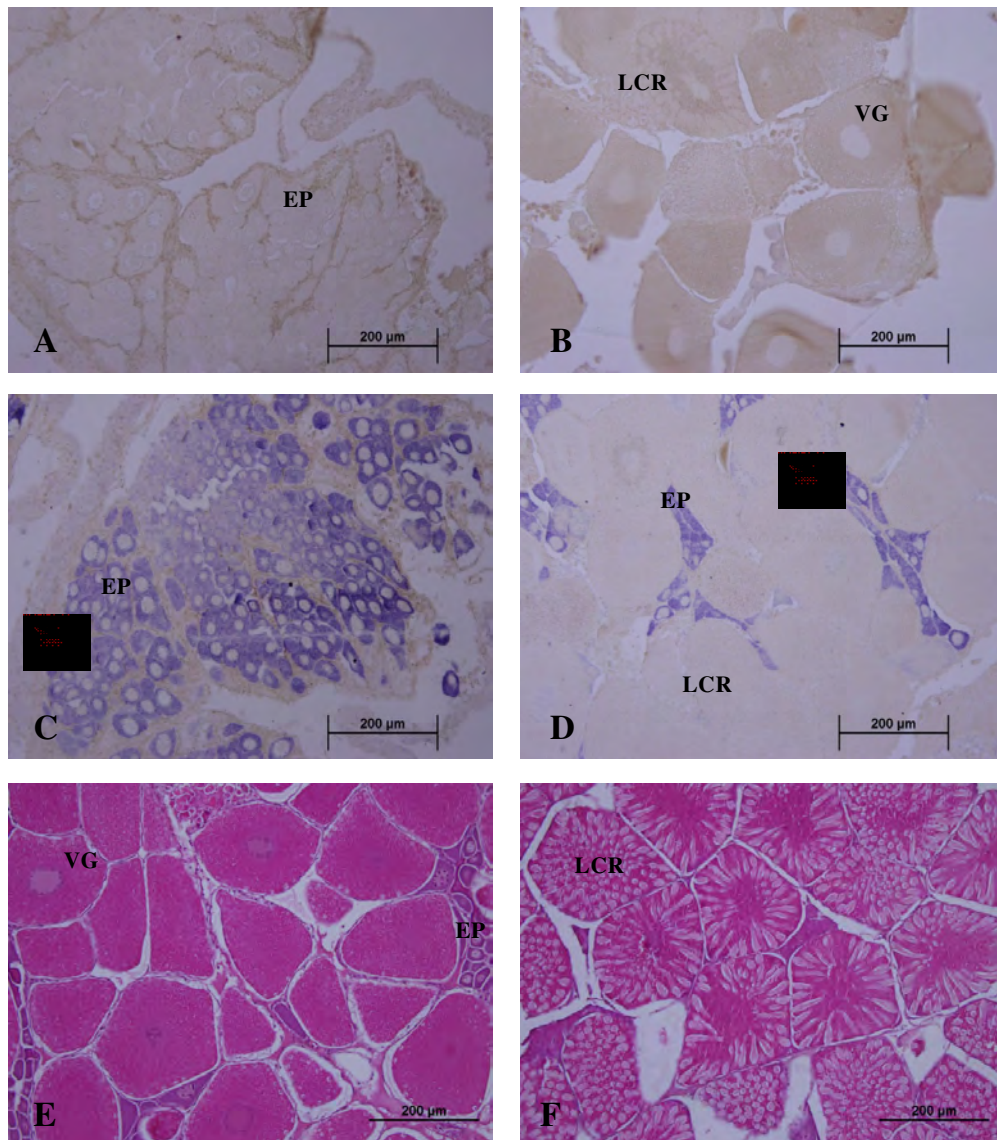


Figure 3.27 Localization of *PmMEK* transcript during ovarian development of eyestalk-ablated *P. monodon* broodstock visualized by *in situ* hybridization using the sense *PmMEK* probe (A and B), antisense *PmMEK* probe (C and D). Conventional HE staining was carried out for identification of oocyte stages (E and F). EP = early previtellogenic oocytes; VG = vitellogenic oocytes and LCR = late cortical rod oocytes.

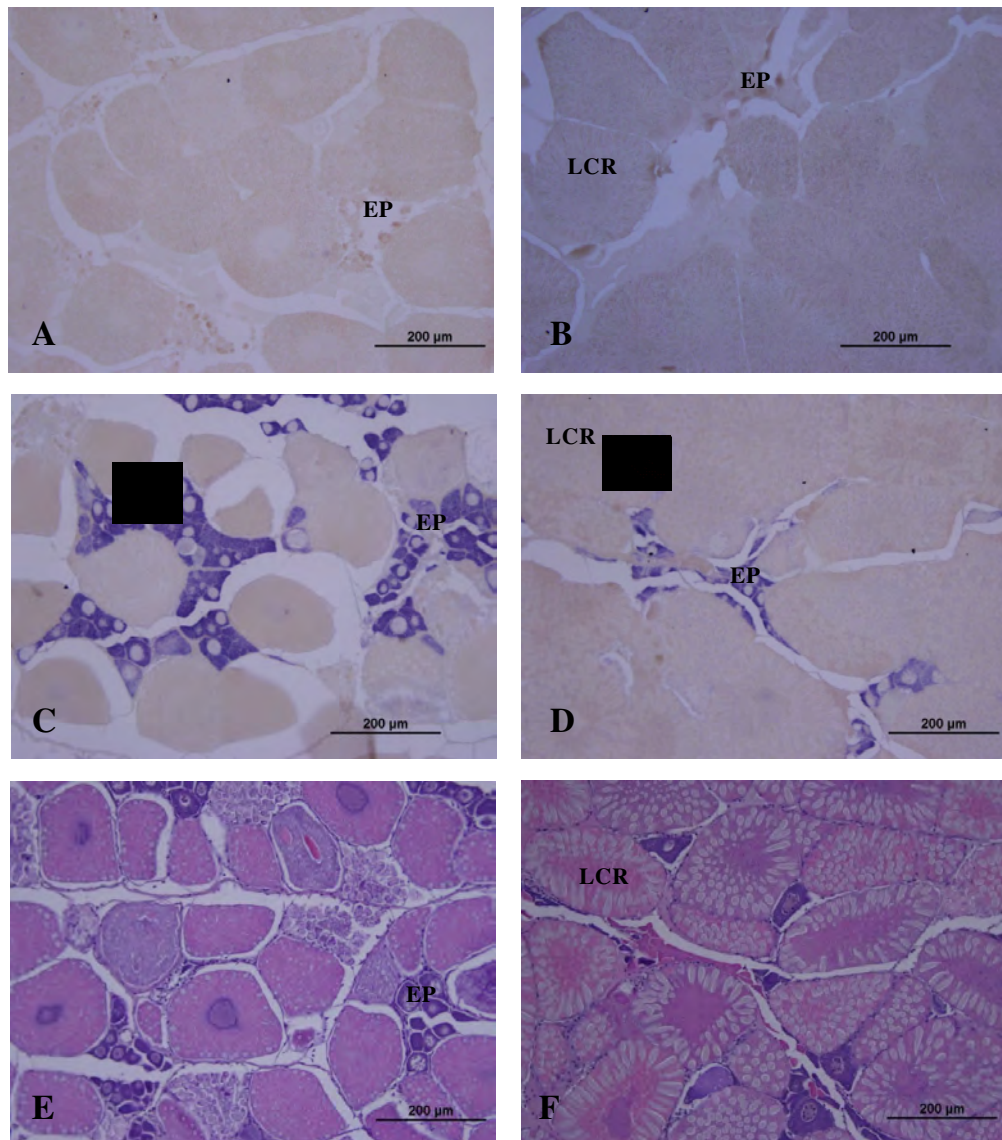


Figure 3.28 Localization of *PmLATS1* transcript during ovarian development of normal *P. monodon* broodstock visualized by *in situ* hybridization using the sense *PmLATS1* probe (A and B), antisense *PmLATS1* probe (C and D). Conventional HE staining was carried out for identification of oocyte stages (E and F). EP = early previtellogenic oocytes and LCR = late cortical rod oocytes.

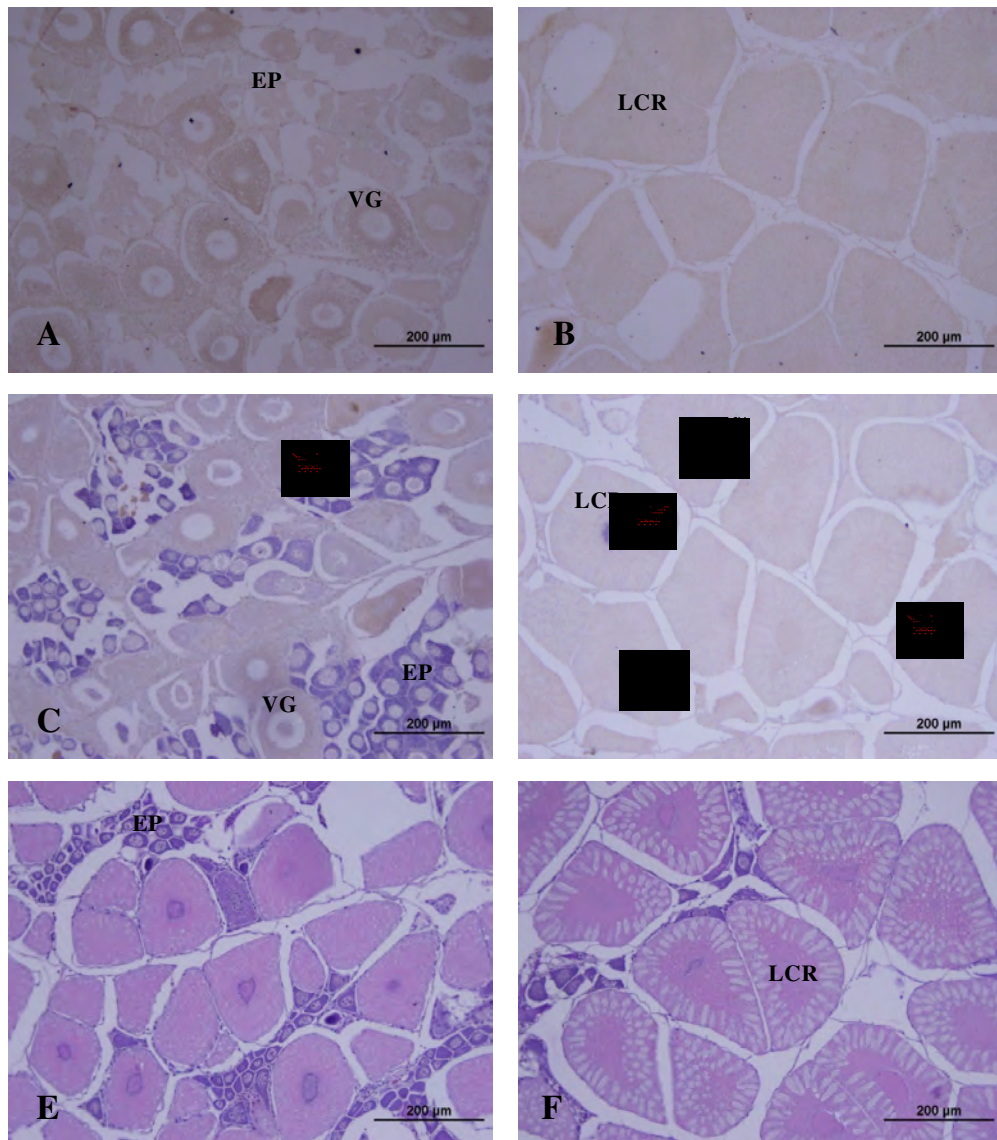


Figure 3.29 Localization of *PmLATS1* transcript during ovarian development of eyestalk-ablated *P. monodon* broodstock visualized by *in situ* hybridization using the sense *PmLATS1* probe (A and B), antisense *PmLATS1* probe (C and D). Conventional HE staining was carried out for identification of oocyte stages (EP). EP = early previtellogenic oocytes; VG = vitellogenic oocytes and LCR = late cortical rod oocytes.

3.7 *In vitro* expression of recombinant MEK and RAS proteins using the bacterial expression system

Recombinant plasmid carrying the full length cDNA of MEK and RAS was prepared for *in vitro* expression of the corresponding protein. For the ORF of MEK was characterized by RACE PCR prior (Figure 3.6).

RAS was initially found from the ovary from the ovary cDNA library (EAT38763) and the full length cDNA of this gene was 936 bp corresponding to 185 amino acids (Figure 3.28). This transcript significantly matched Ras-related protein Rap-1b precursor of *Scylla serrata* (E-value = 4e-96). Before construction of recombinant plasmid, the ORF amplified primers of MEK and RAS that covered from start to stop codon were designed from RACE-full length cDNA. The amplified full length cDNA of MEK and RAS was ligated to pGEM[®]-T easy vector and transformed into *E. coli* JM109. The recombinant plasmid of the positive clone was re-sequenced to confirm the orientation and nucleotide sequence of a partial recombinant clone.

```

GTCGGACCTGGTACTGCTGCAGCAAGTGTCTGAGGATGCGTGAATACAAGATTGTGGTGT 60
                                     M R E Y K I V V L 9
GGGGTCAGGAGGTGTTGGAAAACTGCACTTACAGTTCAGTTTGTGCAGGGCATCTTTGT 120
G [S] G G V G K S A L [T] V Q F V Q G I F V 29
CGAGAAATATGATCCCACGATAGAGGATTCATATCGTAAGCAAGTGAAGTGGATGGCCA 180
E K Y D P T I E D S Y R K Q V E V D G Q 49
GCAGTGTATGCTTGAAATCCTTGATACTGCTGGAACGAACAATTTACAGCAATGCGTGA 240
Q C M L E I L D T A G T E Q F T A M R D 69
TCTCTATATGAAGAATGGACAGGGCTTTGTTTTGGTGTACAGTATCACCGCACAAAGTAC 300
L Y M K N G Q G F V L V Y S I T A Q S T 89
CTTCAATGATTTACAAGATCTCCGTGAACAGATTCTCAGAGTCAAGGACACGGATGACGT 360
F N D L Q D L R E Q I L R V K D T D D V 109
CCCAATGATCCTAGTGGGTAACAAGTGTGACTTGGAGGATGAGCGTGTGTTGGGAAAGA 420
P M I L V G N K C D L E D E R V V G K D 129
CCAGGGCCTCAACCTGGCCAAGTCATTCTCTTGCGCCTTCTAGAAATCATCTGCAAAAGC 480
Q G L N L A K S F S C A F L E [S] [S] A K A 149
TAAGATCAATGTCAATGAGATCTTCTATGACTTAGTTTCGGCAGATTAACCGTAAATCCCC 540
K I N V N E I F Y D L V R Q I N R K S P 169
TGAGAGAAAGTCAAATGGAAGGAGTAATAAAAAAGAGTGTGCTTTTATAAGGTTGGAT 600
E R K S N G R [S] N K K K C C L L * 185

ATTACTCATTATAAGACTAGGTAAAGAATGGCTGGATGTTATGCCTTCATCCTCTCAGG 660
TGTAACCTGCGATTTTGTGTTCTGTTGCCAAGACATGCTGTAAAGTAATCATTCTAGGA 720
ATATTATTGAAGAGCTAATGTGTACAAGTGTTTAGAAGTGAAAAGCAGTGTGTGTGGGGA 780
TGCATGTGTTTGTGTGTGTTTGTGTGTGTAAGTATTAAAGCATAATTTCTTATCTCTAC 840
TTTAAATACAAGTCTGGAAGTGTGATCAGTGTGAGAAGGCAAAAATCTTGCATATCTTGG 900
TAATAGAAACAAAATTCACAGTAAAAAAAAAAAAAAAAA 940

```

Figure 3.30 The full length cDNA and deduced amino acid sequences of RAS of *P. monodon* (1559 bp in length with an ORF of 936 bp corresponding to a deduced polypeptide of 185aa). The putative start (ATG) and stop (TAA) codons are

underlined. The poly A tail is illustrated in boldface. The predicted Ras subfamily of RAS small GTPases (RAS; 2.53e-75, positions 1st-167th) domains are highlighted. The predicted PKC phosphorylation site (NetPhosK 1.0 Server, <http://www.expasy.com>) were framed at residue position 145.

```

BomigRASlike      -----MREYKIVVLGSGGGVGSKALTVQFVQGFVVEKYDPTIEDSYRKQVEVDGQQCMLEI
CamflRaslike3    -----MREYKIVVLGSGGGVGSKALTVQFVQGFVVEKYDPTIEDSYRKQVEVDGQQCMLEI
NasviRAS         -----MREYKIVVLGSGGGVGSKALTVQFVQGFVVEKYDPTIEDSYRKQVEVDGQQCMLEI
AedaeRAS        -----MREYKIVVLGSGGGVGSKALTVQFVQGFVVEKYDPTIEDSYRKQVEVDGQQCMLEI
Bommoras        -----MREYKIVVLGSGGGVGSKALTVQFVQGFVVEKYDPTIEDSYRKQVEVDGQQCMLEI
EsoluRasrelated -----MREYKIVVLGSGGGVGSKALTVQFVQGFVVEKYDPTIEDSYRKQVEVDGQQCMLEI
Danrerasrelated -----MREYKIVVLGSGGGVGSKALTVQFVQGFVVEKYDPTIEDSYRKQVEVDGQQCMLEI
PenmoRAS        -----MREYKIVVLGSGGGVGSKALTVQFVQGFVVEKYDPTIEDSYRKQVEVDGQQCMLEI
FenchRAS        -----MREYKIVVLGSGGGVGSKALTVQFVQGFVVEKYDPTIEDSYRKQVEVDGQQCMLEI
ScypaRasrelated -----MREYKIVVLGSGGGVGSKALTVQFVQGFVVEKYDPTIEDSYRKQVEVDGQQCMLEI
AmbvaRasrelated -----MREYKIVVLGSGGGVGSKALTVQFVQGFVVEKYDPTIEDSYRKQVEVDGQQCMLEI
AspfuRAS        MASKFLREYKLVVVGSGGGVGSCLTIQLIQSHFVDEYDPTIEDSYRKQCVIDDEVALLDV
                :***:***:*.*****.***:*:*  ***:***** *..*.:*:*

BomigRASlike      LDTAGTEQFTAMRDLYMKNGQGFVLVYSITAQSTFNDLQDLREQILRVKDTDDVPMVLVG
CamflRaslike3    LDTAGTEQFTAMRDLYMKNGQGFVLVYSITAQSTFNDLQDLREQILRVKDTDDVPMVLVG
NasviRAS         LDTAGTEQFTAMRDLYMKNGQGFVLVYSITAQSTFNDLHDLREQILRVKDTDDVPMVLVG
AedaeRAS        LDTAGTEQFTAMRDLYMKNGQGFVLVYSITAQSTFNDLQDLREQILRVKDTDDVPMVLVG
Bommoras        LDTAGTEQFTAMRDLYMKNGQGFVLVYSITAQSTFNDLQDLREQILRVKDTDDVPMVLVG
EsoluRasrelated LDTAGTEQFTAMRDLYMKNGQGFALVYSITAQSTFNDLQDLREQILRVKDTDDVPMILVG
Danrerasrelated LDTAGTEQFTAMRDLYMKNGQGFALVYSITAQSTFNDLQDLREQILRVKDTDDVPMILVG
PenmoRAS        LDTAGTEQFTAMRDLYMKNGQGFVLVYSITAQSTFNDLQDLREQILRVKDTDDVPMILVG
FenchRAS        LDTAGTEQFTAMRDLYMKNGQGFVLVYSITAQSTFNDLQDLREQILRVKDTDDVPMILVG
ScypaRasrelated LDTAGTEQFTAMRDLYMKNGQGFVLVYSITAQSTFNDLQDLREQILRVKDTDDVPMILVG
AmbvaRasrelated LDTAGTEQFTAMRDLYMKNGQGFVLVYSITAQSTFNDLQDLREQILRVKDDVPMILVG
AspfuRAS        LDTAGQEYSAMREQYMRTEGEGFLVYSITSRQSFEEIMTFQQQILRVKDKDYFPIIVVG
                ***** *.:*:*:*  ***:*** *:*:* *:*:* *:*:* *:*:* *:*:* *:*:*

BomigRASlike      NKCDLEDERVVGKDGQVNLARQFN-CAFNETSAAKAKINVNDIFYDLVRQINK-----
CamflRaslike3    NKCDLEDERVVGKDGQVNLARQFN-CVFNETSAAKAKINVRDIFYDLVRQINK-----
NasviRAS         NKCDLEDERVVGKDGQVNLARQYN-CAFNETSAAKAKINVNDIFYDLVRQINK-----
AedaeRAS        NKCDLEDERVVGKELGKSLANQFN-CAFNETSAAKAKINVNDIFYDLVQQINK-----
Bommoras        NKTDLEAERVVKGKEQGQNLARHFN-CAFNETSAAKAKIHVNDVIFYDLVRQINK-----
EsoluRasrelated NKCDLEDERVVGKEQGQNLARQWSSCAFLESSAKSKINVNEIFYDLVRQINR-----
Danrerasrelated NKCDLEEERVVKGKEQGQNLARQWSNCAFLESSAKSKINVNEIFYDLVRQINR-----
PenmoRAS        NKCDLEDERVVGKDGQGLNLAKSFS-CAFLESSAKAKINVNEIFYDLVRQINR-----
FenchRAS        NKCDLEDERVVGKDGQGLNLAKSFS-CAFPESSAKAKINVNEIFYDLVRQINR-----
ScypaRasrelated NKCDLEDERVVGKDGQVNLAKNFN-CAFLESSAKAKINVNEIFYDLVRQINR-----
AmbvaRasrelated NKCDLEDERVVGKDGQGANLARSFNCAFLESSAKAKINVNEIFYDLVRQINR-----
AspfuRAS        NKCDLEKERAVSQEAGEALARQFG-CKFIETSAKSRINVENAFYDLVREIRRYNKEMSSY
                ** ** * * * * * . : * * * . : * * * : * * * : * * * : * * * : * * * :

BomigRASlike      -----KSPE-----KKMKQKK--KSLCLLL
CamflRaslike3    -----KSPE-----KKMKQKK--KSLCLLL
NasviRAS         -----KSPE-----KKMKQKK--KSLCIVL
AedaeRAS        -----KSPE-----RKPNKKK--KSLCVLL
Bommoras        -----KSPK-----KDEHKPN--KRKCIIL
EsoluRasrelated -----KTPVP----GK-ARKK---SNCQLL
Danrerasrelated -----KTPVE----KKRAKKK---SNCVLL
PenmoRAS        -----KSPE-----RKSNGRS-NKKKCCLL
FenchRAS        -----KSPD-----RKLNGKSGNKKKCCLL
ScypaRasrelated -----KSPIN----TKINKKS---RPCCLL
AmbvaRasrelated -----KNPE-----KKPNTKK--KSKCVLL
AspfuRAS        PSGSGAAGTRAPEGKMDVSEPGDNAGCCGKCVIM
                : * . * :

```

Figure 3.31 Multiple alignments of the deduced amino acid sequence of PmRAS and RAS of various species. The analysis include PmRAS; RAS sequence of *Bombus ignitus* (ACA64426.1), *Camponotus floridanu* (EFN61568.1), *Nasonia vitripennis* (XP_001608221.1), *Aedes aegypti* (XP_001653812.1), *Bombyx mori* (NP_001036972.1), *Esox lucius* (ACO14317.1), *Daphnia pulex* (EFX66674.1),

Fenneropenaeus chinensis (ACJ66625.1), *Scylla paramamosain* (ACX54109.1), *Amblyomma variegatum* (DAA34581.1). Asterisks, colons, and dots indicate residues identical in all sequence, conserved substitutions, and semiconserved substitutions, respectively.

PmMEK amplification products were digested with *Bam* HI and *Xho*I, eluted and ligated into pGEX 4T-1 expression vector. The amplification product of mature PmRAS product was digested with *Nde*I and *Bam*HI before elution and ligation with pET32a (+) expression vector. After that four ligated expression vectors were transformed into *E. coli* JM109 and re-sequenced to confirm the orientation and nucleotide sequence. The last, they were transformed into *E. coli* BL21 (DE3) codon+RIPL.

The clones were screened using gene specific primers of the corresponding vectors used. A sample of screening for recombinant clones in shuttle and expressed host (JM109 and BL21CodonPlus, respectively).

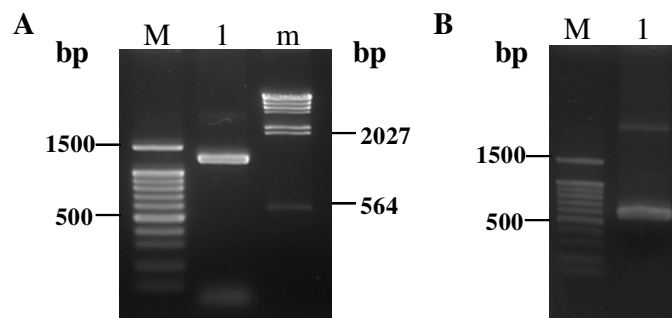


Figure 3.32 Agarose gel electrophoresis showing RT-PCR of the mature transcript of *MEK* (A) and *RAS* (B). Fragments were cloned and sequenced. A hundred-fold dilution of plasmid DNA was used as the template to amplify the ORF overhang with *Bam*HI and *Xho*I for *MEK* and *Nde* I-*Bam* HI for *RAS*.

3.7.1 *In vitro* expression of recombinant protein

Expression of recombinant clone of PmMEK including pGEX (71 kDa) and PmRAS (20.85 kDa) were induced by 1 mM IPTG at 37°C for 1-6 hours. Expression of the recombinant protein was observed at 3 hours after IPTG induction. Recombinant MEK and RAS were stably expressed at 6 hours post induction (Figure 3. 33 and Figure 3. 34).

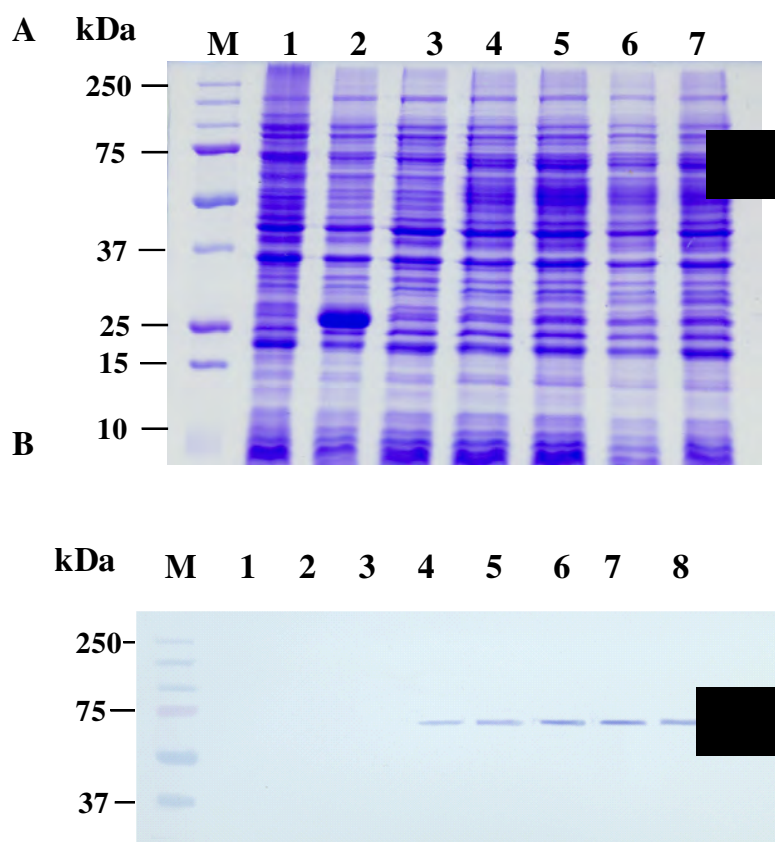


Figure 3.33 A 15% SDS-PAGE (A) and Western blot (B) showing *in vitro* expression of PmMEK at 0 hr (lanes 3; A and B), 1 hr (lanes 4; A and B), 2 hr (lanes 5; A and B), 3hr (lanes 6; A and B) and 6 hr (lanes 7; A and B) after IPTG induction (1 mM), *E.coli* BL21-CodonPlus (DE3)-RIPL (lanes1 ; A). A pGEX 4T-1 vector without insert in *E.coli* BL21-CodonPlus (DE3)-RIPL (lanes 2; A and B) was included as the control and 1;A)

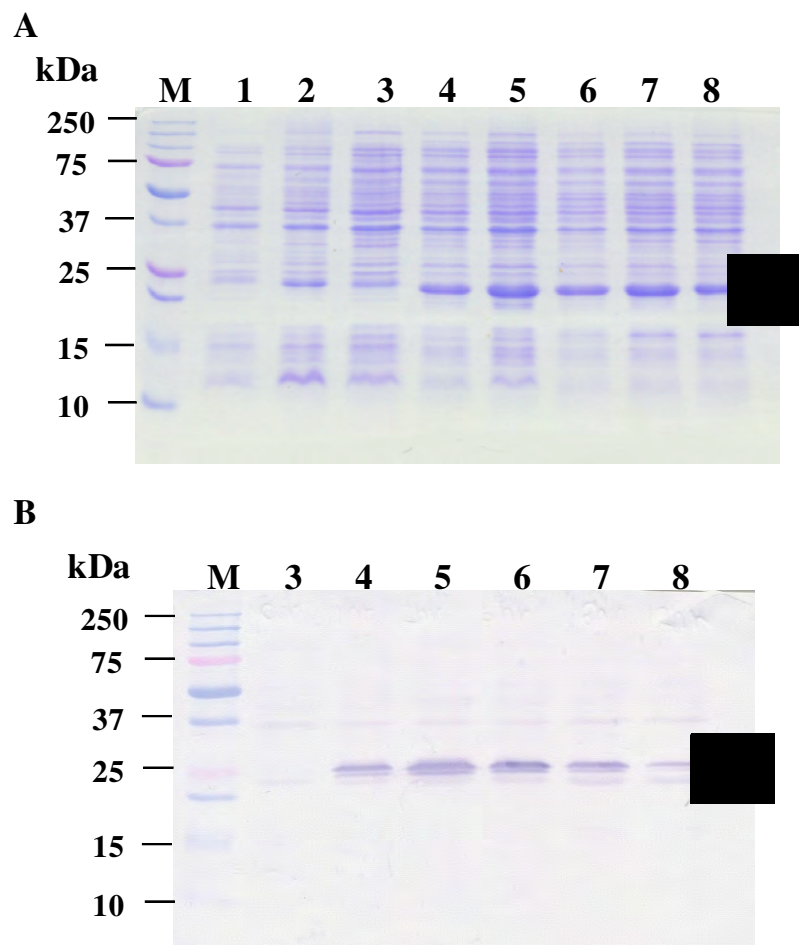


Figure 3.34 A 12% SDS-PAGE (A) and Western blot (B) showing *in vitro* expression of PmRAS at 0 hr (lanes 3; A and B), 1 hr (lanes 4; A and B), 2 hr (lanes 5; A and B), 3hr (lanes 6; A and B) and 6 hr (lanes 7; A and B) after IPTG induction (1 mM). *E.coli* BL21-CodonPlus (DE3)-RIPL (lanes1; A). A pET32 vector without insert in *E.coli* BL21-CodonPlus (DE3)-RIPL (lanes 2; A and B) was included as the control and 1;A)

A recombinant clone of each protein was selected and the expression profile of the corresponding recombinant protein was cultured at 37°C and induced with 1 mM IPTG for 0, 1, 2, 3 and 6 hours after IPTG induction. Recombinant PmMEK was overexpressed since 6 hour after IPTG induction (Figures 3.33). The expression level of recombinant PmRAS was highest at 2 hours post-induction (Figure 3.34).

For determination of expressed proteins, an aliquot of the IPTG-induced culture (OD = 1) of each protein was collected. The soluble and insoluble protein

fractions of each gene were analyzed by 12% and 15% SDS-PAGE for PmMEK and PmRAS respectively (Figures 3.35 and 3.36). Recombinant PmMEK cultured at 37°C for 6 hours after IPTG induction was mainly expressed in an insoluble form and a lower level of recombinant PmMEK was expressed in the soluble form (Figure 3.35). In contrast, the recombinant PmRAS was expressed as the soluble form than the insoluble form and used for further purification (Figure 3.36).

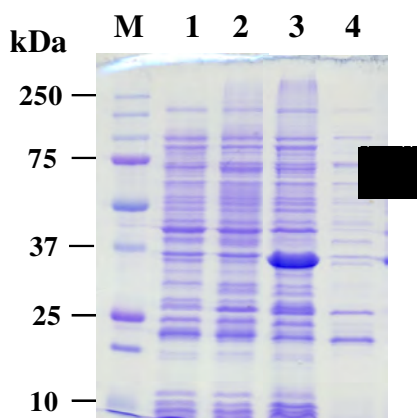


Figure 3.35 A 12% SDS-PAGE showing expression of recombinant PmMEK in a clone cultured for 6 hours at 37°C after IPTG induction (1 mM). Arrowheads indicated the expected protein products. Lanes 1-2 are whole cells ($OD_{600} = 1.0$) at 0 hr and 6 hr. Lanes 3 and 4 are insoluble and soluble fractions, respectively.

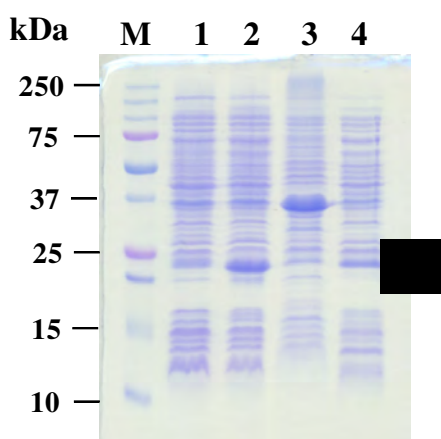


Figure 3.36 A 15% SDS-PAGE showing expression of recombinant PmRAS in a clone cultured for 6 hours at 37°C after IPTG induction (1 mM). Arrowheads indicated the expected protein products. Lanes 1-2 are whole cells ($OD_{600} = 1.0$) at 0 hr and 6 hr. Lanes 3 and 4 are insoluble and soluble fractions, respectively.

3.7.2 Purification of recombinant proteins

The insoluble fraction of recombinant PmMEK was purified under denaturing conditions whereas the soluble fraction of recombinant PmRAS was purified as native proteins.

The insoluble protein of recombinant PmMEK was purified in the denaturing condition. The cells were washed using 10 ml of the binding buffer (20 mM sodium phosphate, 500 mM NaCl, pH 7.4), sonicated and centrifuged at 14000 rpm for 30 min. The insoluble fraction was loaded into the column and washed with the binding buffer. The recombinant protein was eluted with 7 ml of the elution buffer (20 mM sodium phosphate, 500 mM NaCl, 500 mM imidazole, pH 7.4 and 8M urea). Fraction from the washing and eluting steps were analyzed by 15% SDS-PAGE. The purified fractions (Fig) were concentrated by ultrafiltration and kept at 4°C. The obtained protein were subjected to polyclonal antibody production in rabbit.

For the soluble fraction of recombinant PmRAS was purified as native protein. Recombinant proteins were run through the column three times. The first washing step was carried out using 10 ml of the binding buffer (20 mM sodium phosphate and 500 mM NaCl) including 20 mM imidazole, pH 7.4. The recombinant proteins were eluted from the column with 7 ml of the elution buffer (20 mM sodium phosphate, 500 mM NaCl and 500 mM imidazole, pH 7.4). Aliquots of 1 ml were collected from washing and elution of the purified protein. The collected fractions were analyzed by 12% SDS-PAGE (Figures 3.126 and 3.127). The fractions kept at 4°C were concentrated by ultrafiltration and the purified recombinant protein was sent to Faculty of Associated Medical Sciences, Chiangmai University, for production of the polyclonal antibody in rabbit as the insoluble fraction.

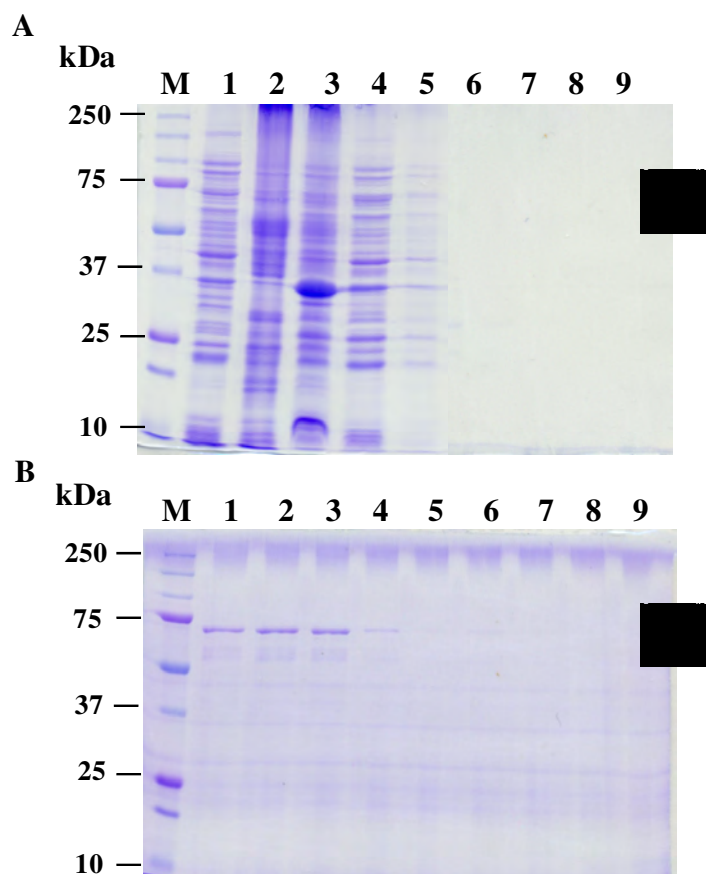


Figure 3.37 15% SDS-PAGE of purified recombinant PmMEK. The culture was carried at 37°C and induced with 1 mM IPTG for 6 hr. A; lane 1-2 is whole cells ($OD_{600} = 1.0$) at 0 hr and 6 hr., lanes 3-4 are the insoluble fraction and insoluble fraction after pass through the column respectively, lanes 5 - 7 are the first washing solution fractions 1, 5 and 9 and lanes 8 - 9 are the second washing solution fractions 1 and 5, respectively. B; lanes 1 - 2 are the third washing insoluble fractions 1 and 5 and lanes 3 - 9 are eluted protein fractions 1-7, respectively.

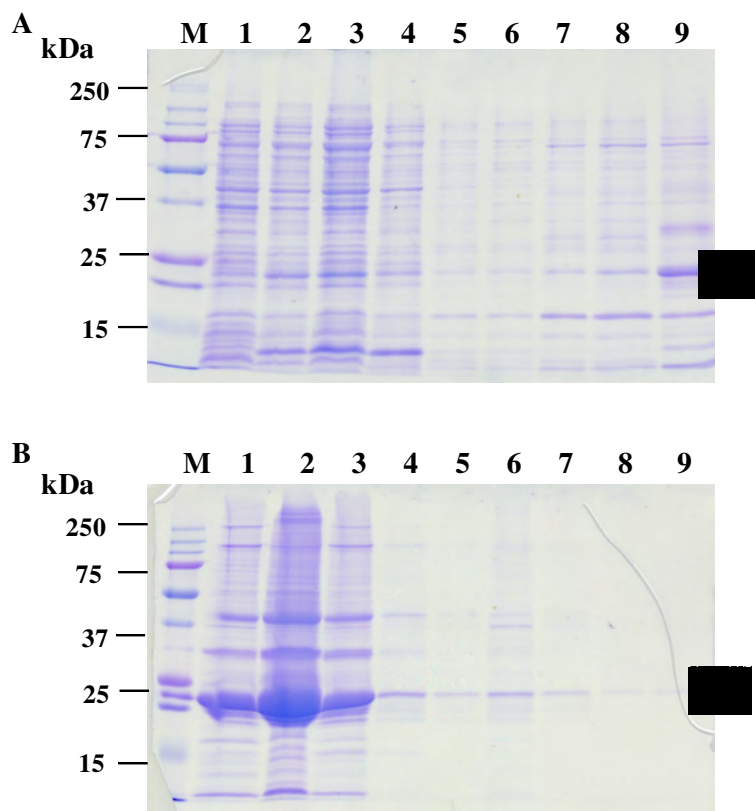


Figure 3.38 12%SDS-PAGE of purified recombinant PmRAS. The culture was carried at 37°C and induced with 1 mM IPTG for 2 hr. A; lane 1-2 is whole cells ($OD_{600} = 1.0$) at 0 hr and 6 hr., lanes 3-4 are the soluble fraction and soluble fraction after pass through the column respectively, lanes 5 - 7 are the first washing solution fractions 1, 5 and 9 and lanes 8 - 9 are the second washing solution fractions 1 and 5, respectively. B; lanes 1 - 2 are the third washing solution fractions 1 and 5 and lanes 3 - 9 are eluted protein fractions 1-7, respectively.

3.8 The production of polyclonal antibodies against recombinant PmMEK

Anti-PmMEK was successfully produced in rabbits. The titer of PmMEK polyclonal antibody (PAb) was high after the five immunizations (Table 3.4). Rabbit was sacrificed and their serum was collect, filtrated through 0.22 μ M membrane and kept at -20 °C.

Table 3.4 Titers of polyclonal antibodies using indirect ELISA assay and read the optical density at 450 nm after rabbits was immunized with recombinant PmMEK for 5 times

Dilution of serum	Polyclonal antibody PmMEK	
	Pre-immunized serum (OD ₄₅₀)*	Immunized serum (OD ₄₅₀)**
1:500	0.044	2.398
1:2000	0.021	1.967
1:8000	0.011	0.994
1:32000	0.007	0.337

*Pre-immunized serum = serum from normal rabbit

**Immunized serum = serum from rabbit injected with the recombinant protein

3.9 Expression profiles of PmMEK protein during ovarian development of *P. monodon*

AntiMEK was tested for its specificity by Western blot analysis. A positive band was obtained along with several discrete bands (data not shown).

To examine levels of MEK during ovarian development of *P. monodon*, Western blot analysis of this protein was carried out (Figure 3.39). After transferring, a portion of the PVDF membrane containing proteins with the molecular weight approximately 71 kDa. The intensity of each immunoreactivity bands was indicated in Table 3.5

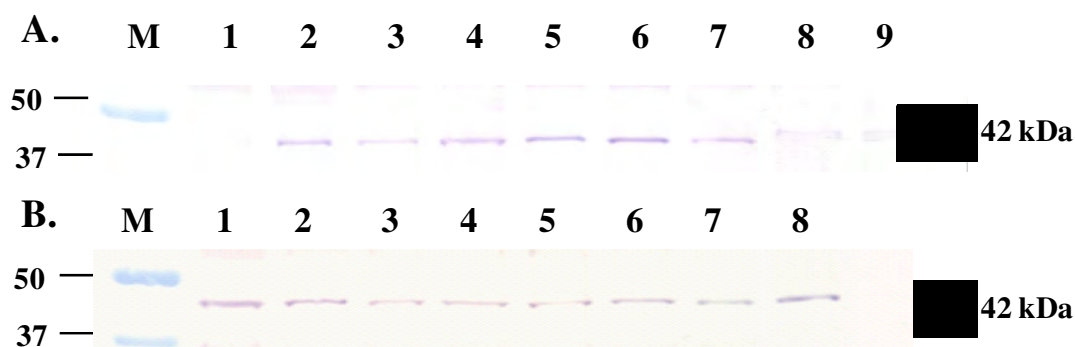


Figure 3.39 Western blotting analysis of anti-MEK PcAb (dilution 1:200, expected MW approximately 71 kDa) using total protein extracted from ovaries of ovaries of normal (A) and eyestalk-ablated (B) broodstock of wild *P. monodon*. Ovarian proteins (20 μ g) were size-fractionated by 15% SDS-PAGE.

Figure A: Lanes 1 = ovaries of 4 months-old shrimps; lanes 2-3 = stage I ovaries (GSI = 0.27% and 0.66%, respectively); lanes 4-5 = stage II ovaries (GSI = 4.01% and 5.75%, respectively); lanes 6-7= stage III ovaries (GSI = 6.16% and 6.23% respectively); lanes 8-9 = stage IV ovaries (GSI = 10.01% and 11.66%).

Figure B: Lanes 1-2 = stage I ovaries (GSI = 0.76 and 1.22%, respectively); lanes 3-4 = stage II ovaries (GSI = 3.31 and 5.08%, respectively); lanes 5-6 = stage III ovaries (GSI = 6.87% and 6.92%, respectively); lanes 7-8= stage IV ovaries (GSI = 6.36% and 6.92%, respectively).

Table 3.5 The intensity of MEK signals in different stages of ovaries in both normal and eyestalk-ablated of *P. monodon* broodstock.

Stage of samples	Intensity	Average
Normal broodstock		
4 months-old shrimps ovaries	19.52857	19.52857
Stage I ovaries (GSI = 0.89%)	29.63492	27.03196
	24.42901	
Stage II ovaries (GSI = 2.24%)	30.35182	31.22373
	32.09563	
Stage III ovaries (GSI = 5.91%)	35.50059	31.26859
	27.03659	
Stage IV ovaries (GSI = 10.41%)	23.50177	23.11157
	22.72136	
Eyestalk-ablated broodstock		
Stage I ovaries (GSI = 0.89%)	21.35244	22.53618
	23.71992	
Stage II ovaries (GSI = 0.89%)	12.29417	18.24671
	24.19925	
Stage III ovaries (GSI = 2.24%)	17.51410	23.40226
	29.29041	
Stage IV ovaries (GSI = 5.91%)	19.74812	22.03994
	24.33177	

Expression of PmMEK in ovaries of *P. monodon* during ovarian development in intact juvenile and broodstocks showed increasing of the target protein from juveniles to stage III before decreasing at stage IV, at which the band seemed to be shifted and almost detectable. More intense signals of ovarian PmMEK were observed in stages I, II and III than those in 4 months-old shrimp and stages IV ovaries of normal *P. monodon* broodstock (Figure.3.39A).

The MEK protein level in stage II ovaries was decreased increased from stage I ovaries and the expression level of this protein was increased when oocyte development proceeds (Figure 3.39B). Notably, statistical analysis was not performed because only 2 individuals from each ovarian stage of eyestalk-ablate *P. monodon* broodstock (except stage II) were examined.

CHAPTER IV

DISCUSSION

Molecular mechanisms and functional involvement of genes and proteins involved in the signal transduction pathway of meiotic maturation of oocytes is necessary for better understanding of *P. monodon* reproduction. The basic knowledge may lead to the possible ways to effectively induce ovarian maturation in economically important species like *P. monodon*.

The development of oocytes consists of a series of complex cellular events, in which different genes express to ensure the proper development of oocytes and to store transcripts and proteins as maternal factors for early embryogenesis (Qiu *et al.*, 2005; Tosti, 2006). The signal transduction such as the MAP kinase signaling cascade is one of the mechanisms that converts a biological stimulus to specific cellular responses. It is mediated by the network of proteins, transmitting stimuli across the plasma membrane through the cytoplasm and finally, into nucleus (Reece, 2002).

During oogenesis in eukaryotes, oocytes are naturally arrested at prophase I (Okano-Uchida *et al.*, 1998). Induction of meiosis in the eukaryotic cells requires the coordinated activation of multiple M phase-inducing protein kinases and are also contributed by the dynamics of the MAPK pathway. Induction leads to the activation of maturation promoting factor (MPF), a cdc2-cyclin B complex (Matten *et al.*, 1996; Gross *et al.*, 2000; Islam *et al.*, 2005) that initiates meiotic resumption of oocytes (Kishimoto, 2003; Liang *et al.*, 2007), which is marked by rapid accumulation of vitellin, a yolk protein, and the presence of the cortical rods, spherical or rod-like bodies that appear in the peripheral cytoplasm of oocytes of penaeid shrimp.

Meiotic oocyte maturation is resumed by a specific hormone (i.e. progesterone in lower vertebrates) and undergone germinal vesicle breakdown (GVBD) afterward (Yano, 1998). The actions of progesterone and its derivatives are mediated through its nuclear receptor, the progesterone receptor (nPR), as the classical pathway (Rao *et al.*, 1974). Subsequently, two totally distinct classes of putative membrane-bound progestin receptors have been reported in vertebrates: membrane progestin receptors (mPR subtypes α , β , γ ; Peluso *et al.*, 2006) and

progesterin membrane receptor component (PGMRC subtypes 1 and 2; Mourot *et al.*, 2006; Cahill, 2007; Thomas, 2008).

The full-length cDNAs and genes of nuclear progesterone receptor and mPR have not been reported in any penaeid shrimp at present. Recently, the full-length cDNA of *progesterin membrane receptor component 1* (*Pgmrc1*) in ovaries of *P. monodon* was successfully characterized (2015 bp in length with an ORF of 573 bp deducing to 190 amino acids; GenBank accession no. GQ505293). A predicted transmembrane domain (IFTSPLNVFLLGVCTVLIY) was found in the deduced *P. monodon* Pgmrc1 protein. Immunohistochemistry revealed that the ovarian Pgmrc1 protein was localized in cell membrane of various oocyte stages and follicular cells, and in the follicular layers. *Pgmrc1* was up-regulated in stage IV (mature) ovaries of intact broodstock ($P < 0.05$). Unilateral eyestalk ablation resulted in an earlier up-regulation of *Pgmrc1* since the stage II (vitellogenic) ovaries. Moreover, the expression level of *Pgmrc1* in stages II–IV (vitellogenic, early cortical rod and mature) ovaries of eyestalk-ablated broodstock was significantly greater than that of the same ovarian stages in intact broodstock ($P < 0.05$) (Preechaphol *et al.*, 2010).

In all animal species examined so far, the meiotic maturation of oocytes is regulated by maturation promoting factor (MPF), a complex of cdc2 (Cdk1) and cyclin B and other Cdk/cyclin complexes. Recently, *P. monodon cyclin B* was isolated and characterized. Expression levels of *PmCyB* in ovaries of broodstock were much greater than those of juveniles. During ovarian development, the level of *PmCyB* in mature ovaries (stage IV) was greater than that of previtellogenic (I) ovaries of *P. monodon* ($P < 0.05$) (Visudtiphole *et al.*, 2009). The differential expression profiles of *PmCyB* indirectly suggested the possible roles of the MAPK signal transduction cascade in the control of oocyte meiotic resumption in *P. monodon*. Accordingly, genes in the MAPK and related signal transduction pathways are studied.

Expression patterns of genes functionally related to ovarian development of *P. monodon* by RT-PCR

RT-PCR was used to determine differentially expressed genes during ovarian maturation of *P. monodon*. Expression analysis across different tissues of a female and testes of a male broodstock revealed that all examined transcripts were not tissue-specific but differentially or comparably expressed in examined tissues. Results were

further confirmed by examining the differential expression between ovaries and testes of *P. monodon* broodstock.

Four genes; *Mitogen-activated protein kinases-ERK kinase (MEK)*, *Large Tumor Suppressor1 (LATS1)*, *Kinase Suppressor of RAS (KSR)* and *RAS*, displaying more preferential expression towards ovaries were selected for further studies. The information suggested that they should play more important roles in oogenesis than in spermatogenesis of *P. monodon*.

Isolation and characterization of the full-length cDNA of genes expressed in ovaries of *P. monodon*

RACE-PCR was carried out for isolation of the full-length cDNA of *P. monodon MEK*, *LATS1* and *KSR*. Of these, that of *PmMEK*, and *PmKSR* were successfully characterized while the partial cDNA sequence of *PmLATS1* was obtained.

PmMEK exhibits a relatively high degree of sequence similarity with Serine/Threonine protein kinase catalytic domain in other species implying the conserved function of this gene family across taxa. The deduced MEK protein contains substrate-interaction or docking domains that required for high-affinity interactions with the enzymes. The importance of MEK-ERK docking has also been suggested by the use of MEK1 peptide encompassing the D domain. These peptides affected the subcellular distribution of ERK2 and also blocked cell cycle progression (Gotoh *et al.*, 1999). Docking site at the carboxyl terminal of PmMEK was conserved across phyla exhibited (K/R) XXX#X#, where # referred to hydrophobic residues and X is any amino acid. Bardwell *et al.* (2001) reported the importance of docking site that this conserved motif binds directly to MAPKs, ERK1 and ERK2. The interaction between these molecules is crucial for accurate transmission of many intracellular signals.

The putative *PmKSR* contained a protein kinase C conserved region 1(C1) and serine/threonine protein kinase (S_TKc) domains. *Drosophila* KSR amino acid sequences shares some similarity to MKKK Raf-1, which is quite similar to this study (C1 in the N-terminal and a potential kinase domain in the C-terminal; Whitmarsh and Davis, 1998). In *Drosophila melanogaster* and *C. elegans*, domain organization of the

KSR proteins share five conserved areas called CA1–CA5 (Kolch, 2005). However, only 2 domains were predicted from the deduced amino acid sequences of *PmKSR*. These two domains were conserved in arthropods, lower vertebrates and human.

The C1 domain, or protein kinase C conserved domain region 1 in *Drosophila* and mammals has been shown to participate in the formation of a ternary KSR–MEK–RAF complex that facilitates MEK phosphorylation (McKay *et al.*, 2009). This domain binds Ras GTPase and diacylglycerol *in silico*. Zhou *et al.* (2002) reported that the C1 domain in KSR is similar to that found in Raf and PKC γ possessing conserved cysteine and histidine residues. This domain are generally found in proteins involved in the signal transduction mediating interaction with lipids and proteins affecting the localization and biological function of the proteins.

In addition, a serine/threonine protein kinase (S_TKc) domain was identified in the carboxyl terminal of the deduced PmKSR polypeptide indicating its possible function in serine/threonine phosphorylation. Whitmarsh and Davis (1998) reported that KSR is able to bind MEK1 and MAPK/ERK2 indicating that KSR acts as scaffold protein that bring MEK1 to ERK2. Kolch (2006) recognized KSR as a scaffolding protein, assisting the phosphorylation of MAPK and MEK.

CA4 is a Ser/Thr-rich region. CA4 contains an FXFP motif that continues a stimulus-dependent ERK docking site (McKay *et al.*, 2009). There was no result for domain searching but FXFP site was located downstream of C1 domain and presented just before the S_TKc domain. Whether this region is a putative the S/T rich region or CA4 remains to be further characterized. Moreover, the deduced PmKSR protein lacks a CA5 (kinase-like) domain. Typically, the CA5 domain binds constitutively to MEK, and to RAF following stimulation (Roy *et al.*, 2002; Muller *et al.*, 2001; Ory *et al.*, 2003 and Yu *et al.*, 1998). The CA5 domain binds constitutively to MEK, and to RAF following stimulation.

A study of KSR1 knockout mice indicates that mammalian KSR1 plays an important role in growth factor- and RAS-dependent RAF activation (Lozano J, 2003). From multiple sequence alignments, the kinase domain in KSR would be divided into 2 sets; the S_TKc and the STKYC domains. The former phosphorylates specifically on serine/threonine residues, while the latter phosphorylates serine/threonine/tyrosine. The S_TKc domain found in the N-terminal of PmKSR is

likely the CA5 domain regarded in Kolch (2005). Functional studies of the PmKSR protein should be carried out.

The partial nucleotide sequence of *PmLATS1* contained serine/threonine protein kinases domain (S_TKc) and the extension to Ser/Thr type protein kinase domain (S_TK_X). *LATS* was first identified in *Drosophila melanogaster* (Xu *et al.*, 1995). Recently, Chen *et al.*, (2009) characterized the full-length cDNA of *LATS1* (1068 amino acid). Moreover, Dhillon *et al.* (2007) reported *LATS1/2* functions in the RAS-MAPK-ERK pathway, which regulates cell proliferation, apoptosis, and migration. The information implies that *LATS* gene products should also play a functionally important role in the signal transduction pathway during oocyte/ovary development of *P. monodon*.

Expression levels of *PmMEK* and *PmLATS1* during ovarian development of *P. monodon*

Quantitative real-time PCR indicated that *PmMEK* plays their important roles during the late stage of ovarian development. The expression levels of *PmMEK* at stages IV ovaries was greater than those other stages ($P > 0.05$). Like results in *Xenopus laevis*, the level of *MEK* mRNA examined also increased in late developmental stages of oocytes (Furuno *et al.*, 2002). This transcript was not significantly different during development of eyestalk-ablated *P. monodon* brooder.

The expression level of *PmLATS1* was significantly increased at the final stage (IV) of ovarian development in intact broodstock. The result suggested that *PmLATS1* may play an important role during reproductive maturation of *P. monodon* ovaries. In eyestalk-ablated broodstock, its expression level was up-regulated during vitellogenesis and final maturation of ovaries. This critically suggested that the gene might involve in both development and maturation of *P. monodon* ovaries. Expression of *LATS* mRNAs during development in the zebrafish (*Danio rerio*) was observed. Chen *et al.* (2009) reported that *LATS1* exhibited ubiquitous expression patterns while *LATS2* was highly expressed in the muscle, spleen, testis and oocyte in zebrafish adults. During embryogenesis, a different expression profiles between zebrafish *LATS1* and *LATS2* after gastrulation suggested that these genes might play important roles during late embryogenesis in addition to some shared fundamental functions in early development. The tissue expression pattern of *D. rerio LATS1* and *LATS2*

mRNAs and localization of mRNAs during oogenesis is in part similar to that of *PmLATS1*. Functional analysis of *PmLATS1* gene products should be carried out to evaluate the importance on ovarian development and oogenesis in *P. monodon*.

In addition, the expression level of *PmKSR* transcript was higher in stages I and III ovaries of eyestalk-ablated broodstock than that of the same stages in intact *P. monodon* broodstock. Eyestalk ablation has been widely practiced in the hatcheries to induce ovarian maturation and spawning in shrimp (Benzie, 1998) as it reduces the secretion of gonad inhibiting hormone (GIH) from the sinus gland. GIH had been identified from *P. monodon* and showed its impact on gonad development.

The transmission of GIH signals to the ovary has not been well established. Nevertheless, eyestalk ablation caused an increase in the mRNA levels of *vitellogenin* and *cortical rod protein* in ovaries of *M. japonicus* (Tsutsui *et al.*, 2005; Okumura *et al.*, 2006). Results from quantitative real-time PCR analysis showed the effect of this maturation-inducing method on expression of reproduction-related genes. The increase in *PmKSR* mRNA during ovarian development in eyestalk-ablated female broodstock suggests that gonad inhibiting hormone (GIH; Meusy and Payen, 1988) affects *PmKSR* transcription. Accordingly, the transcriptional profile of *PmKSR* may be used to follow reproductive maturation of *P. monodon* as a consequence of maturation inducing feed and/or hormonal treatment.

Localization of *PmMEK* and *PmLATS1* transcripts in ovaries of *P. monodon*

Localization of *PmMEK* and *PmLATS1* was carried out using *in situ* hybridization. The positive signals were observed from the antisense probe of abundantly expressed *PmMEK* and *PmLATS1* transcripts in both intact and eyestalk-ablated shrimp.

PmMEK was localized in ooplasm of previtellogenic oocytes in all ovarian stages of intact and eyestalk-ablated broodstock. *PmMEK* transcript was not observed in follicular cells, oogonia, vitellogenic, cortical rod and mature oocytes. *PmLATS1* showed similar subcellular localization in ooplasm of previtellogenic oocytes with the exception that it was also found in ooplasm and at the nuclear membrane during the GVBD process (the transitional phase between early cortical rod to mature oocytes).

The results clearly indicating both *PmMEK* and *PmLATS1* mRNA were transcribed within oocytes and they should play the functional role during ovarian development of *P. monodon*.

The expression level and localization of *PmLATS1* mRNA were in agreement as the expression level of *PmLATS1* transcript was high in stage IV oocytes in both intact and eyestalk-ablated ovaries and the hybridization signals were also found in ooplasm of late cortical rod (mature) oocytes. Interestingly, *PmLATS1* mRNA was also found at nuclear membrane which is extraordinary. This may have been due to specificity of *in situ* hybridization probe (ISH probe) used in the experiment as the ISH probe was synthesized from the partial *PmLATS1* cDNA sequence. Therefore, a new ISH probe covering the full-length cDNA of *PmLATS1* should be tested for more specific results. Development of a new method to gain high resolution imaging of mRNA localization in tissue samples such as fluorescence tagging probe can also be an alternative to provide a clearer result (Martin and Ephrussi, 2009) leading to the unambiguous conclusion about untypical localization of *PmLATS1* during the late stage of oocyte development.

The disappearance of positive signals of *PmMEK* mRNA in ooplasm of more mature stages (vitellogenic, early cortical rod and mature; stages II-IV) of oocytes may be due to significantly increasing oocytes sizes as oogenesis proceeded and low sensitivity of *in situ* hybridization on detecting gene expression per se (Klinbunga *et al.*, 2009).

From *in situ* hybridization, more intense signals of transcripts were generally found in ovaries of eyestalk-ablated broodstock than that of intact broodstock. This simply revealed the effects of eyestalk ablation on expression of reproduction-related genes in this study. The finding suggested that these genes should be involved in oogenesis and ovarian development of *P. monodon*.

In vitro* expression of rPmMEK and the expression profile of PmMEK during ovarian development of *P. monodon

In this study, rPmMEK was successfully expressed as the insoluble protein in *E. coli*. The polyclonal antibodies against this recombinant protein was successfully

produced in rabbit and anti PmMEK PcAb was used to study expression profiles of the corresponding protein by western blot analysis.

The PmMEK protein seemed to be more preferentially expressed in vitellogenic and early cortical rod ovaries than other stages in intact broodstock but it was comparably expressed during ovarian development in eyestalk-ablated broodstock of wild *P. monodon*.

The expression profiles of PmMEK mRNA and protein in intact broodstock were different. The PmMEK transcript was more abundantly transcribed during the final maturation of ovarian development. Nevertheless, the PmMEK protein observed in vitellogenic ovaries (stage II) and cortical rod (stage III) than those in mature ovaries of intact *P. monodon* broodstock. A lower level of this protein observed in mature ovarian stages suggested more rapid translation of the PmMEK protein during vitellogenic (stage II) and cortical rod (stage III) ovarian stages in intact *P. monodon*. The expression of PmMEK in mature (stage IV) ovaries was not increased but it was rather post-translational modified (e.g. glycosylation and/or phosphorylation) as revealed by its higher molecular weight observed from western blotting.

In eyestalk-ablated broodstock, the expression profile of PmMEK mRNA and protein was similar. This suggested that the accumulated *PmMEK* mRNA in oocytes is probably sufficient for its multiple translations during ovarian development of ablated *P. monodon*.

In the present study, the expression profiles of interesting genes/proteins were examined in different stages of ovarian development of intact and eyestalk-ablated *P. monodon* broodstock. The findings suggested that several key genes from the MAPK signal transduction pathway seems to contribute in ovarian development and maturation in *P. monodon*. With the increased knowledge about functions of these genes and/or proteins, it opens the possibility to control reproductive maturation of female *P. monodon* in captivity in the future.

CHAPTER V

CONCLUSIONS

1. Screening of expression patterns of genes functionally related to ovarian development of *P. monodon* by RT-PCR, 4 genes including *Mitogen-activated protein (MAP) kinases (MEK)*, *Large Tumor Suppressor1 (LATS1)*, *Kinase Suppressor of RAS (KSR)* and *RAS* with differentially expresses pattern as reveal by RT-PCR were further characterized.

2. The full length cDNAs of *PmMEK* was 1559 bp in length containing the ORFs of 1227 bp to polypeptide of 408 amino acid. Molecular mass and *pI* of the deduced *PmMEK* protein was 45.27 kDa and 6.13, respectively. *PmMEK* contained Serine/Threonine protein kinases (S_TKc).

3. *In situ* hybridization indicated that *PmMEK* was localized only in the cytoplasm of previtellogenic oocytes while *PmLATS1* was localized in ooplasm of late cortical rod oocytes as well as previtellogenic oocytes.

4. Quantitative real-time PCR indicated that In normal broodstock, expression levels of *PmMEK* at stages IV ovaries was greater than those other stages ($P > 0.05$), and this transcript was not significantly different during development of eyestalk-ablated brooder *P. monodon*. The expression level of *PmLATS1* was significantly increased at the final stage (IV) of ovarian development in normal broodstock. And the expression level of *PmKSR* transcript was higher in stage I, II and III ovaries of eyestalk-ablated broodstock than that of intact broodstocks *P. monodon*.

5. Recombinant protein of *PmMEK* was successfully expressed *in vitro*. Polyclonal antibody against this recombinant protein was produced in rabbit. Western blot analysis indicated that *PmMEK* in ovaries of *P. monodon* during ovarian development in intact juvenile and broodstocks showed increasing of the target protein from juveniles to stage III before decreasing at stage IV. More intense signals of ovarian *PmMEK* were observed in stages I, II and III than those in 4 months-old

shrimp and stages IV ovaries of normal *P. monodon* broodstock. At post spawning stage, the target protein increased again.

REFERENCES

- Abe, S. I. 1987. Differentiation of spermatogenic cells from vertebrates in vitro. Cytology. 109, 159–209.
- Alfaro, A., Zunga, G., and Komen, J. 2004. Induction of ovarian maturation and spawning by combined treatment of serotonin and a dopamine antagonist, spiperone in *Litopenaeus stylirostris* and *Litopenaeus vannamei*. Aquaculture. 236, 511–522.
- AIMS, Manual for the Determination of Egg Fertility in *Penaeus monodon* [Online]. 2009. Available from: <http://www.aims.gov.au/pages/research/mdef/mdef-00.html> [2009, February 20].
- Bayaa, M., Booth, R. A., Sheng, Y., and Liu, X. J. 2000. The classical progesterone receptor mediates *Xenopus* oocyte maturation through a nongenomic mechanism. Proceedings of the National Academy of Sciences USA. 97, 12607–12612.
- Benzie, J. A. H. 1997. A review of the effect of genetics and environment on the maturation and larval quality of the giant tiger prawn *Penaeus monodon*. Aquaculture. 155, 69–85.
- Benzie, J. A. H. 1998. Penaeid genetics and biotechnology. Aquaculture. 164, 23-47.
- Berridge, M. J., Bootman, M.D., and Roderick, H. L. 2003. Calcium signaling: Dynamics, homeostasis and remodeling. Molecular and Cellular Biology. 4, 517–529.
- Bourne, H. R., Sanders, D. A., and McCormick, F. 1991. The GTF'ase superfamily: conserved structure and molecular mechanism. Nature. 349, 117–127.
- Bradford, M. M. 1976. A rapid and sensitive method for the quantitation of microgram quantities of protein utilizing the principle of protein-dye binding. Analytical Biochemistry. 72, 248–254.
- Brusca, R. C., and Brusca, G. J. 1990. Invertebrates. Sinauer Associates, Inc., Massachusetts, 922.
- Bundschu, K., Walter, U., and Schuh, K. 2007. Getting a first clue about SPRED functions. BioEssays. Reviews Molecular Cell Biology. 29 (9), 897–907.
- Campbell, S. L., Khosravi-Far, R., Rossman, K. L., Clark, G. J., and Der, C. J. 1998. Increasing complexity of Ras signaling. Oncogene. 17, 1395–1413.

- Chang, E. S. 1993. Comparative endocrinology of molting and reproduction: insects and crustaceans. Annual Review of Entomology. 38, 161–180.
- Chang, F., et al. 2003. Regulation of cell cycle progression and apoptosis by the Ras/Raf/MEK/ERK pathway. International Journal of Oncology. 22, 469–480.
- Chan, S. M., Gu, P. L., Chu, K. H., and Tobe, S. S. 2003. Crustacean neuropeptide genes of the CHH/MIH/GIH family: implications from molecular studies. General and Comparative Endocrinology. 134, 214–219.
- Chen, C. H., Sun, Y. H., Pei, D. S., and Zhu, Z. Y. 2009. Comparative expression of Zebrafish *Lats1* and *Lats2* and their implication in gastrulation movements. Developmental dynamics. 238, 2850–2859.
- Christian, M. U., Thanashan, R., Frank, S., and Marc, T. 2010. Mechanistic principles of RAF kinase signaling. Cellular and Molecular Life Sciences. 68, 553–565.
- Cobb, M. H. 1999. Progress in Biophysics and Molecular Biology. 71, 479.
- Coman, G. J., et al. 2006. Reproductive performance of reciprocally crossed wild-caught and tank reared *Penaeus monodon* broodstock. Aquaculture. 252, 372–384.
- Crews, C. M., Alessandrin, A., and Erikson, R. L. 1992. The primary structure of MEK, a protein kinase that phosphorylates the ERK gene product. Science. 258, 478–480.
- Cuzon, G. Guillaume, J., and Cahu, C. 1994. Composition, preparation and utilization of feeds for Crustacea. Aquaculture. 124, 253–267.
- De Kleijn, D. P. V., and Van Herp, F. 1995. Molecular biology of neurohormonal precursors in the eyestalks of crustacean. Biochemistry and Molecular Biology of Comparative Biochemistry. 112, 573–579.
- Devlin, R. H., and Nagahama, Y. 2002. Sex determination and sex differentiation in fish: an overview of genetic, physiological, and environmental influences. Aquaculture. 208, 191–364.
- Dhillon, A. S., Hagan, S., Rath, O., and Kolch, W. 2007. MAP kinase signalling pathways in cancer. Oncogene. 26 (22), 3279–3290.
- DiKic, I., Tokiwa, G., Lev, S., Courtneidge, S. A., and Schlessinger, J. 1996. A role for Pyk2 and Src in linking G-protein-coupled receptors with MAP kinase activation. Nature. 383, 547–550.

- Duncan, P. I., Stojdl, D. F., and Marius, R. M. 1998. The *Clk2* and *Clk3* dual-specificity protein kinases regulate the intranuclear distribution of SR proteins and influence pre-mRNA splicing. Experimental Cell Research. 241, 300–308.
- Dupre, A., Jesus, C., Ozon, R., and Haccard, O. 2002. Mos is not required for the initiation of meiotic maturation in *Xenopus* oocytes. European Molecular Biology Organization. 21, 4026–4036.
- FAO, Fishery Statistic [Online]. 2009. Available from: <http://www.fao.org/fishery/statistics/en> [2009, February 20].
- Garrington, T. P., and Johnson, G. L. 1999. Organization and regulation of mitogen-activated protein kinase signaling pathways. Current Opinion in Cell Biology. 11, 211–218.
- Gross, S. D., Schwaba, M. S., Taieb, F. E., Lewellyn, A. L., Qian Y. W., and Maller, J. L. 2000. The critical role of the MAP kinase pathway in meiosis II in *Xenopus* oocytes is mediated by p90 Rsk. Current Biology. 10, 430–438.
- Gu, P. L., Tobe, S. S., Chow, B. K., Chu, K. H., He, J. G., and Chan, S. M. 2002. Characterization of an additional molt inhibiting hormone-like neuropeptide from the shrimp *Metapenaeus ensis*. Peptides. 23, 1875–1883.
- Hehl, S., Stoyanov, B., Oehrl, W., Schonherr, R., and Heinemann, S. H. 2001. Phosphoinositide 3-kinase-gamma induces *Xenopus* oocyte maturation via lipid kinase activity. Biochemical Journal. 360, 691–698.
- Hori, T., Takaori-Kondo, A., Kamikubo, Y., and Uchiyama, T. 2000. Molecular cloning of a novel human protein kinase, kpm, that is homologous to warts/lats, a *Drosophila* tumor suppressor. Oncogene. 19 (27), 3101–3109.
- Hu, Q., Klippel, A., Muslin, A. J., and Williams, L. 1995. Ras-dependant induction of cellular responses by constitutively active phosphatidylinositol-3 kinase. Science. 268, 100–102.
- Huberman, A. 2000. Shrimp endocrinology a review. Aquaculture. 191, 191-208.
- Inoue, M., Naito, K., Nakayama, T., and Sato, E. 1996. Mitogen-activated protein kinase activity and microtubule organization are altered by protein synthesis inhibition in maturing porcine oocytes. Zygote. 4, 191–198.
- Islam, A., et al. 2005. AT The distinct stage-specific effects of 2-(pamylcinnamoyl) amino-4-chlorobenzoic acid on the activation of MAP kinase and Cdc2 kinase in *Xenopus* oocyte maturation. Cell Signal. 17, 507–523.

- Johnson, G. L., and Lapadat, R. 2002. Mitogen-activated protein kinase pathways mediated by ERK, JNK, and p38 protein kinases, Science. 298, 1911–1912.
- Katso, R., Okkenhaug, K., Ahmadi K, White, S., Timms, J., and Waterfield MD, 2001. Cellular function of phosphoinositide 3- kinase: implications for development, homeostasis, and cancer. Annual Review of Plant Biology. 17, 615–675.
- Kishimoto, T. 2003. Cell-cycle control during meiotic maturation. Current Opinion in Cell Biology. 15, 654–663.
- King, J. E. 1948. A study of the reproductive organs of the common marine shrimp, *Penaeus setiferus* (Linnaeus). Biological Bulletin. 94, 244–262.
- Kishimoto, T. 2003. Cell-cycle control during meiotic maturation. Current Opinion in Cell Biology. 15, 654–663.
- Klinbunga, S. 1996. Genetic variation population structure of the giant tiger shrimp (*Penaeus monodon* Fabricius). PhD's thesis. University of Stirling, Scotland. 356.
- Klinbunga, S., Penman, D. J., McAndrew, B. J., and Tassanakajon, A. 1999. Mitochondrial DNA diversity in three populations of the giant tiger shrimp, *P. monodon*. Journal of Marine Biotechnology. 1, 113–121.
- Kornfeld, K., Hom, D. B., and Horvitz, H. R. 1995. The ksr-1 gene encodes a novel protein kinase involved in Ras-mediated signaling in *C. elegans*. Cell. 83, 903–913
- Kondoh, E., Tachibana, K., and Deguchi, R. 2006. Intracellular Ca²⁺ increase induces post-fertilization events via MAP kinase dephosphorylation in eggs of the hydrozoan jellyfish *Cladonema pacificum*. Developmental Biology. 293, 228–241.
- Kumagai, A., and W. G. Dunphy. 1992. Regulation of the cdc25 protein during the cell cycle in *Xenopus* extracts. Cell. 70, 139–141.
- Laemmli, U. K. 1970. Cleavage of structural proteins during the assembly of the head of bacteriophage T4. Nature. 227 (5259), 680–685.
- Lee, D. O'C., and Wickins, J. F. 1992. Crustacean farming. Blackwell Scientific Publications, The University Press, Cambridge. 392.
- Lewis, T. S., Shapiro, P. S., and Ahn, N. G. 1998. Advances in Cancer Research, 74, 49.

- Li, Y., Pei, J., Xia, H., Ke, H., Wang, H., and Tao, W. 2003. Lats2, a putative tumor suppressor, inhibits G1/S transition. Oncogene. 22 (28), 4398–4405.
- Liu, L., Laufer, H., Gogarten, P. J., and Wang, M. 1997. cDNA cloning of a mandibular organ inhibiting hormone from the spider crab *Libinia emarginata*. Invertebrate Neuroscience. 3, 199–204.
- Lohka, M. J., Hayes, M. K., and Maller, J. L. 1988. Purification of maturation promoting factor, an intracellular of early mitotic events. Proceedings of the National Academy of Sciences USA. 85, 3009–3013.
- Lopez-Illasaca, M., Crespo, P., Pellici, P. G., Gutkind, J. S., and Wetzker, R. 1997. Linkage of G protein-coupled receptors to the MAPK signaling pathway through PI 3-kinase gamma. Science 275, 394–397.
- Lozano, J., et al. 2003. Deficiency of kinase suppressor of Ras1 prevents oncogenic ras signaling in mice. Cancer Research. 63, 4232–4238.
- Marin, K.C. and Ephrussi, A. 2009. mRNA localization: Gene Expression in the spatial dimension. Cell 136, 719–730.
- Martoriati, A., Duchamp, G., and G´erard, N. 2003a. In vivo effect of epidermal growth factor, interleukin-1beta, and interleukin-1RA on equine preovulatory follicles. Biology of Reproduction. 68, 1748–1754.
- Martoriati, A., Caillaud, M., Goudet, G., and G´erard, N. 2003b. Inhibition of *in vitro* maturation of equine oocytes by interleukin 1beta via specific IL-1 receptors. Reproduction. 126, 509–515.
- Matten, W. T., Copeland, T. D., Ahn, N. G., and Vande, G. F. 1996. Positive feedback between MAP kinase and Mos during *Xenopus* oocyte maturation. Developmental Biology. 179, 485–492.
- Maxam, A. M., and Gilbert, W. 1977. A new method for sequencing DNA Proceedings of the National Academy of Sciences, 74, 560.
- McKay, M. M., Ritt, D. A., and Morrison, D. K. 2009. Signaling dynamics of the KSR1 scaffold complex. Proceedings of the National Academy of Sciences USA. 106, 11022–11027.
- McPherson, J. P., et al. 2004. Lats2/Kpm is required for embryonic development, proliferation control and genomic integrity. European Molecular Biology Organization .23 (18), 3677–3688.

- Michaud, N. R., Therrien, M., Cacace, A., Edsall, L. C., Spiegel, S., Rubin, G. M., Morrison, D. K. 1997. KSR stimulates Raf-1 activity in a kinase-independent manner. Proceedings of the National Academy of Sciences U.S.A 94, 12792–12796.
- Morrison, D. K. 2001. KSR: A MAPK scaffold of the Ras pathway. Journal of Fuel Cell Science and Technology. 114, 1609–1612.
- Motoh, H. 1984. Biology and ecology of *Penaeus monodon*. Proceedings of the First International Conference on the Culture of Penaeid Prawns/Shrimp. Aquaculture Department. 27–36.
- Muller, J., Ory, S., Copeland, T., Piwnica-Worms, H., and Morrison, D. K. 2001. C-TAK1 regulates Ras signaling by phosphorylating the MAPK scaffold, KSR1. Molecular Cell. 8, 983–993.
- Nagabhushanam, R., Joshi, P. K., and Kulkarni, G. K. 1980. Induced spawning in the prawn *Parapenaeopsis stylifera* (H. Milne Edwards) using a steroid hormone 17α -hydroxyprogesterone. Indian Journal of Science and Technology. 9, 227.
- Nishiyama, Y., et al. 1999. Federation of European Biochemical Societies Letters. 459, 159–165.
- Okano-Uchida, T., Sekiai T, Lee K. S., Okumura, E., Tachibana, K., Kishimoto, T. 1998. In vivo regulation of cyclin A/cdc2 and cyclin B/cdc2 through meiotic and early cleavage cycles in starfish. Developmental Biology. 197, 39–53.
- O’Keefe, S. J., Wolfes, H., Kiessling, A. A., and Cooper, G. M. 1989. Microinjection of antisense c-mos oligonucleotides prevents meiosis II in the maturing mouse egg. Proceedings of the National Academy of Sciences USA. 86, 7038–7042.
- Okumura, T., Aida, K. 2001. Effects of bilateral eyestalk ablation on molting and ovarian development in the giant freshwater prawn, *Macrobrachium rosenbergii*. Fisheries Science. 67, 1125–1135.
- Ory, S., Zhou, M., Conrads, T. P., Veenstra, T. D., and Morrison, D. K. 2003. Protein phosphatase 2A positively regulates Ras signaling by dephosphorylating KSR1 and Raf-1 on critical 14-3-3 binding sites. Current Biology. 13, 1356–1364.
- Primavera, J. H. 1990. External and internal anatomy of adult penaeid prawns/shrimps. SEAFDEC, Aquaculture Department, The Philippines, Poster.

- Quackenbush, L. S. 2001. Yolk synthesis in the marine shrimp, *Penaeus vannamei*. Computational Biology. 41 (3), 458–464.
- Quinitio, E. T., Hara, A., Yamaguchi, K., and Fuji, A. 1994. Changes in the steroid hormone and vitellogenin levels during the gametogenic cycle of the giant tiger shrimp, *Penaeus monodon*. Comparative Biochemistry and Physiology. 109, 21–26.
- Reece, J. 2002. Campbell Biology. San Francisco: Benjamin Cummings.
- Rodriguez, E. M., Medesani, D. A., Greco, L. L., Fingerman, M. 2002. Effects of some steroids and other compounds on ovarian growth of the red swam crayfish, *Procambarus clarkii*, during early vitellogenesis. Journal of Experimental Zoology. 292, 82–87.
- Rosenberry, B. 1997. World Shrimp Farming 1997. Shrimp News International.
- Roy, F., Laberge, G., Douziech, M., Ferland-McCollough, D., and Therrien, M. 2002. KSR is a scaffold required for activation of the ERK/MAPK module. Genes & Development. 16, 427–438.
- Sadler, K. C., and Ruderman, J. V. 1998. Components of the signaling pathway linking the 1-methyladenine receptor to MPF activation and maturation in starfish oocytes. Developmental Biology. 197, 25–38.
- Saneyoshi, T., kume, S., Amasaki, Y., and Mikoshiba, K. 2002. The Wnt/calcium pathway activates NF-AT and promotes ventral cell fate in *Xenopus* embryos. Nature. 417, 295–299.
- Sanger, F., Nicklen, S., and Coulson, A. R. 1977. DNA sequencing with chain-terminating inhibitors. Proceedings of the National Academy of Sciences U.S.A. 74, 5463.
- Segata, N., Daar, I., Oskarsson, M., and Showalter, S. D. 1989. The product of the *mos* Proto-oncogene as a candidate “initiator” for oocyte maturation. Science. 245, 643–646.
- Sambrook, J. and Russell, D. W. 2001. Molecular Cloning: A Laboratory Manual, 3rd ed., Cold Spring Harbor Laboratory Press, New York, USA.
- St John, M.A., et al. 1999. Mice deficient of *Lats1* develop soft-tissue sarcomas, ovarian tumours and pituitary dysfunction. Nature Genetics. 21 (2), 182–186.

- Steelman, L. S., Pohnert, S. C., Shelton, J. G., Franklin, R. A., Bertrand, F. E., and McCubrey, J. A. 2004. JAK/STAT, Raf/MEK/ERK, PI3K/Akt and BCR-ABL in cell cycle progression and leukemogenesis. Leukemia. 18, 189–218.
- Stein, P., Svoboda, P., and Schultz, R. M. 2003. Transgenic RNAi in mouse oocytes: a simple and fast approach to study gene function. Developmental Biology. 256, 188–194.
- Stephen, A., Stricker, and Toni, L. 2001. 5-HT causes an increase in cAMP that stimulates, rather than inhibits, oocyte maturation in marine nemertean worms. Development. 128, 1415–1427.
- Stewart, S., Sundaram, M., Zhang, Y., Lee, J., Han, M., and Guan, K. L. 1999. Kinase suppressor of Ras forms a multiprotein signaling complex and modulates MEK localization. Molecular Biology of the Cell. 19, 5523–5534.
- Stoyanov, B., et al. 1995. Cloning and characterization of a G protein-activated human phosphoinositide-3 kinase. Science. 269, 690–693.
- Sundaram, M., and Han, M. 1995. The *C. elegans* ksr-1 gene encodes a novel Raf-related kinase involved in Ras-mediated signal transduction. Cell. 83, 889–901.
- Tachibana, K., Tanaka, D., Isobe, T., and Kishimoto, T. 2000. c-Mos forces the meiotic cell cycle to undergo meiosis II to produce haploid gametes. Proceedings of the National Academy of Sciences USA. 97, 14301–14306.
- Tao, W., et al. 1999. Human homologue of the *Drosophila melanogaster* last tumour suppressor modulates CDC2 activity. Nature Genetics. 21 (2), 177–181.
- Takehara, Y., Dharmarajan, A. M., Faufman, G., and Wallach, E. E. 1994. Effect of interleukin-1b on ovulation in the in vitro perfused rabbit ovary. Endocrinology. 134 (4), 1788–1793.
- Therrien, M., Chang, H. C., Solomon, N. M., Karim, F. D., Wassarman, D. A., and Rubin, G. M. 1995. KSR, a novel protein kinase required for RAS signal transduction. Cell. 83, 879–888.
- Therrien, M. 2002. KSR is a scaffold required for activation of the ERK/MAPK module. Genes & Development 16, 427–438.
- Tian, J., Kim, S., Heilig, E., and Ruderman, J.V. 2000. Identification of XPR-1, a progesterone receptor required for *Xenopus* oocyte activation. Proceedings of the National Academy of Sciences U.S.A. 97, 14358–14363.

- Tosti, E. 2006. Calcium ion currents mediating oocyte maturation events. Endocrinol. 4 (26), 1–9.
- Towbin, H., Starhelin, T., and Gordon, J. 1979. Electrophoretic transfer of proteins from polyacrylamide gels to nitrocellulose sheets: procedure and some applications. Proceedings of the National Academy of Sciences U.S.A. 76, 4350–4354.
- Treerattrakool, S., Panyim, S., Chan, S.-M., Withyachumnarnkul, B., and Udomkit, A. 2007. Molecular characterization of gonad-inhibiting hormone of *Penaeus monodon* and elucidation of its inhibitory role in vitellogenin expression by RNA interference. Federation of the Societies of Biochemistry and Molecular Biology. 275 (5), 970–980.
- Tsukimura, B., and Kamemoto, F. I. 1991. *In vitro* stimulation of oocytes by presumptive mandibular organ secretions in the shrimp, *Penaeus vannamei*. Aquaculture. 92, 59–66.
- Tunquist, B. J., and Maller, J. L. 2003. Under arrest: cytostatic factor (CSF)-mediated metaphase arrest in vertebrate eggs. Genes & Development. 17, 683–710.
- Turenchalk, G. S., and John, A. R. 1999. The role of lats in cell cycle regulation and tumorigenesis. Biochimica Acta, 1424, 9–16.
- VanGuilder, H., Vrana, K. E., and Freeman, W. M. 2008. Twenty-five years of quantitative PCR for gene expression analysis. Biotechniques. 44, 619–626.
- Wongprasert, K., Asuvapongpatana, S., Poltana, P., Tiensuwan, M., and Withyachumnarnkul, B. 2006. Serotonin stimulates ovarian maturation and spawning in the black tiger shrimp *Penaeus monodon*. Aquaculture. 261, 1447–1454.
- Wymann, M. P., and Pirola, L. 1998. Structure and function of phosphoinositide 3-kinases. Biochimica et Biophysica Acta. 1436, 127–150.
- Xia, H., et al. 2002. LATS1 tumor suppressor regulates G2/M transition and apoptosis. Oncogene. 21 (8), 1233–1241.
- Xia, H. J., and Yang, G. 2005. Inositol 1,4,5-triphosphate 3-kinases: functions and regulations. Cell Research. 15 (2), 83–91.
- Xu, T., Wang, W., Zhang, S., Stewart, R. A., and Yu, W. 1995. Identifying tumor suppressors in genetic mosaics: the *Drosophila* lats gene encodes a putative protein kinase. Development. 121 (4), 1053–1063.

- Yabuta, N., et al. 2000. Structure, expression, and chromosome mapping of LATS2, a mammalian homologue of the *Drosophila* tumor suppressor gene *lats/warts*. Genomics. 63 (2), 263–270.
- Yabuta, N., et al. 2007. Lats2 is an essential mitotic regulator required for the coordination of cell division. Journal of Biological Chemistry. 282 (26), 19259–19271.
- Yano, I. 1987. Effect of 17- α -OH-progesterone on vitellogenin secretion in kuruma prawn, *Penaeus japonicus*. Aquaculture. 61, 46–57.
- Yano, I. 1988. Oocyte development in the kuruma prawn *Penaeus japonicus*. Marine Biology. 99, 547–553.
- Young, N. J., Quinlan, P. T., and Goad, L. J. 1992. Cholesteryl esters in the decapod crustacean, *Penaeus monodon*. Comparative Biochemistry and Physiology. 102, 761–768.
- Yu, W., Fantl, W. J., Harrowe, G., and Williams, L. T. 1998. Regulation of the MAP kinase pathway by mammalian Ksr through direct interaction with MEK and ERK. Current Biology. 8, 56–64.

APPENDIX

APPENDIX

Table 1 Relative expression levels of *MEK* in different ovarian developmental stages of *P. monodon* based on Quantitative real-time PCR analysis

Sample Groups		Mean conc.		Ratio (target / <i>EF-1α</i>)	Average	STDEV
		<i>MEK</i>	<i>EF-1α</i>			
Juvenile	JNOV2	2.66E+03	6.59E+04	0.04035	0.07721	0.04298
	JNOV3	8.60E+03	2.08E+05	0.04143		
	JNOV4	9.29E+03	6.75E+04	0.13754		
	JNOV5	1.31E+03	2.15E+04	0.06065		
	JNOV6	1.94E+04	1.83E+05	0.10611		
	N-BD-Stage I	BUFOV3	2.90E+04	1.42E+05		
	BUFOV6	1.33E+04	6.04E+04	0.22116		
	BUFOV4	3.03E+04	2.60E+05	0.11660		
	BUFOV7	2.12E+04	1.00E+05	0.21143		
	AGYLOV1	5.91E+04	9.29E+05	0.06357		
	AGYLOV4	6.02E+04	4.43E+05	0.13578		
	AGYLOV2	4.23E+04	5.36E+05	0.07886		
N:BD-Stage II	BFNOV32	3.44E+04	1.37E+05	0.25081	0.28398	0.15946
	ASPOV10	4.38E+04	9.47E+04	0.46210		
	ASPOV6	5.17E+04	1.72E+05	0.29955		
	BFNOV38	3.25E+04	6.65E+04	0.48837		
	BFNOV33	1.49E+04	2.90E+05	0.05125		
	BFNOV35	2.46E+04	7.79E+04	0.31579		
	BFNOV31	4.14E+04	2.97E+05	0.13944		
N:BD-Stage III	BFNOV4/1	1.72E+04	7.42E+04	0.23137	0.19041	0.04380
	BFNOV18	1.24E+04	7.50E+04	0.16535		
	BFNOV4	1.54E+04	7.57E+04	0.20321		
	BFNOV24	1.17E+04	6.43E+04	0.18208		
	BFNOV5	1.67E+04	6.47E+04	0.25815		
N:BD-Stage IV	BFNOV1	1.47E+04	1.02E+05	0.14324	0.42388	0.23488
	BFNOV2	1.07E+04	2.16E+04	0.49627		
	BFNOV14	1.40E+04	2.12E+04	0.66235		
	BFNOV10	9.59E+03	7.77E+04	0.12343		
	BFNOV12	9.12E+03	3.71E+04	0.24604		
	BFNOV15	8.52E+03	4.06E+04	0.20988		
	BFNOV20	1.16E+04	1.43E+04	0.81285		
	BFNOV16	6.14E+03	1.81E+04	0.33931		
	BFNOV17	8.15E+03	1.31E+04	0.62076		
	BFNOV13	8.46E+03	2.78E+04	0.30402		
N:BD Post-spawning	BFNOV30	1.39E+04	8.31E+04	0.16706	0.23405	0.19209
	BFNOV34	1.91E+04	2.26E+05	0.08442		
	BFNOV37	1.94E+04	4.31E+04	0.45067		

Table 1(cont.)

Sample Groups		Mean conc.		Ratio (target / <i>EF-1α</i>)	Average	STDEV
		<i>MEK</i>	<i>EF-1α</i>			
EA:BD-Stage I	BFEOV18	3.65E+04	8.80E+04	0.41448	0.30995	0.10666
	YLBOV01	9.51E+04	4.74E+05	0.20065		
	YLBOV06	2.50E+04	1.06E+05	0.23735		
	BFEOV15	3.18E+04	8.21E+04	0.38731		
EA:BD-Stage II	YLBOV05	7.24E+04	5.88E+05	0.12317	0.17944	0.04847
	YLBOV08	5.63E+04	2.84E+05	0.19813		
	BFEOV19	2.41E+04	1.13E+05	0.21203		
	BFEOV17	1.02E+04	7.69E+04	0.13290		
	YLBOV07	2.29E+04	9.90E+04	0.23096		
EA:BD-Stage III	BFEOV16	3.47E+04	4.73E+04	0.73508	0.31410	0.13967
	YLBOV04	3.86E+04	1.36E+05	0.28345		
	BFEOV21	3.10E+04	1.10E+05	0.28187		
	YLBOV02	3.37E+04	9.24E+04	0.36488		
	YLBOV03	2.25E+04	9.55E+04	0.23522		
	BFEOV05	5.69E+04	1.92E+05	0.29676		
	BFEOV05	4.40E+04	1.31E+05	0.33668		
	BFEOV02	3.16E+04	1.30E+05	0.24371		
	BFEOV11	2.24E+04	1.11E+05	0.20210		
	BFEOV03	3.46E+04	1.38E+05	0.25092		
EA:BD-Stage IV	BFEOV01	1.95E+04	9.77E+04	0.19988	0.32192	0.11473
	BFEOV07	4.28E+04	9.83E+04	0.43503		
	BFEOV06	2.20E+04	5.08E+04	0.43376		
	BFEOV24	2.34E+04	1.00E+05	0.23353		
	BFEOV10	3.11E+04	8.32E+04	0.37402		
	BFEOV12	2.82E+04	6.09E+04	0.46285		
	BFEOV13	3.45E+04	1.56E+05	0.22112		
	BFEOV22	1.52E+04	7.07E+04	0.21519		
EA:BD-Stage I	BFEOV18	3.65E+04	8.80E+04	0.41448	0.30995	0.10666
	YLBOV01	9.51E+04	4.74E+05	0.20065		
	YLBOV06	2.50E+04	1.06E+05	0.23735		
	BFEOV15	3.18E+04	8.21E+04	0.38731		
EA:BD-Stage II	YLBOV05	7.24E+04	5.88E+05	0.12317	0.17944	0.04847
	YLBOV08	5.63E+04	2.84E+05	0.19813		
	BFEOV19	2.41E+04	1.13E+05	0.21203		
	BFEOV17	1.02E+04	7.69E+04	0.13290		
	YLBOV07	2.29E+04	9.90E+04	0.23096		
EA:BD-Stage III	BFEOV16	3.47E+04	4.73E+04	0.73508	0.31410	0.13967

Table 2 Relative expression levels of *LATS1* in different ovarian developmental stages of *P. monodon* based on Quantitative real-time PCR analysis

Sample Groups		Mean conc.		Ratio (target / <i>EF-1α</i>)	Average	STDEV
		<i>LATS1</i>	<i>EF-1α</i>			
Juvenile	JNOV2	1.92E+04	6.59E+04	0.29124	0.40470	0.23902
	JNOV3	4.02E+04	2.08E+05	0.19376		
	JNOV4	5.49E+04	6.75E+04	0.81359		
	JNOV5	8.10E+03	2.15E+04	0.37656		
	JNOV6	6.38E+04	1.83E+05	0.34837		
	N-BD-Stage I	BUFOV3	1.24E+05	1.42E+05		
	BUFOV6	3.82E+04	6.04E+04	0.63300		
	BUFOV4	1.23E+05	2.60E+05	0.47262		
	BUFOV7	5.21E+04	1.00E+05	0.52094		
	AGYLOV1	1.44E+05	9.29E+05	0.15536		
	AGYLOV4	2.37E+05	4.43E+05	0.53549		
	AGYLOV2	6.09E+04	5.36E+05	0.11374		
	BFNOV32	9.19E+04	1.37E+05	0.67023		
N:BD-Stage II	ASPOV10	1.63E+05	9.47E+04	1.72041	0.80482	0.54003
	ASPOV6	1.38E+05	1.72E+05	0.80186		
	BFNOV38	7.09E+04	6.65E+04	1.06577		
	BFNOV33	3.55E+04	2.90E+05	0.12230		
	BFNOV35	7.45E+04	7.79E+04	0.95689		
	BFNOV31	6.28E+04	2.97E+05	0.21159		
	BFNOV4/1	5.60E+04	7.42E+04	0.75490		
N:BD-Stage III	BFNOV18	2.54E+04	7.50E+04	0.33839	0.55692	0.21258
	BFNOV4	5.36E+04	7.57E+04	0.70752		
	BFNOV24	3.47E+04	6.43E+04	0.53975		
	BFNOV5	5.37E+04	6.47E+04	0.83015		
	BFNOV1	3.77E+04	1.02E+05	0.36879		
N:BD-Stage IV	BFNOV2	3.17E+04	2.16E+04	1.46866	1.16073	0.49644
	BFNOV14	2.92E+04	2.12E+04	1.37961		
	BFNOV10	3.16E+04	7.77E+04	0.40618		
	BFNOV12	3.43E+04	3.71E+04	0.92463		
	BFNOV15	3.55E+04	4.06E+04	0.87490		
	BFNOV20	3.00E+04	1.43E+04	2.10066		
	BFNOV16	2.57E+04	1.81E+04	1.41988		
	BFNOV17	1.48E+04	1.31E+04	1.12378		
	BFNOV13	2.08E+04	2.78E+04	0.74822		
N:BD Post-spawning	BFNOV30	4.80E+04	8.31E+04	0.57786	0.74218	0.57147
	BFNOV34	6.13E+04	2.26E+05	0.27087		
	BFNOV37	5.94E+04	4.31E+04	1.37781		

Table 2 (cont.)

Sample Groups		Mean conc.		Ratio (target / <i>EF-1a</i>)	Average	STDEV
		<i>LATS1</i>	<i>EF-1a</i>			
EA:BD-Stage I	BFEOV18	3.44E+04	8.80E+04	0.39102	0.37636	0.08880
	YLBOV01	2.32E+05	4.74E+05	0.48897		
	YLBOV06	2.91E+04	1.06E+05	0.27624		
	BFEOV15	2.87E+04	8.21E+04	0.34921		
EA:BD-Stage II	YLBOV05	1.57E+05	5.88E+05	0.26802	0.24295	0.01957
	YLBOV08	6.59E+04	2.84E+05	0.23178		
	BFEOV19	2.95E+04	1.13E+05	0.26009		
	BFEOV17	1.76E+04	7.69E+04	0.22883		
	YLBOV07	2.24E+04	9.90E+04	0.22603		
EA:BD-Stage III	BFEOV16	4.85E+04	4.73E+04	1.02713	0.61306	0.17465
	YLBOV04	9.65E+04	1.36E+05	0.70868		
	BFEOV21	5.04E+04	1.10E+05	0.45775		
	YLBOV02	3.62E+04	9.24E+04	0.39180		
	YLBOV03	6.17E+04	9.55E+04	0.64531		
	BFEOV05	1.35E+05	1.92E+05	0.70575		
	BFEOV05	9.88E+04	1.31E+05	0.75583		
	BFEOV02	8.40E+04	1.30E+05	0.64761		
	BFEOV11	5.76E+04	1.11E+05	0.52056		
	BFEOV03	7.49E+04	1.38E+05	0.54268		
EA:BD-Stage IV	BFEOV01	2.46E+04	9.77E+04	0.47171	0.669725	0.277833
	BFEOV07	4.28E+04	9.83E+04	0.48193		
	BFEOV06	4.46E+04	5.08E+04	0.45593		
	BFEOV24	9.53E+04	1.00E+05	0.96968		
	BFEOV10	2.64E+04	8.32E+04	0.52015		
	BFEOV12	4.63E+04	6.09E+04	0.46258		
	BFEOV13	8.47E+04	1.56E+05	1.01707		
	BFEOV22	6.19E+04	7.07E+04	1.01638		
EA:BD-Stage I	BFEOV18	3.44E+04	8.80E+04	0.39102	0.37636	0.08880

Table 3 Relative expression levels of *KSR* in different ovarian developmental stages of *P. monodon* based on Quantitative real-time PCR analysis

Sample Groups		Mean conc.		Ratio (target / <i>EF-1α</i>)	Average	STDEV
		<i>KSR</i>	<i>EF-1α</i>			
Juvenile	JNOV2	1.00E+04	6.59E+04	0.15221	0.32630	0.30710
	JNOV3	2.02E+04	2.08E+05	0.09742		
	JNOV4	2.29E+04	6.75E+04	0.33866		
	JNOV5	1.83E+04	2.15E+04	0.85184		
	JNOV6	3.50E+04	1.83E+05	0.19137		
	N:BD-Stage I	BUFOV3	2.06E+04	1.42E+05		
	BUFOV6	1.17E+04	6.04E+04	0.19408		
	BUFOV4	2.39E+04	2.60E+05	0.09205		
	BUFOV7	1.43E+04	1.00E+05	0.14247		
	AGYLOV1	2.04E+04	9.29E+05	0.02198		
	AGYLOV4	5.18E+04	4.43E+05	0.11701		
	AGYLOV2	2.52E+04	5.36E+05	0.04708		
	BFNOV32	2.78E+04	1.37E+05	0.20303		
N:BD-Stage II	ASPOV10	3.93E+04	9.47E+04	0.41500	0.19345	0.13229
	ASPOV6	2.48E+04	1.72E+05	0.14358		
	BFNOV38	2.13E+04	6.65E+04	0.31954		
	BFNOV33	1.24E+04	2.90E+05	0.04253		
	BFNOV35	1.61E+04	7.79E+04	0.20640		
	BFNOV31	2.47E+04	2.97E+05	0.08322		
	BFNOV4/1	1.07E+04	7.42E+04	0.14390		
N:BD-Stage III	BFNOV18	9.37E+03	7.50E+04	0.12479	0.13483	0.0564
	BFNOV4	1.14E+04	7.57E+04	0.15030		
	BFNOV24	1.28E+04	6.43E+04	0.19912		
	BFNOV5	9.97E+03	6.47E+04	0.15401		
	BFNOV1	4.70E+03	1.02E+05	0.04595		
N:BD-Stage IV	BFNOV2	8.87E+03	2.16E+04	0.41064	0.38374	0.17954
	BFNOV14	6.33E+03	2.12E+04	0.29894		
	BFNOV10	9.89E+03	7.77E+04	0.12725		
	BFNOV12	9.39E+03	3.71E+04	0.23140		
	BFNOV15	9.67E+03	4.06E+04	0.67785		
	BFNOV20	9.48E+03	1.43E+04	0.52400		
	BFNOV16	6.63E+03	1.81E+04	0.50493		
	BFNOV17	8.21E+03	1.31E+04	0.29491		
	BFNOV13	2.12E+04	2.78E+04	0.25548		
N:BD Post-spawning	BFNOV30	1.98E+04	8.31E+04	0.08754	0.23478	0.13805
	BFNOV34	1.56E+04	2.26E+05	0.36131		
	BFNOV37	7.40E+04	4.31E+04	0.84061		

Table 3 (cont.)

Sample Groups		Mean conc.		Ratio (target / <i>EF-1a</i>)	Average	STDEV
		<i>KSR</i>	<i>EF-1a</i>			
EA:BD-Stage I	BFEOV18	1.76E+05	8.80E+04	0.37222	0.64166	0.34378
	YLBOV01	3.49E+04	4.74E+05	0.33057		
	YLBOV06	8.40E+04	1.06E+05	1.02324		
	BFEOV15	1.04E+05	8.21E+04	0.17651		
EA:BD-Stage II	YLBOV05	1.37E+05	5.88E+05	0.48230	0.38964	0.14509
	YLBOV08	3.44E+04	2.84E+05	0.30296		
	BFEOV19	3.60E+04	1.13E+05	0.46846		
	BFEOV17	5.13E+04	7.69E+04	0.51797		
	YLBOV07	3.62E+04	9.90E+04	0.76624		
EA:BD-Stage III	BFEOV16	5.68E+04	4.73E+04	0.41684	0.41858	0.16340
	YLBOV04	3.32E+04	1.36E+05	0.30215		
	BFEOV21	4.54E+04	1.10E+05	0.49072		
	YLBOV02	3.20E+04	9.24E+04	0.33527		
	YLBOV03	4.97E+04	9.55E+04	0.2594		
	BFEOV05	9.18E+04	1.92E+05	0.70181		
	BFEOV05	3.78E+04	1.31E+05	0.29133		
	BFEOV02	4.16E+04	1.30E+05	0.37545		
	BFEOV11	5.03E+04	1.11E+05	0.36412		
	BFEOV03	2.31E+04	1.38E+05	0.44243		
EA:BD-Stage IV	BFEOV01	2.46E+04	9.77E+04	0.27720	0.29152	0.12242
	BFEOV07	1.54E+04	9.83E+04	0.15804		
	BFEOV06	1.94E+04	5.08E+04	0.19756		
	BFEOV24	2.48E+04	1.00E+05	0.48924		
	BFEOV10	2.91E+04	8.32E+04	0.29050		
	BFEOV12	2.62E+04	6.09E+04	0.31535		
	BFEOV13	2.61E+04	1.56E+05	0.42783		
	BFEOV22	2.35E+04	7.07E+04	0.15049		

Table 4 The percentage of GSI and another data of *p. monodon* using in this thesis

No.	Body weight (g.)	Gonad weight (g.)	GSI (%)	Total length (cm.)	Original codes	Gonad colour	Remark
1	115.28	0.32	0.27	23.5	BUFOV03	light white	Stage I
2	76.37	0.47	0.61	23.0	BUFOV06	light white	Stage I
3	105.70	0.70	0.66	24.5	BUFOV04	light white	Stage I
4	99.96	0.77	0.77	23.5	AGYLOV03	white	Stage I
5	170.28	1.46	0.86	-	PMBF2	white	Stage I
6	112.35	1.00	0.89	23.0	BUFOV07	light yellow	Stage I
7	82.71	0.90	1.08	21.5	BUFOV05	turbid white	Stage I
8	157.33	1.73	1.10	27.0	AGYLOV01	white + light pink	Stage I
9	104.97	1.18	1.12	23.0	AGYLOV04	white	Stage I
10	120.58	1.60	1.33	23.5	AGYLOV02	white	Stage I
11	186.69	2.69	1.44	26.0	BFNOV32	yellow	Stage I
12	188.30	2.76	1.47	-	PMBF1	light yellow	Stage I
13	218.71	4.70	2.15	28.0	BFNOV38	light green + yellow	Stage II
14	205.67	4.61	2.24	27.5	BFNOV33	light yellow	Stage II
15	128.74	2.25	2.25	24.5	ASPOV10	light yellow	Stage II
16	205.05	5.29	2.58	28.0	BFNOV35	light yellow	Stage II
17	149.64	2.68	2.68	26.7	ASPOV06	light yellow	Stage II
18	208.54	6.16	2.95	26.0	BFNOV31	light green	Stage II
19	181.30	6.00	3.31	28.5	BFNOV04/1	yellow + green	Stage II
20	159.80	6.40	4.01	27.7	BFNOV07	light green	Stage III
21	187.10	8.27	4.42	30.0	BFNOV18	green + yellow	Stage III
22	173.40	8.00	4.61	28.0	BFNOV03	green	Stage III
23	164.50	7.60	4.64	27.5	BFNOV04	green	Stage III
24	230.93	12.12	5.28	32.0	BFNOV23	green + yellow	Stage III
25	235.98	12.69	5.37	33.0	BFNOV24	green	Stage III
26	172.30	9.90	5.75	28.0	BFNOV05	green	Stage III
27	172.60	10.20	5.91	28.0	BFNOV01	green	Stage III
28	136.40	8.40	6.16	26.5	BFNOV09	dark green	Stage IV
29	133.20	8.30	6.23	26.0	BFNOV08	green	Stage IV
30	176.20	12.90	7.32	29.0	BFNOV06	dark green	Stage IV
31	272.20	20.30	7.46	32.0	BFNOV02	green	Stage IV
32	152.20	12.80	8.42	27.0	BFNOV14	green	Stage IV
33	139.90	13.10	9.36	25.5	BFNOV10	dark green	Stage IV
34	162.20	16.20	9.99	28.0	BFNOV12	dark green	Stage IV
35	166.90	16.70	10.01	27.5	BFNOV11	light green	Stage IV
36	239.86	24.98	10.41	33.0	BFNOV21	green	Stage IV
37	207.40	23.20	11.19	30.5	BFNOV15	dark green	Stage IV
38	232.57	26.08	11.21	30.0	BFNOV20	green	Stage IV
39	156.10	18.20	11.66	27.0	BFNOV16	dark green	Stage IV
40	252.11	31.30	12.41	30.0	BFNOV17	green	Stage IV
41	158.60	19.90	12.55	27.5	BFNOV13	dark green	Stage IV
42	300.12	10.47	3.49	32.5	BFNOV30	light green + yellow	post-spawn
43	194.49	3.61	1.86	27.5	BFNOV36	light yellow + little green	post-spawn

Table4 (cont.)

No.	Body weight (g.)	Gonad weight (g.)	GSI (%)	Total length (cm.)	Original codes	Gonad colour	Remark
44	256.40	8.39	3.27	29.5	BFNOV34	light yellow	post-spawn
45	264.70	7.66	2.89	30.0	BFNOV37	light yellow	post-spawn
46	285.97	8.30	2.90	32.0	BFNOV39	yellow	post-spawn
47	200.79	5.18	2.58	28.0	BFNOV40	light yellow	post-spawn
48	236.51	1.79	0.76	27.50	BFEOV18	white	Eyestalk-ablated; Stg I
49	111.00	1.00	0.90	24.50	YLBOV01	white + light yellow	Eyestalk-ablated; Stg I
50	163.00	2.00	1.22	25.00	YLBOV06	white	Eyestalk-ablated; Stg I
51	272.20	3.71	1.36	30.00	BFEOV15	yellow	Eyestalk-ablated; Stg I
52	125.00	2.00	1.60	24.50	YLBOV05	white + light yellow	Eyestalk-ablated; Stg II
53	118.00	2.00	1.69	24.50	YLBOV08	white	Eyestalk-ablated; StgII
54	173.37	4.72	2.72	25.50	BFEOV19	light green + yellow	Eyestalk-ablated;Stg II
55	252.03	7.16	2.84	29.50	BFEOV17	green + yellow	Eyestalk-ablated;Stg II
56	151.00	5.00	3.31	25.00	YLBOV07	light green	Eyestalk-ablated;Stg II
57	291.39	10.31	3.54	30.50	BFEOV16	green	Eyestalk-ablated;Stg II
58	164.00	6.00	3.66	26.00	YLBOV04	light green	Eyestalk-ablated;Stg II
59	193.65	8.82	4.55	27.00	BFEOV21	dark green	Eyestalk-ablated;Stg III
60	153.00	7.00	4.57	25.50	YLBOV02	light green	Eyestalk-ablated;Stg III
61	125.00	6.00	4.80	25.00	YLBOV03	light green	Eyestalk-ablated;Stg III
62	118.80	5.90	4.97	24.50	BFEOV08	green	Eyestalk-ablated;Stg III; BIOTEC shrimp
63	186.50	9.40	5.04	27.50	BFEOV05	light green	Eyestalk-ablated;Stg III
64	196.90	10.00	5.08	29.50	BFEOV02	light green + yellow	Eyestalk-ablated;Stg III
65	96.20	4.90	5.09	23.30	BFEOV11	green	Eyestalk-ablated;Stg III; BIOTEC shrimp
66	182.70	9.40	5.15	28.00	BFEOV03	yellow + little green	Eyestalk-ablated;Stg III
67	278.23	14.37	5.16	29.50	BFEOV20	dark green + little yellow	Eyestalk-ablated;Stg III
68	197.40	10.80	5.47	29.50	BFEOV04	light green + yellow	Eyestalk-ablated;Stg III
69	229.60	14.60	6.36	30.00	BFEOV01	green + yellow	Eyestalk-ablated; StgIV
70	220.10	14.00	6.36	28.50	BFEOV07	light green + yellow	Eyestalk-ablated; StgIV
71	170.20	11.60	6.82	27.00	BFEOV06	light green + yellow	Eyestalk-ablated; StgIV
72	365.38	25.08	6.86	33.00	BFEOV24	green	Eyestalk-ablated; StgIV
73	116.40	8.00	6.87	25.50	BFEOV10	dark green	Eyestalk-ablated; StgIV; BIOTEC shrimp
74	128.70	8.90	6.92	25.20	BFEOV12	dark green	Eyestalk-ablated; StgIV; BIOTEC shrimp
75	188.20	13.80	7.35	27.50	BFEOV13	dark green	Eyestalk-ablated; StgIV
76	167.54	14.33	8.55	25.00	BFEOV22	dark green	Eyestalk-ablated; StgIV
77	256.34	22.41	8.74	29.50	BFEOV23	dark green	Eyestalk-ablated; StgIV
78	249.50	22.30	8.94	31.50	BFEOV09	light green	Eyestalk-ablated; StgIV
79	115.60	12.80	11.07	23.50	BFEOV14	dark green	Eyestalk-ablated; StgIV; BIOTEC shrimp

BIOGRAPHY

Miss Somkamon Keereepruk was born on July 28, 1986 in Bangkok. She graduated with the degree of Bachelor of Science from the Faculty of Science Technology at King Mongkut's Institute of Technology Ladkrabang in 2007. She has studied for the Degree of Master of Science (Biotechnology) at the Program of Biotechnology, Chulalongkorn University since 2008.

Publication related with this thesis

Keereepruk, S., Ponza, P., Kllinbunga, S., and Menasveta, P., 2010. Screening of genes involving signal transduction pathways and their significance in ovarian maturation of the giant tiger shrimp *Penaeus monodon*. The 22nd Annual Meeting of the Thai Society for Biotechnology "International Conference on Biotechnology for Healthy Living", 20-22 October, Trang, Thailand (poster presentation).